ISTANBUL TECHNICAL UNIVERSITY ★ GRADUATE SCHOOL OF SCIENCE ENGINEERING AND TECHNOLOGY

DESIGN OF NANOSIZED FOOD DELIVERY SYSTEMS FOR ANTIOXIDANTS BY USING NANOEMULSION, NANOSUSPENSION AND LAYER BY LAYER DEPOSITIONING OF LIPOSOMES

Ph.D. THESIS

Ayşe KARADAĞ

Department of Food Engineering

Food Engineering Programme

FEBRUARY 2013

ISTANBUL TECHNICAL UNIVERSITY ★ GRADUATE SCHOOL OF SCIENCE ENGINEERING AND TECHNOLOGY

DESIGN OF NANOSIZED FOOD DELIVERY SYSTEMS FOR ANTIOXIDANTS BY USING NANOEMULSION, NANOSUSPENSION AND LAYER BY LAYER DEPOSITIONING OF LIPOSOMES

Ph.D. THESIS

Ayşe KARADAĞ
(506072503)

Department of Food Engineering

Food Engineering Programme

Thesis Advisor: Prof. Dr. Beraat ÖZÇELİK

FEBRUARY 2013

İSTANBUL TEKNİK ÜNİVERSİTESİ ★ FEN BİLİMLERİ ENSTİTÜSÜ

ANTİOKSİDANLAR İÇİN NANOBOYUTTA GIDA TAŞINIM SİSTEMLERİNİN NANOEMULSİYON, NANOSÜSPANSİYON VE KAT-KAT KAPLANMA TEKNİĞİ İLE HAZIRLANAN LİPOZOMLARIN TASARIMI

DOKTORA TEZİ

Ayşe KARADAĞ
(506072503)

Gıda Mühendisliği Anabilim Dalı

Gıda Mühendisliği Programı

Tez Danışmanı: Prof. Dr. Beraat ÖZÇELİK

ŞUBAT 2013

Ayşe Karadağ, a **Ph.D.** student of ITU **Graduate School of Science, Engineering and Technology** 5006072503, successfully defended the **thesis** entitled "**DESIGN OF NANOSIZED FOOD DELIVERY SYSTEMS FOR ANTIOXIDANTS BY USING NANOEMULSION, NANOSUSPENSION AND LAYER BY LAYER DEPOSITIONING OF LIPOSOMES**", which she prepared after fulfilling the requirements specified in the associated legislations, before the jury whose signatures are below.

Thesis Advisor :	**Prof. Dr. Beraat ÖZÇELİK** İstanbul Technical University	.....
Jury Members :	**Prof. Dr. Muhammet ARICI** Yildiz Technical University	.....
	Doç. Dr. Gürbüz GÜNEŞ Istanbul Technical University	.....
	Doç. Dr. Rana SANYAL Bogazici University	.....
	Yrd. Doç. Dr. Esra ÇAPANOĞLU GÜVEN Istanbul Technical University	.....

Date of Submission : 10 December 2012
Date of Defense : 18 February 2013

FOREWORD

The completion of my PhD studies and writing thesis has been an amazing and painful journey accompanied with bitterness, hardships, frustration. I suppose similar to the most of PhD candidates around the world, I had questioned whether my motives to start this journey as solid and precise as the day I decided or my ideas/perceptions had been changed throughout this experience. However at this point of my life, when I look over I could only remember all the best things happened to me and many outstanding people without whose support, encouragement and guidance it would not have been possible to accomplish this long but challenging and fulfilling road

I have been very fortunate to be able to work in three universities in three countries. First and foremost, I would like to express my heartfelt gratitude to my supervisor and mentor, Prof. Dr. Beraat OZCELIK for all her contributions, time, guidance and support to make my Ph.D. experience productive and stimulating. The joy and enthusiasm she has for research was motivational and I hope I could be able to turn pass on the research values and the inspirations that she has given to me.

This thesis was a product of long and intensive study which was partly realized in Rutgers, The State University of New Jersey, USA and University of Hohenheim, Germany.I am deeply grateful to Prof. Dr. Qingrong HUANG for giving me this exciting opportunity to work in his laboratory for a year and provided all sources to pursuit a research on nanoemulsion and nanosuspension systems. He had been a strong and supportive advisor giving enough space and freedom but always very close to my work and follow its progress carefully.

It is my privilige to express my genuine thanks and appreciations to Prof. Dr. Jochen WEISS who accepted me to conduct a study on nanoliposomes for a year in his laboratory under his valuable supervision. I will always indebted to him sharing his tremendous knowledge on colloidal dispersion systems and many motivating discussions which changed my perspectives and made me think out of the box. I will always consider myself very luck to be his student.

I also thank my friends and lab-mates in Turkey, Stuttgart and New Jersey (too many to list here but you know who you are) for providing support and friendship and making my life enjoyable and delightful.

Lastly, and most importantly I would like to thank, my mom, dad and my brothers. My parents have given their unconditional care, support and always believed in me. I love them so much, and I would not have made it this far without them. Special thanks to my brother Kemal for providing every easiness and comfort during my stay in USA and to my dearest brother Veysel who has been one of my best friends and stood by me through every crisis and struggles. I would like to give this thesis as a gift to my family.

February, 2013 Ayse KARADAG (M.Sc)

TABLE OF CONTENTS

Page

FOREWORD ..... **vii**
TABLE OF CONTENTS ..... **ix**
ABBREVATIONS ..... **xiii**
LIST OF TABLES ..... **xv**
LIST OF FIGURES ..... **xvii**
SUMMARY ..... **xxi**
ÖZET ..... **xxv**
1. INTRODUCTION **1**
1.1Purpose of Thesis 4
2. LITERATURE **7**
2.1Antioxidants 7
2.1.1 Antioxidant capacity determination methods 10
2.1.1.1 DPPH (1,1-Diphenyl-2- picrylhydrazyl) radical scavenging capacity assay 11
2.1.1.2 FRAP (Ferric reducing antioxidant potential) assay 12
2.1.1.3 ORAC (Oxygen radical absorbance capacity) assay 12
2.2 Delivery Systems 13
2.2.1 Nanoemulsions 14
2.2.1.1 Nanoemulsion Composition 16
2.1.1.2 Preparation methods 24
2.2.2 Liposomes/Nanoliposomes 34
2.2.2.1 Preparation methods 35
2.2.3 Nanosuspensions 37
2.2.3.1 Preparation methods 37
2.2.4 Stability 40
2.2.4.1 Gravitational separation 44
2.2.4.2 Flocculation 45
2.2.4.3 Coalescence 46
2.2.4.4 Ostwald ripening 47
2.2.5 Layer by layer (LBL) depositioning technique 47
2.2.5.1 Preparation methods 48
2.3 Characterization Methods 51
2.3.1 Light scattering methods 51
2.3.2 Microscopy 53
2.3.2.1 Conventional optical microscopy 54
2.3.2.2 Laser scanning confocal microscopy (LSCM) 55
2.3.2.3 Electron microscopes 55
2.3.2.4 Atomic force microscopy (AFM) 56
2.3.3 Measurement of surface charge 56

3. OPTIMIZATION OF CONDITIONS FOR THE PREPARATION OF QUERCETIN NANOEMULSIONS USING RESPONSE SURFACE METHODOLOGY 61
3.1 Introduction 61
3.2 Materials and Methods 622
3.2.1 Materials 622
3.2.2 Solubility of quercetin 63
3.2.3 Screening of emulsion formulations by constructing of phase diagram 63
3.2.4 Preparation of quercetin nanoemulsion 633
3.2.5 Particle size analysis 64
3.2.6 Stability of quercetin nanoemulsions 64
3.2.7 Experimental design 65
3.2.8 Statistical analysis 66
3.3 Results and Discussion 66
3.3.1 Solubility of quercetin 66
3.3.2 Screening of emulsion formulations by constructing of phase diagram 699
3.3.3 Analysis of response surface model 70
3.3.3.1 Fitting the models 70
3.3.3.2 Verification of model and optimal conditions 74
3.3 Quercetin Loading 74
3.4 Conclusion 78
4. PREPARATION OF QUERCETIN NANOSUSPENSIONS BY HIGH-PRESSURE HOMOGENIZATION 79
4.1 Introduction 79
4.2 Materials and Methods 80
4.2.1 Materials 80
4.2.2 High pressure homogenization processing 80
4.2.3 Lyophilization 81
4.2.4 Spray drying 81
4.2.5 Particle size measurements 81
4.2.6 Solubility/Dispersity test 81
4.2.7 Dissolution rate measurements 82
4.2.8 Atomic force microscopy (AFM) 82
4.2.9 Differential scanning calorimetry (DSC) measurements 82
4.2.10 Antioxidant activity assays 83
4.2.10.1 DPPH free radical scavenging activity Assay 83
4.2.10.2 Ferric reducing/antioxidant power (FRAP) assay 83
4.2.10.3 Oxygen radical antioxidant capacity (ORAC) assay 83
4.2.11 Scanning electron microscopy (SEM) 84
4.2.12 Statistical analysis 85
4.3 Results and Discussion 85
4.3.1 Effect of high pressure conditions on particle size 85
4.3.2 Effect of high pressure conditions on water dispersity 88
4.3.3 Thermal properties of quercetin before and after HPH treatment 93
4.3.4 Dissolution Rate 94
4.3.5 Antioxidant assays 95
4.4 Conclusion 97
5. PRESENCE OF ELECTROSTATICALLY ADSORBED POLYSACCHARIDES IMPROVES SPRAY DRYING OF LIPOSOMES 99

5.1 Introduction 99
5.2 Materials and Methods 101
5.2.1 Materials 101
5.2.2 Solution preparation 102
5.2.3 Chitosan molecular weight determination 102
5.2.4 Preparation of uncoated and coated liposomes 103
5.2.5 Particle size distribution and mean size 103
5.2.6 ζ –Potential measurement 104
5.2.7 Optical microscopy 104
5.2.8 Spray drying 104
5.2.9 Moisture content 105
5.2.10 Water activity 105
5.2.11 Powder yield 105
5.2.12 Particle size distribution of reconstituted liposomes 105
5.2.13 Scanning electron microscopy (SEM) 105
5.3 Statistical Analysis 106
5.4 Results and Discussion 106
5.4.1 Influence of chitosan addition on the properties of liposomes 106
5.4.2 Effect of maltodextrin addition on the properties of uncoated and coated liposomes 112
5.4.2.1 Uncoated liposomes 112
5.4.2.2 Coated liposomes 116
5.4.3 Moisture content and water activity of spray dried liposomal powders 118
5.4.4 Powder morphology 121
5.4.5 Reconstitution of coated liposomes 125
5.5 Mechanistic insights 127
5.6 Conclusions 128
REFERENCES 131
CURRICULUM VITAE 145

ABBREVATIONS

AAPH	: 2,2′-azobis(2amidinopropane dihydro- chloride
AFM	: Atomic force microscopy
ANOVA	: Analysis of variance
DDA	: Degree of Deacylation
DE	: Dextrose Equivalent
DLS	: Dynamic light scattering
DPPH	: 1,1-Diphenyl-2- picrylhydrazyl) FRAP
DSC	: Differential scanning calorimetry
ET	: Electron transfer
HAT	: Hydrogen atom transfer
HMW-C	: High molecular weight chitosan
HMW-MD	: High molecular weight maltodextrin
kDa	: kilodalton
LBL	: Layer-by-layer depositioning method
LMW-C	: Low molecular weight chitosan
LMW-MD	: Low molecular weight maltodextrin
LSCM	: Laser scanning confocal microscopy
ORAC	: Oxygen radical absorbance capacity
PCS	: Photon correlation spectroscopy
RSM	: Response surface methodology
SEM	: Scanning electron microscopy
SPC	: Soybean phosphatidylcholine
TEM	: Transmission electron microscopy
TPTZ	: 2, 4,6-tripyridyl-s-triazine

LIST OF TABLES

Page

Table 2.1: Structure of main flavonoid groups. 8
Table 2.2: Comparison of thermodynamic stability and physicochemical properties of colloidal dispersions prepared from oil, water and emulsifier 15
Table 2.3: Examples of some common stabilizers that can be used in the food industry to formulate nanoemulsions..... 20
Table 2.4: Applications and corresponding HLB values 23
Table 2.5: Some factors related to emulsion stability. 41
Table 2.6: Comparison of steric and electrostatic stabilization mechanisms..... 42
Table 3.1: Uncoded and coded independent variables used in RSM design..... 65
Table 3.2: Experimental values of particle size and emulsion stability of QT nanoemulsions obtained from the central composite experimental design. 67
Table 3.3: Solubility of quercetin (mg/g) in limonene oil and medium chain triglyceride (MCT) and their combination with emulsifiers Tween 80 (T80) and Span 20 (S20). 68
Table 3.4: Analysis of variance of the regression coefficients of the fitted quadratic equations for the particle size, and stability (droplet growth ratio and quercetin stability) of nanoemulsions. 712
Table 3.5: Particle sizes of emulsions loaded with different amount quercetin 75
Table 4.1: Water dispersity of HPH treated quercetin nanosuspensions in different T80 (w/w) concentrations for cycle 0 and 30 at 25°C and 150 MPa pressure. 90
Table 5.1: Molecular characteristics of chitosan used in this study. 102
Table 5.2:. The particle size change of uncoated liposomal dispersions by the addition of low molecular weight maltodextrin (LMW-MD)..... 114
Table 5.3: ζ-Potential of uncoated and HMW-C and LMW-C (0.175 w/v%) coated liposomes (0.5 w/v%), droplets mixed with LMW-MD and HMW-MD (20 w/v%) prior to spray drying and reconstituted coated liposomes after spray drying. 116
Table 5.4: Particle diameter of HMW-C and LMW-C (0.175 w/v%) coated liposomes (0.5 w/v%), coated liposomes mixed with LMW-MD and HMW-MD (20 w/v%) prior to spray drying and reconstituted coated liposomes after spray drying (0.5 (w/v%) liposome; 0.175 (w/v%) chitosan; 20 (w/v%) maltodextrin). 118
Table 5.5: Yield, moisture content and water activity of chitosan coated liposome powders 119

LIST OF FIGURES

Page

Figure 2.1: Molecular structure of quercetin. 9
Figure 2.2: Antioxidant mechanism of action in HAT and ET..... 10
Figure 2.3: Depiction of (a) oil-in-water (O/W), (b) water-in-oil (W/O), (c) water-in-oil-in-water (W/O/W) emulsions and (d) oil-in-water-in-oil (O/W/O)..... 15
Figure 2.4: Emulsion formation. 19
Figure 2.5: Schematic representation of high-pressure valve homogenizers..... 25
Figure 2.6: Schematic representation of microfluidizers. 27
Figure 2.7: Schematic representation of ultrasonic probe homogenizer. 29
Figure 2.8: Schematic representation of proposed mechanism for spontaneous emulsification 30
Figure 2.9: Schematic diagram of the temperature-dependence of the spontaneous curvature of surfactant monolayers. 32
Figure 2.10: Schematic representation of the proposed mechanism for low- intensity emulsification by the catastrophic phase inversion (CPI) method 33
Figure 2.11: The schematic diagram of the nanosizing process using wet milling technology 388
Figure 2.12: Food emulsions may become unstable through a variety of physical mechanisms, including creaming, sedimentation, flocculation, coalescence, and phase inversion 43
Figure 2.13: Schematic for formation of a number of nanolayers around particles. 49
Figure 2.14: Effect of ionic strength on layer thickness and polymer orientation at the substrate surface; (A) at low ionic strength, and (B) at high ionic strength 50
Figure 2.15: The Stern and diffuse layer..... 57
Figure 3.1: Solubility of quercetin in different environments at room temperature (T80: Water (1:16, w/w); S20: MCT (1:2, w/w); S20: Limonene oil (1:2, w/w) and T80: Limonene oil (1:2 w/w))..... 67
Figure 3.2: Pseudoternary phase diagram and stability of limonene oil-emulsifier (S20:T80 (1:1, w/w)-water system homogenized by HSH. 69
Figure 3.3: Contour plots of the particle size (nm) of the nanoemulsions as a function of pressure and emulsifier concentration % (a) at the oil concentration of 10%, and as a function of pressure and oil concentration% (b) at the emulsifier concentration of 10%. 711
Figure 3.4: Contour plots of droplet growth ratio (a) and quercetin stability (b) of the nanoemulsions as a function of emulsifier and oil concentration % at the Pressure of 120 MPa. 73
Figure 3.5: Stability of the emulsion with different quercetin content; 10:10:80 (oil: emulsifier: water) on day 2. 76

Figure 4.1: Change in particle size and polydispersity of quercetin in water (left) and in 1% Tween 80 (w/w) solution (right) as a function of HPH cylces. HPH pressure and processing temperature were fixed at 150 MPa and 25°C, respectively. Duplicate samples were prepared and the results are reported as the mean and standard deviation of three measurements made per sample ..... 86.

Figure 4.2: Change in particle size and polydispersity of quercetin in water as a function of homogenization pressure. HPH cycle and processing temperature were fixed at 20 and 25°C, respectively. Duplicate samples were prepared and the results are reported as the mean and standard deviation of three measurements made per sample. 87

Figure 4.3: (A). AFM height image of HPH-treated quercetin nanosuspension deposited on a precleaned silicaon surface (B) SEM images of pure non-treated quercetin and (C) lyophilized HPH-treated quercetin nanosuspension. HPH was carried at 150 MPa for 20 cycles at 25°C. Pictures were taken at X3500 magnifications. 91

Figure 4.4: Water dispersity of quercetin nanosuspensions in water (A) and in 1% T80 (w/w) solution (B) as a function of cycle at 150 MPa and 25°C. Photographic pictures shows the quercetin nanosuspensions in water (left) and in 1% T80 (w/w) solution (right) for cycle 0 and 40 at 150 MPa and 25°C, insoluble part of quercetin was removed by ultracentrifugation. 92

Figure 4.5: Water dispersity of HPH treated quercetin nanosuspensions in water at different pressures for cycle 20 at 25°C, insoluble part of quercetin was removed by ultracentrifugation. 92

Figure 4.6: DSC thermograms of pure quercetin and lyophilized quercetin HPH-treated nanosuspensions prepared in water and in 1% T80(w/w). HPH was carried at 150 MPa for 20 cycles at 25°C. 93

Figure 4.7: Dissolution of HPH-treated quercetin powder as a function of the agitation time. Predried suspension prepared in water (A) and in 1% T80 (w/w) solution (B). HPH was carried at 150 MPa for 20 cycles at 25°C. 94

Figure 4.8: The scavenging activities (1), reducing abilities (2) and oxygen radical absorbing capacities (3) of spray dried quercetin suspension powders prepared in 1%T80 (w/w): (A) HPH treated samples (A') non-treated samples ; and prepared in water: (B) HPH treated samples (B') non-treated samples. 96

Figure 5.1: Change in ζ-potential and mean particle diameter after addition of 0 to 0.75, w/v % chitosan to liposomes (0.5, w/v%) for (A) HMW-C and (B) LMW-C. Photographic images of dispersions (chitosan concentration increasing from 0.001-0.75% from left to right) were taken after 2 weeks of storage at room temperature. 109

Figure 5.2: Microscopic images at x100 magnification, A: Liposome (1%) with initial size of ~0.4µm; B-G: After addition of high molecular weight chitosans, B: 0.01%, C: 0.05%, D: 0.1%, E: 0.25%, F: 0.5%, G: 0.75%; H and I : After addition of low molecular weight chitosans, H:0.5% and I: 0.75%. 110

Figure 5.3: Microscopic images (x100 magnification) of dispersions after addition of LMW-MD and HMW-MD to uncoated liposomes (0.5 w/v %). 1: uncoated liposomes; 2: addition of LMW-MD (20 w/v %), 3: addition of HMW-MD (20 w/v %). The scale bar denotes a length 10µm.... 113
Figure 5.4: Optical microscopic images (at x100 magnification) of uncoated liposomal dispersions containing at various maltodextrin molecular weights and concentrations. The region below the dotted line shows the concentrations where dispersions did not flocculate..... 115
Figure 5.5: Microscopic images (x100 magnification) of structures formed after addition of HMW-MD and LMW-MD (20 w/v %) to HMW-C (0.175 w/v %) (A series) and LMW-C (0.175 w/v %) (B series) coated liposomes (0.5 w/v %) and the change in the structure upon redispersion of spray dried powders. 1: coated liposomes; 2: after addition of LMW-MD; 3: reconstituted spray dried samples prepared with LMW-MD; 4: after addition of HMW-MD; 5: reconstituted spray dried samples prepared with HMW-MD..... 120
Figure 5 6: Volume based particle diameter distribution of uncoated liposomes (0.5 w/v %) before and after low and high molecular weight maltodextrin addition (20% w/v%)..... 121
Figure 5.7: Volume based particle diameter distribution of low and high molecular weight chitosan (0.175 v/w %) coated liposomes before and after low and high molecular weight maltodextrin (20 w/v %) addition and after reconstitution of spray dried samples 122
Figure 5.8: SEM images of coated liposomes (A: High molecular weight chitosan; B: Low molecular weight chitosan) spray dried in the presence of low molecular weight maltodextrin. Pictures were taken at X1000 and X4000 magnifications. 124
Figure 5.9: SEM images of coated liposomes (A: High molecular weight chitosan; B: Low molecular weight chitosan) spray dried in the presence of high molecular weight maltodextrin. Pictures were taken at x1000 and x4000 magnifications. 125
Figure 5.10: Mechanistic image of different events occurred when chitosan added to liposomes (A) and when maltodextrin added to uncoated and chitosan coated liposomes and when spray dried liposome powders reconstituted (B)..... 129

DESIGN OF NANOSIZED FOOD DELIVERY SYSTEMS FOR ANTIOXIDANTS BY USING NANOEMULSION, NANOSUSPENSION AND LAYER BY LAYER DEPOSITING OF LIPOSOMES

SUMMARY

Emulsion based delivery systems have been used in food industry to protect active ingredients against harsh conditions, to enhance their stability and bioavailibiliy, to mask bad odors and tastes. Due to their small droplet sizes, nanoemulsions provide high kinetic stability.

In the first part of the thesis, response surface methodology (RSM) was used to optimize the conditions for quercetin nanoemulsion preparations. The solubility of quercetin has been determined using two kinds of oils, namely limonene oil and medium chain triglyceride (MCT), and their combinations with emulsifiers (Tween 80 and Span 20). Among all systems highest solubility was observed in limonone oil and Tween 80 mixtures. Coarse emulsions prepared by only high speed homogenizer which represents the different points in the pseudoternary phase diagram. 24 hours later from preparation, the emulsions that stored at room conditions were visually evaluated and classified according to their stability. The stable coarse emulsion region found in pseudoternary phase diagram was further processed by high pressure homogenization (HPH) to produce the secondary nanoscale emulsions. The effect of independent variables of homogenization pressure (52–187 MPa), emulsifier (5-15%, w/w) and oil concentration (10-20%, w/w) on particle size, droplet growth ratio and quercetin stability in nanoemulsion formulations was studied by RSM. Quercetin loading was kept constant (0.25%, w/w) in all formualtions.

Experimental data could be adequately fitted into a second-order polynomial model with multiple regression coefficients of (R^2) of 0.9171 for the particle size. 0.8545 for droplet growth ratio by storage and 0.7795 for quercetin stability. The lineer and quadratic term of homogenization pressure and oil concentration and the interaction between pressure and oil concentration had a significant effect on the particle size of the nanoemulsions. Concurrently, the interaction between oil and emulsifier concentration had significant effect on the stability of quercetin in nanoemulsions. Optimum conditions to have the formulation with minimum particle size and highest stability were found as 13% emulsifier, 17% oil concentration and 70 MPa homogenization pressure.

This study also showed that, particle size of the droplets changed according to quercetin loading and oil to emulsifier ratio in the system. When the oil/emulsifier ratio was low, increasing the amount of quercetin exhibited an increase in particle size. However when there was high amount of oil in the system, quercetin loading did not affect the size. We suggested that this was the result of tendency of quercetin accumulation on the oil/water interface and in the oil droplets. When there was enough space as a result of having more oil in the system, quercetin may find more place to occupy without changing the particle size. In addition to that, regardless of

its initial particle size, the formulations loaded with less amount of quercetin were less stable than those loaded with higher amount of quercetin.

An alternative procedure to improve the dispersibility of a drug is the use of physical processing methods which increase the surface area and wettability of drug particles by means of particle size reduction or generation of amorphous states Among physical processing methods, HPH is a simple and highly recommended process with high efficiency, high reproducibility, needless of organic solvents and the ease of scaling up this process in industry.

In the second part of the thesis, HPH was used to increase the water dispersity of quercetin crystals which exhibits antioxidant, anti-inflammatory, anti-cancer properties but poor water solubility and oral bioavailability. Generally, the energy delivered into system is proportional to the pressure and higher the homogenization pressure, the smaller particle size obtained. Particle size got a steady value (~ 400 nm) after 10 cycles. The force required to break down the crystals seems to increase rather exponentially with decreasing particle size. Because HPH process breaks the particles/crystals preferentially at weaker points, i.e. imperfections and by decreasing the size, the number of imperfections is becoming less and remaining crystals are getting more perfect. The atomic force microscopy (AFM) images suggested that most particles were mainly irregular shaped and scanning electron microscopy (SEM) images showed that HPH-treated particles exhibited particle size uniformity and lack of larger needle type crystalline structures. Melting peak of HPH-treated quercetins shifted to lower temperature and lower entalpy of fusion values as an indication of a certain loss of crystallinity.Easily water redispersible powders were fabricated by using spray drying process. HPH-treated powders showed higher antioxidant activities than non-treated samples in terms of radical scavenging activity, reducing ability and oxygen radical absorbance capacity determinations through increased water dispersibility.

Liposomes have attracted considerable attention in the food and agricultural, biomedical industries in recent years because they are biocompatible, biodegradable, nontoxic, and have the ability to encapsulate both water and oil-soluble functional compounds such as antimicrobials, flavors, antioxidants. However maintaining the stability in aqueous dispersion represents a challenge for commercialization. Since much deterioration processes take place in an aqueous environment, one possible approach is to generate dry powders. Spray drying as less expensive, time and energy consuming process. However, liposomes had either completely collapsed or rearranged into multilamellar liposomes with membranes being composed of two or more bilayers after rehydration of powders followed by spray drying. Recently, a method referred to as the layer-by-layer (LBL) depositioning method has been utilized to increase the stability of liposomes. This method is based on the adsorption of different oppositely charged biopolymers such as proteins and carbohydrates on the liposomal interfaces. However, to date, little is known as to how these layers may be used to create better food structures that have superior performances in the dried state.

In the third part of the thesis, fine-disperse anionic lecithin liposomes were prepared by membrane filtration and coated with lower and higher molecular weight cationic chitosan using the layer-by-layer depositioning method. The surface charge on liposomes (0.5%, w/w) changed from negative to positive when chitosan was added to liposomal dispersions. For both high and low molecular weight chitosan, the surface charge of the initially anionic liposomes increased from -32 mV to ~+56 mV

with addition of chitosan (0-0.75 w/v %). The mean diameter of particles depended on the chitosan concentration added. The particle diameter of uncoated liposomes was ~0.4 μm and increased to around 50 μm after addition of low amounts of chitosan (0.0025 to 0.01, [w/v %]). Formation of aggregated structures could be observed under the microscope, and these were eventually followed by phase separation after a few hours. The mean diameter of aggregates that were formed at low chitosan concentrations decreased with increasing chitosan concentration above 0.025 (w/v %). The mean diameter was lowest (0.5 μm) at a chitosan concentration of ~0.4 (w/v %), where the ζ-potential had reached a constant value. There, microscopic images were void of any aggregated structures and no phase separation was visible. Further addition of chitosan to the system induced depletion flocculation, due to presence of free polyelectrolytes in the continuous phase.

Low and high molecular weight maltodextrins were added to facilitate spray drying of liposomes. Regardless of its molecular weight, addition of maltodextrin (20%, w/w) to uncoated liposomes immediately caused extensive flocculation and a complete breakdown of the system. The results led us to the conclusion that uncoated liposomes combined with high concentrations of maltodextrin may not be suitable for spay drying. In contrast to uncoated liposomes, the structure of chitosan-coated liposomal dispersions did not change after maltodextrin addition. This suggests that the presence of a "protective coat" of an adsorbed biopolymer decreased susceptibility against subsequent depletion flocculation caused by a second non-adsorbing polymer. The adsorption of chitosan to the liposomal surfaces increases the thickness of the interfacial layer and alters its charge. In consequence, there may be an increased steric and electrostatic repulsion between different liposomes which would reduce the extent of flocculation. A~100 nm decrease in diameter of coated liposomes was observed when they mixed with low molecular weight maltodextrin due to an osmotic driving force. In contrast upon the addition of high molecular weight maltodextrin, the dispersions still showed unimodal particle size distribution but increased in particle size. Since a high molecular weight chitosan layer on the particle surface can be expected to be thicker, liposomes coated with high molecular weight chitosan appear to be less susceptible to depletion interaction upon addition of maltodextrin. According to the SEM pictures, the powders had less dents, and a smoother surface when the molecular weight of the wall material (maltodextrin) was lower. The less-dented structure of particles dried with low molecular weight maltodextrin may be attributed to the lower glass transition temperature and difference in sugar composition. High DE maltodextrins typically consist of a greater amount of low molecular weight sugars which may act as a plasticizer preventing irregular shrinkage during drying.

Upon redispersion, all samples yielded back particle size distributions similar to the original liquid dispersion, except the low-molecular weight chitsan coated samples that had been spray dried with high molecular weight maltodextrin which yielded aggregated liposomes (~30 μm). The better protection provided by high molecular weight chitosan against spray drying stresses could be attributed to its molecular weight. Results suggest that an appropriate design of the liquid precursor system using both adsorbing and non-adsorbing polysaccharides is crucial to produce a spray-dried powder that yields much of the original liquid liposomal dispersion back upon redispersion.

ANTİOKSİDANLAR İÇİN NANOBOYUTTA GIDA TAŞINIM SİSTEMLERİNİN NANOEMULSİYON, NANOSÜSPANSİYON VE KAT-KAT KAPLANMA TEKNİĞİ İLE HAZIRLANAN LİPOZOMLARIN TASARIMI

ÖZET

Emülsiyon bazlı taşınım sistemleri gıda endüstrisinde aktif bileşenleri çevresel koşullardan korumak, dayanıklılığı ve biyoyararlılığını arttırmak, istenmeyen koku ve tatların maskelenmesi amacıyla kullanılmaktadır. Nanoemülsiyonlar düşük parçaçık boyutlarından dolayı oldukça yüksek kinetik dayanıklılık göstermektedir.

Tezin ilk kısmında yapılan çalışmada, yüzey yanıt yöntemi quercetin nanoemülsiyon hazırlanma koşullarının optimize edilmesi için kullanılmıştır. Quercetin'in limonen yağında, orta zincirli trigliseritte ve bu yağların emülgatör Tween 80 ve Span 20 ile karışımında çözünürlüğü belirlenmiştir. Quercetin'in en fazla çözündüğü sistem limonene yağı-Tween 80 karışımı olarak belirlenmiştir. Emülsiyon formülasyonunda limonen yağı kullanıldığında emülgatör olarak Tween 80-Span 20 (1:1) karışımının en düşük partikül boyutlu sistemleri ürettiği bilindiğinden çalışmada emülgatör olarak Tween 80-Span 20 karışımı kullanılmıştır. Üçlü faz diyagramındaki noktalara karşılık gelen birincil-ham emülsiyonlar sadece yüksek hızlı homojenizatör kullanılarak hazırlanmış, oda koşullarında 24 saat depolanmış ve formülasyonlar depolama sonunda gözlemsel kararla faz ayrımı olup olmamasına bağlı olarak dayanıklı/dayanıksız şeklinde ayrılmıştır. Dayanıklı birincil-ham emülsiyonlar daha sonra yüksek basınçlı homojenizatörler kullanılarak ikincil-nano emülsiyonlar üretilmiştir. Bağımsız değişkenlerden homojenizasyon basıncı (52–187 MPa), emülgatör (%5-15) ve yağ (%10-20) konsantrasyonunun partikül boyutu, partikül büyüme oranı ve formülasyondaki quercetin dayanıklılığı üzerine etkileri yüzey yanıt sistemi kullanılarak incelenmiştir. Formülasyonlara yüklenen quercetin miktarı (0.25%) sabit tutulmuştur. Deneysel veriler göstermiştir ki, partikül boyutu, partikül büyüme oranı ve formülasyondaki quercetin dayanıklılığına ait çoklu regresyon katsayıları (R2) sırasıyla 0.9171, 0.7795 ve 0.8545 olarak bulunmuş ve ikinci dereceden polinom modeli uygun kabul edilmiştir. Partikül boyutu üzerine homojenizasyon basıncı ve yağ konsantrasyonuna ait lineer ve quadratik terim ve basınç ve yağ konsantrasyonun interaksiyonuna ait terim istatistiksel açıdan önemli bulunmuştur. Bununla birlikte, emülsiyonların dayanıklılığı üzerine ise emülgatör ve yağ konsantrasyonun interaksiyonuna ait terim önemli olmuştur. Minimum partikül boyutu ve en yüksek dayanıklılığı sağlayan formülasyona ait optimum koşullar %13 emülgatör, %17 yağ içeriği ve 70 MPa homojenizasyon basıncı olarak belirlenmiştir. Bu çalışma aynı zamanda, partikül boyutunun yüklenen quercetin miktarına ve formülasyondaki yağ/emülgatör oranına bağlı olduğunu da göstermiştir. Yağ/emülgatör oranı düşük olan sistemlerde, yüklenen quercetin miktarının arttırılması partikül boyutunun da artmasına sebep olmuştur. Ancak, yüksek miktarda yağ içeren sistemlerde ise partikül boyutu yüklenen quercetin miktarına bağlı

olmamıştır. Bu durum, hidrofobik bir antioksidan olan quercetin'in yağ/su ara yüzeyinde ve yağ damlacığı içinde birikme eğiliminde olması ile açıklanabilir. Sistemde daha fazla yağ olması, daha fazla su/yağ ara yüzeyi ve dolayısıyla quercetin için birikebilecek daha fazla alan olması demektir. Bu durumda quersetin ara yüzeyin kalınlığını veya damlacığın boyutunu arttırmaksızın var olan alanlara birikebilir. Buna ilaveten, aynı formülasyon farklı miktarlarda quersetin ile yüklendiği zaman, başlangıç boyutundan bağımsız olarak daha az quercetin yüklenen sistem daha dayanıksız olmuştur.

Sudaki çözünürlüğü düşük olan biyoaktif maddelerin suda çözünürlüğününün arttırılmasında uygulanan alternatif yöntemlerden biri de fiziksel yöntemlerin kullanılması olabilir. Bu yöntemler partikül boyutunun küçülmesi ve daha amorf yapıların eldesi ıle yüzey alanını ve biyoaktif maddelerin ıslanabilirliğini arttırabilmektedir. Fiziksel proses yöntemleri arasında yüksek basınçlı homojenizatörler (HPH) verimliliğinin, tekrar edilebilirliğinin yüksek olması, organik çözelti kullanılmaması ve endüstriyel kullanıma uygun olmaları dolayısıyla oldukça rağbet görmektedirler.

Tezin ikinci kısmında yapılan çalışmada, HPH, antioksidan, antikanserojen ve antiinflamatuar özellik gösteren ancak suda çözünürlüğü ve biyoyararlılığı düşük quercetin kristallerinin sudaki dispersibilitelerini arttırmak için kullanılmıştır. Quercetin'in suda çözünürlüğünün bu yolla artması arkasındaki mekanizma nanoboyutta yapılar elde edilmesi ile açıklanabilir. Genelde sisteme verilen enerji homojenizasyon basıncı ile orantılıdır ve artan basınç ile daha düşük boyutta partiküller elde edilmiştir. Partikül boyutu 10 devir sonrasında sabit bir değere (~ 400 nm) ulaşmıştır. Kristal yapıyı parçalamak için gereken kuvvet azalan partikül boyutu ile eksponensiyel olarak artmaktadır. Çünkü HPH prosesi, kristalleri zayıf noktalarından parçalar ve boyut azaldıkça, kristaller daha mükemmel yapıya sahip olup zayıf nokta sayısı azalır ve partiküller ilave devirler uygulansa da daha küçük boyutlara indirilemezler. Atomik kuvvet mikroskopu (AFM) görüntüleri üretilen partiküllerin yapılarının düzgün olmadığı, Taramalı elektron mikroskopu (SEM) görüntüleri de HPH ile işlem görmemiş saf quercetin kristallerin partikül boyutunun uniform olmadığını buna karşılık HPH ile muamele edilmiş quercetin nanokristallerin ise partikül boyutunun çok daha uniform olduğu ve büyük iğnemsi yapıdaki kristal yapıların kaybolduğunu göstermiştir.

Quercetin'in sudaki dispersibilitesi azalan partikül boyutu ve beraberinde artan yüzey alanını ile artmaktadır. Yüksek basınç uygulaması quercetinin kristal yapısının amorf yapısına geçişini ve dolayısıyla çözünürlüğünü arttırmaktadır. HPH ile işlem görmemiş quercetin sudaki süspansiyonları neredeyse renksiz iken, HPH işlemi ile sarımsı renk elde edilmiş ve sistemdeki Tween 80 varlığı ile bu renk farkı daha belirgin olmuştur. HPH ile işlem görmüş örneklere ait termogramlarda erime noktasına ait pikin daha düşük sıcaklık değerlerine kayması ve daha düşük entalpi değeri göstermesi belli miktarda kristalliğin kaybolduğunu göstermektedir. Suda kolaylıkla çözülebilen maltodekstrinin taşıyıcı olarak kullanıldığı toz örnekler, püskürtmeli kurutucuda elde edilmiştir. HPH ile muamele edilmiş toz örnekler, HPH ile muamele edilmeyen toz örneklere göre radikal yakalama, indirgeme özelliği ve oksijen radikali absorbans kapasitesi açısından daha yüksek antioksidan aktivitesi göstermişlerdir. Çalışma sonrasında, HPH uygulaması ve püskürtmeli kurutucu kombinasyonunun suda kolaylıkla disperse olabilen ve çözünürlüğü artmış nano-formülasyonların geliştirilmesinde başarıyla kullanılabildiği gözlenmiştir.

Lipozomlar, yapı ve içerik açısından hücre zarına benzemelerinden dolayı biyouyumlu ve biyobozunur olup herhangi bir toksik özellik göstermezler. Gıda sanayinde uzun yıllardır çok çeşitli amaçlarla kullanılmakta olan soya veya yumurta lesitininin kullanılmasıyla elde edilebilen lipozom yapılar aynı zamanda hem yağda hem de suda çözünen fonksiyonel bileşiklerin enkapsülasyonunda, isteğe göre salınım gösterebilecek sistemlerin tasarlanmasında da kullanılabilir. Tüm bu özelliklerinden dolayı, son yıllarda biyomedikal, gıda ve tarım alanında kullanımları oldukça dikkat çekmektedir. Ancak lipozomlar sıvı formda genellikle uzun süre muhafaza edilmeye dayanıklı değildirler ve bu durum ticari olarak da kullanımlarını zorlaştırmaktadırlar. Lipozomlar, sıvı formda depolama boyunca küresel yapıların birleşmesi, bir araya gelerek kümeleşmesi ve enkapsüle olan maddenin zamanla yapıdan sızması gibi fiziksel bozulma proseslerine maruz kalabilirler. Lipozom yapıların dayanıklıklarını arttırmanın bir yolu da suyu uzaklaştırarak toz lipozom üretimi şeklinde olabilir. Bu amaçla kullanılabilecek püskürterek kurutma yöntemi dondurarak kurutma gibi diğer yöntemlere nazaran hem daha az enerji hem de daha az zaman harcadığından dolayı ticari anlamda ürün elde etmeye uygun bir alternatif olarak karşımıza çıkmaktadır. Ancak püskürtmeli kurutma sonrası elde edilen tozların tekrar rehidrasyonu sonrasında yapılar ya tamamıyla yıkılmışlar veya çok lamelli yapılar şeklinde tekrar oluşmuşlardır.

Son zamanlarda, emulsiyonlarda sıklıkla uygulanan tabaka tabaka kaplanma tekniği adı verilen yöntem, lipozomların dayanıklılığını da arttırmak için de kullanılmaktdır. Bu metod, proteinler ve karbonhidratlar gibi farklı yüklere sahip biyopolimerlerin lipozom yüzeylerine adsorbe olmasına dayanmaktadır. Ancak bu katmanların kuru fazda daha üstün özellik gösteren gıda yapılarının tasarımında kullanılması ile ilgili çok az bilgi mevcuttur.

Tezin üçüncü kısmında yapılan çalışmada, anyonik lipozomlar (~400 nm), yüksek hızda homojenizasyonu takiben membran filtrasyon yöntemi ile elde edilmiş sonrasında düşük ve yüksek molekül ağırlıklı katyonik polisakkarit kitosanlar kullanılarak kaplanmıştır. Kitosan miktarı (0-0.75 w/v %) arttıkça lipozomların yüzey yükü -32 mV'den +56 mV'a değişmiştir. Partikül boyutu da eklenen kitosan miktarına göre değişmektedir. Düşük miktarda kitosan ilavesi (0.0025 - 0.01, [w/v %]) sonucu partikül boyutu ~50 μm'ye ulaşmış ve bu aralıkta kümelenerek bir araya gelmiş, oluşan yapılar mikroskopta gözlenebilmiş ve devamında birkaç saat içinde faz ayrımı gözlenmiştir. Bu durum bridging flokülasyon mekanizması ile açıklanabilir. Ortamda yetersiz miktarda polimer olmasından dolayı aynı polimerler birden fazla lipozom yüzeyine bağlanmış ve onların bir araya gelip dayanıklılıklarını kaybetmeklerine ve yapının çökmesine sebep olmuştur. Bu kümelenmiş-agrege yapıların boyutları kitosan ilavesiyle [> 0.025 (w/v %)] azalmıştır. Kitosan konsantrasyonu % 0.4 (w/v %), olduğunda en düşük partikül boyutu (~500 nm) elde edilmiş ve bu konsantrasyonda yüzey yükü de sabit değere ulaşmıştır. Mikroskop görüntüleri de herhangi bir agrege yapı göstermemiştir.

Bu noktadan sonra sisteme daha fazla kitosan ilavesi ise su fazında serbest miktarda gereğinden fazla bulunan polimer (kitosan) varlığı dolayısıyla depletion flokülasyonuna sebep olmuştur. Mikroskop görüntüleri yüksek molekül ağırlıklı kitosan ile kaplanan lipozomlarda % 0.5 (w/v) kitosan konsantrasyonunda flokların varlığını gösterirken, düşük molekül ağırlıklı kitosan ile kaplanan lipozomlarda ise bu flokların varlığı kitosan konsantrasyonu % 0.75 (w/v) oluncaya kadar gözlenmemiştir. Bu durum depletion flokülasyonunun yüksek molekül ağırlıklı polimerlerin varlığında daha etkin olarak gözlenmesinden dolayı açıklanabilir.

Kitosan ile kaplanan ve kaplanmayan lipozomlar, püskürtmeli kurutma işleminde taşıyıcı matriks olarak sıklıkla kullanılan farklı molekül ağırlığında %20 (w/w) maltodextrin (düşük DE20, ve yüksek molekül ağırlıklı, DE2) çözeltileri ile karıştırılmıştır. Molekül ağırlığından bağımsız olarak kitosan ile kaplanmayan lipozomlar, maltodekstrin ile karışmaya müteakip "depletion" flokülasyon mekanizması sonucu maltodekstrinin molekül ağırlığı ve konsantrasyonuna da bağlı olarak stabilitelerini kaybetmiş, lipozomun istenen küresel yapısı bozulmuş ve sonucunda faz ayrımı gözlenmiştir. Bu durumda kitosanla kaplanmayan lipozomlar, daha kurutma öncesi istenen yapısal özelliklerini kaybetmiş ve püskürtmeli kurutucuda kullanılamaz hale gelmişlerdir.

Diğer yandan kitosanla kaplanan yapılar ise istenen yapıyı maltodekstrin ilavesine karşı koruyabilmiş ve püskürtmeli kurutucuda toz haline getirilebilmişlerdir. Kitosanın lipozom yüzeyine adsorpsiyonu sonucu ara yüzeyin kalınlığı artmış, yükü değişmiş ve sonuç olarak kitosan varlığı lipozom yapıların hem sterik hem de elektrostatik açıdan stabilitelerini arttırmış ve maltodeksrtin ilavesine karşılık sistemde meydana gelen "depletion" flokülasyonuna karşı sistemi korumuştur. Düşük molekül ağırlıklı maltodekstin ilavesi sonrası kaplanmış lipozomların boyutunda ~100 nm'lik azalma gözlenmiştir. Lipozomlar, merkezdeki suyun etrafı fosfolipit çiftkatmanlı membranlarca sarılan yapılardır ve bu yapılar tuz, şeker gibi düşük molekül ağılıklı çözeltilere daldırıldıkları zaman, su ozmotik etki sonucu konsantrasyon farkını azaltmak için lipozomun içindeki merkezden dış ortama doğru hareket eder ve bu durumda boyutta azalmaya sebep olabilir.

Yüksek molekül ağırlıklı maltodekstrin ilave edilen örneklerde ise hala unimodal partikül dağılımı gözlenmesine rağmen partikül boyutu artmıştır ve bu artış yüksek molekül ağırlıklı kitosan ile kaplanan lipozomlarda ~0.5 μm den 1 μm'e çıkarken, düşük molekül ağırlıklı kitosan ile kaplanan lipozomlarda ise 2 μm'e çıkmıştır. Yüksek molekül ağırlıklı kitosan tabakasının partikül yüzeyinde daha kalın bir tabaka oluşturması beklendiğinden, bu kitosanla kaplanan lipozomların da maltodekstrin ilavesinden kaynaklanan depletion interaksiyonuna karşı daha dayanıklı olması beklenebilir. SEM görüntüleri püskürtmeli kurutucu ile üretilen toz örneklerin morfolojisinin maltodekstrinin molekül ağırlığına bağlı olduğunu göstermektedir. Düşük molekül ağırlıklı maltodekstrin varlığında üretilen toz örneklere ait görüntülerde, daha az çökük ve daha düzgün, küresel yapılar gözlenmiştir. Bunun sebebi düşük molekül ağırlıklı maltodekstrinin kompozisyonundan dolayı sahip olduğu plastikleştirici etkiye ve yüksek camsı geçiş sıcaklığı ile açıklanabilir. Rehidrasyon sonrası agrege yapılar oluşturan (~30 μm) yüksek molekül ağırlıklı maltodekstrin varlığında kurutulan düşük molekül ağırlıklı kitosan ile kaplanan lipozomlar hariç tüm sistemler orjinal boyutlarına geri dönmüşlerdir. Bu sonuç, kitosan tabakasının kurutma sırasındaki stres faktörlerine karşı koruyuculuk özelliğinin de molekül ağırlığına bağlı olduğunu göstermektedir. Tüm bu sonuçlar göstermektedir ki, kurutulmuş fonksiyonel lipozom toz örneklerinin hazırlanabilmesi için kurutma öncesindeki sıvı fazın özel olarak tasarlanması gerekmektedir. Bu amaçla lipozom yapıyı koruyacak farklı özellikteki adsorbe olan polisakkaritlerin seçimi, optimum konsantrasyonlarının belirlenmesi ve ayrıca püskürtmeli kurutma sırasında taşıyıcı matriks olarak seçilecek adsorbe olmayan polisakkaritin de seçimi ve kullanım koşullarının belirlenmesi önem taşımaktadır.

1. INTRODUCTION

Flavonoids are a large group of plant polyphenolic compounds that are commonly distributed in the plant kingdom and largely found in the diet. Over 4000 different flavonoids have been described, although a much smaller number is important from a dietary point of view. The average intake of flavonoids was estimated as ranging from 1 to 25 mg/day. However, the latter value covers only five aglycons (myricetin, quercetin, kaempferol, apigenin, and luteolin) of which quercetin's 60% share makes this flavonoid one of the most commonly consumed (Piskula and Terao 1998).

Among flavonoids, quercetin (3,3′,4′,5,7-pentahydroxyflavone), the major representative of the flavonol subclass, accounts for the largest percent of flavonoid intake by diet. Particularly rich sources for quercetin are onions, apples, wine, berries and tea (Hollman and others 1997; Wach and others 2007). Quercetin has been exhibited the highest antiradical scavenging activity toward hydroxyl radical, peroxyl, and superoxide anion compared with other flavonoids (Casagrande and others 2006). Recently, there have been studies reported that quercetin can inhibit the proliferation of multiple cancer cell types, including lung cancer cells, colon cancer cells, prostate carcinoma cells, and pancreatic tumor cells, and promote cells apoptosis at micromolar concentrations (Li and others 2009). The flavonoid quercetin possesses anti-inflammatory, anti-proliferative and gene expression changing capacity in vitro. Its antioxidative and anti-inflammatory effects have been shown in vivo as well (Boots and others 2008).

Administration of active phytochemical components, nutraceuticals, into the human body requires the use of an appropriate vehicle for bringing an effective amount of the active component intact to the desired site in the body. The desired site varies and it may be the blood stream, organs, and cells, and so on (Huang and others 2010). It is known that the delivery of these phytochemicals is significantly influenced by their physicochemical properties, such as water solubility, partition coefficient, lipophilicity, and crystallinity, and so on (Huang and others 2010). Most nutraceutical ingredients are poorly water soluble and a limiting factor to the in vivo

performance of poorly water soluble neutraceticals after oral administration is their inadequate ability to be wetted by and dissolved into the fluid in the gastrointestinal (GI) tract. For example, quercetin's low solubility in water (0.17-7.7 µg/ml), artificial gastric juice (5.5 µg/ml), and artificial intestinal juice (28.9 µg/ml) has limited its absorption upon oral administration (Gao and others 2009), and after being received quercetin aglycone orally, only in a relatively few studies it can be detected in plasma and urine. From the urinary excretion data, it cannot be concluded that <3% of quercetin is bioavailable (Erlund 2004).

Therefore, the enhancement of oral bioavailability of poorly soluble drugs as well as functional food and nutraceutical ingredients remains one of the most challenging aspects of nutraceutical development.

Nutraceutical dispersions can be formulated either as emulsions or suspensions (Jayant 2011). Oil-in-water emulsions are used as delivery systems in many industries, including pharmaceuticals, petrochemicals, health care products, cosmetics, agrochemicals, and foods (McClements and others 2009). Drug penetration was reported to be strongly enhanced by solubilisation in small droplets (below 0.2µm).

Nano-emulsions can be prepared by reasonable surfactant concentrations (less than 10%), and posses very small size and high kinetic stability. For food applications, the delivery vehicle must be prepared from food-grade ingredients and this requirement limits the number of surfactants that can be used and the presence of cosurfactants (short- or medium chain alcohols) is generally considered undesirable because of potential toxicity issues (Flanagan and others 2006). Therefore, one has to balance the benefits brought by the use of bioactives and potential side effects (that is, obesity, cardiovascular diseases, and so on) caused by the use of high amount of lipids (Huang and others 2010).

An another alternative procedure to improve the solubility of a drug is the use of physical processing methods which increase the surface area and wettability of drug particles by means of particle size reduction or generation of amorphous states of drugs. The rate of dissolution is proportional to the surface area.

Owing to the increased surface to volume ratio of the nanocrystals, an increase in saturated solubility and very fast dissolution rate can be seen, especially for the particles those sizes lower than 1µm (Müller and Peters 1998).

Liposome dispersions have also attracted considerable attention in the biomedical, food and agricultural industries in recent years because they are biocompatible, biodegradable, nontoxic, and have the ability to act as targeted release-on-demand carrier systems for both water and oil-soluble functional compounds such as antimicrobials, flavors, antioxidants and bioactive compounds (Keller 2001; Taylor and others 2005; Mozafari and others 2008b; Malheiros and others 2010; Gibis and others 2012).

However, liposomes are generally unstable when suspended in aqueous systems for prolonged periods. They can undergo physical degradation processes, including vesicle fusion, aggregation, and leakage of entrapped material over time. Since much deterioration processes take place in an aqueous environment, one possible approach may be the removal of the water to generate dry powders. Spray drying is a less expensive, time- and energy consuming process. However, there are much fewer studies available that report the results of spray drying of liposomes (Lo and others 2004; Goldbach and others 1993a; Goldbach and others 1993b; Wessman and others 2010). When aqueous dispersions of liposomes were dehydrated in the absence of additives, the result would be the fusion of liposomes, formation of aggregates and leakage of encapsulated materials on rehydration. Therefore, several excipients have been identified and are commonly applied as stabilizers in dry liposomal formulations. Monosaccharides and more frequently disaccharides are utilized as stabilizing excipients during drying (Koster and others 2000; Koster and others 2003).

Recently, a method referred to as the layer-by-layer (LBL) depositioning method has been utilized to increase the stability of liposomes (Quemeneur and others 2007; Laye and others 2008; Chuah and others 2009; Mady and Darwish 2010; Quemeneur and others 2010; Gibis and others 2012). This method is based on the adsorption of different oppositely charged biopolymers such as proteins and carbohydrates on the liposomal interfaces.

This approach has been proven to provide better thermal as well as environmental (pH and ionic strength) stability in liposomes and emulsions (Ogawa and others 2003; Guzey and McClements 2007; Shaw and others 2007; Chun and others 2013; Klinkesorn and McClements 2009). However, to date, little is known as to how these layers may be used to create better food structures that have superior performances in the dried state.

1.1 Purpose of Thesis

Different factors including process conditions and emulsion composition influence the physicochemical properties of the nanoemulsions. Response-surface methodology (RSM) is an effective technique for exploring the relationships between the responses and the independent variables, and optimizing the process conditions or product formulation. In the *first part* of this research, we *aim* to prepare quercetin loaded nanoemulsion with food grade ingredient by using high pressure homogenization, and to optimize the pressure, emulsifier and oil concentration with the smallest particle size and greatest stability by applying RSM.

The *objective* of the *second part* of this study is to utilize HPH for formulating quercetin nanosuspension as a significant potential to enhance its water solubility/dispersity. Among physical processing methods to produce nanosuspensions, high pressure homogenization (HPH) is a simple and highly recommended process with high efficiency, reproducibility, needless of organic solvents and the ease of scaling up this process in industry. The effect of pressure and the number of processing cycles on particle size and solubility/dispersity have been studied to achieve the optimized processing conditions. Quercetin powders prepared by a combination of HPH and the spray drying proven to be able to produce quercetin nanosuspensions with a higher dispersity and fast dissolution rate and provide higher antioxidant activities.

In the *third part* of this research, we *hypothese* that spray dried liposome powders that may yield much of the the original liposomal dispersion back upon rehydration can be produced by utilizing LBL method. Therefore the *objective* of the study is thus to test this hypothesis by using both adsorbing and non-adsorbing polymers in combination with liposomes followed by spray drying.

Followed by a brief literature review on nanodelivery systems specifically nanoemulsion, nanosuspension and nanoliposomes, this research thesis is composed of three individual chapters. In those chapters the research is carried on the optimization conditions of quercetin nanoemulsions by using RSM; preparetion of quercetin nanosuspension by high pressure homogeniztion; and production of spray dried liposomes by utilizing layer by layer depositioning technique, respectively. Each chapter has its own material and methods results and discussion and conclusion sections.

2. LITERATURE

2.1 Antioxidants

In food science, the antioxidant is defined as a substance in foods significantly decreases or prevents the adverse effects of reactive species, such as reactive oxygen and nitrogen species (ROS/RNS), on normal physiological function in humans when present at low concentrations compared to those of an oxidizable substrate (Karadag and others 2009).

Flavonoids are polyphenolic compounds that occur ubiquitously in foods of plant origin. Over 4000 different flavonoids have been described, although a much smaller number is important from a dietary point of view. Due to their low redox potentials ($0.2 < E_0 < 0.8$), increased electron donationg properties, flavonoids are thermodynamically able to reduce most oxidizing free radicals relevant to biological systems such as superoxide, peroxyl, alkoxyl, and hydroxyl radicals (Han and others 2012; Wanasundara and Shahidi 2005).

Flavonoids consist of 2 aromatic benzen rings (A and B), which are connected by an oxygen-containing heterocyclic pyrene ring (C) (Table 2.1). The variation in the C ring forms the basis of the division in various subclasess. In general, the antioxidant activity of flavonoids depends on the structure and substitution pattern of their hydroxyl groups. Three structural requirements seems important: (i) the ortho-dihydroxy (catechol) structure in the B-ring, possessing electron donating properties, increasing the stability of oxidized flavonoid radicals through H-bonding or electron delocalization; (ii) the C2-C3 double bond conjugated with a 4 keto group, enhancing electrontransfer and radical scavenging through electron-delocalization from B group; (iii) the presence of both 3- and 5-OH groups, enabling the formation of stable quinonic structures upon flavonoid oxidation.

Table 2. 1: Structure of main flavonoid groups.

Group	Structural Formula	Examples
Flavone	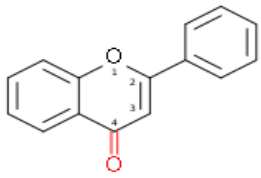	Luteolin, Apigenin, Tangeritin
Flavonol	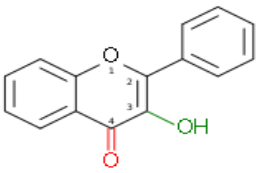	Quercetin, Kaempferol, Myricetin
Flav**an**one	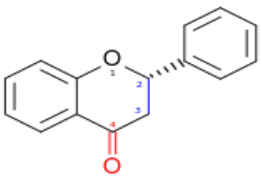	Hesperetin, Naringenin
Flav**an**onol	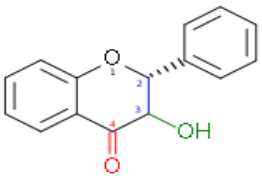	Dihydrokaampferol

Aside from these structural requirements, the number and position of hydroxyl substituents on the flavonoid molecule, the presence of glycosides, and the overall degree of conjugation are important in determining their activities (Han and others 2012).

A typical flavonoid which meets the above three criteria is quercetin (3, 3′, 4′, 5, 7-pentahydroxyflavone)(Figure 2.1), showing the highest antioxidant capacity in the flavonol group. Quercetin, the major representative of the flavonol subclass is a common dietary component. Particularly rich sources for quercetin are onions, apples, wine, berries and tea (Hollman and others 1997; Wach and others 2007a; Wach and others 2007b).

In addition to being an excellent antioxidant, quercetin also possesses anti-inflammatory, anti-proliferative and gene expression changing capacities *in vitro*. Within the flavonoid family, quercetin is the most potent radical scavenger of ROS, icluding $O_2^{\cdot}$, and RNS like $NO^{\cdot}$ and $ONOO^{\cdot}$ (Boots and others 2008b).

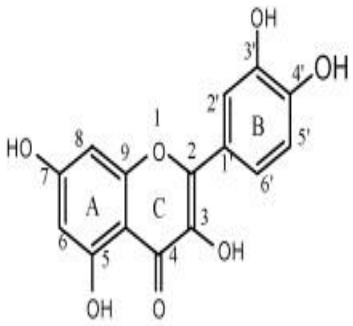

Figure 2. 1: Molecular structure of quercetin.

The average intake of flavonoids was estimated as ranging from 1 g/day to 25 mg/day. However, the latter value covers only five aglycons (myricetin, quercetin, kaempferol, apigenin, and luteolin) of which quercetin's 60% share makes this flavonoid one of the most commonly consumed (Piskula and Terao 1998).

Free radical scavenging activity by flavonoids is highly dependent on the presence of a free 3-OH. Free radical scavenging capacity is primarily attributed to the high reactivities of hydroxyl substituents that participate in the following hydrogen atom ttansfer reaction (HAT):

$$F\text{-}OH + R^{\cdot} \longrightarrow RH + F\text{-}O^{\cdot}$$

This reaction gives the flavonoid phenoxyl radicals ($F\text{-}O^{\cdot}$) and a stable molecule (RH). The formed flavonoid radical is stabilized by resonance. The non-paired electron can be delocalized on the whole of the aromatic cycle. But, it can continue to evolve according to several processes (dimerisation, dismutation, recombination with other radicals, oxidation in quinon) either while reacting with radicals or other antioxidants, or with biomolecules. Thus, flavonoid phenoxyl radicals exhibit a much lower reactivity compared to $R^{\cdot}$. The $F\text{-}O^{\cdot}$ radical can react with another radical to form stable quinones (Seyoum and others 2006).

Hydroxyl groups on the B-ring donate hydrogen and an electron to hydroxyl, peroxyl, and peroxynitrite radicals, stabilizing them and giving rise to a relatively stable flavonoid radical. Among structurally homologous flavones and flavanones,

peroxyl and hydroxyl scavenging increases linearly and curvilinearly, respectively, according to the total number of OH groups, particularly of the B-ring.The superiority of quercetin in inhibiting both metal and nonmetal-induced oxidative damage is partially ascribed to its free 3-OH substituent which is thought to increase the stability of the flavonoid radical and 3′,4′-catechol arrangement. Compared to the flavonols quercetin, myricetin, and kaempferol, the flavone luteolin is a very weak scavenger of DPPH (2,2-diphenyl-1-picrylhydrazyl radical) and substitution of 3-OH by a methyl or glycosyl group completely abolishes the activity of quercetin and kaempferol against-βcarotene oxidation in linoleic acid (Heim and others 2002).

2.1.1 Antioxidant capacity determination methods

The features of any antioxidant capacity method are an oxidation initiator, a suitable substrate, and an appropriate measure of the end point. Initiators may include increased temperature (Laguerre and others 2007) and partial pressure of oxygen, addition of transition metal catalysts (Ou and others 2002), exposure to light to promote photosensitized oxidation by singlet oxygen (Choe and Min 2006).

Generally, there are two possibilities for phenolic antioxidants reacting with free radicals ($R^{\cdot}$): (i) one-step hydrogen atom transfer (HAT), or (ii) electron transfer followed by proton transfer (ET) (Figure 2.2)

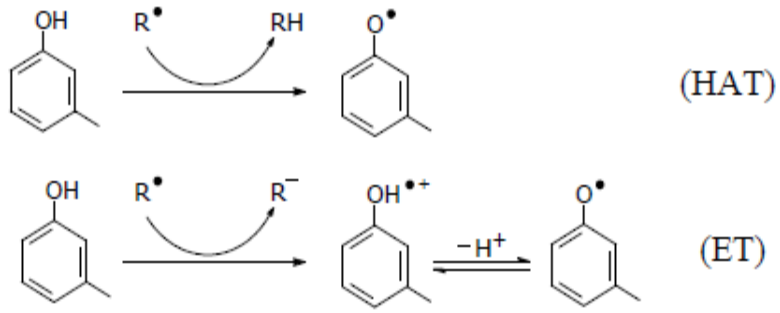

Figure 2. 2: Antioxidant mechanism of action in HAT and ET.

HAT-based methods measure the classical ability of an antioxidant to scavenge free radicals by hydrogen donation to form stable compounds (Prior and others 2005). HAT-based methods are more relevant to the radical chain-breaking antioxidant capacity. HAT reactions are solvent and pH dependent and are generally quite rapid, typically completed in seconds to minutes. HAT-based methods are generally

composed of a synthetic free radical generator AAPH (2,2′-azobis (2amidinopropane dihydro- chloride), ABAP (2,2'-azobis-(2-amidinopropane) hydrochloride), ABTS (2,2′-azinobis(3-ethylbenzothiazolline-6-sulfonic acid (Valkonen and Kuusi 1997; Wolfe and Liu 2007), an oxidizable molecular probe (dichlorofluorescein (DCFH) (Adom and Liu 2005), fluorescein (FL)(Moore and others 2006), and an antioxidant.

ET-based methods detect the ability of a potential antioxidant to transfer one electron to reduce any compound, including metals, carbonyls, and radicals;

$$M(III) + F\text{-}OH \longrightarrow F\text{-}OH^{\cdot} + M(II)$$

ET reactions can be relatively slow and need long times to reach completion. They traditionally measure relative percent decrease in product rather than kinetics or total antioxidant capacity. Compared to HAT, the ET mechanism is strongly solvent dependent due to solvent stabilization of the charged species (Ou and others 2002). ET-based methods involve two components in the reaction mixture, antioxidants and oxidant (probe). The probe itself is an oxidant and abstracts an electron from the antioxidant, resulting in color changes of the probe. The degree of the color change is proportional to the antioxidant concentration. The reaction is reached to end point when color change stops.

Since quercetin sacrificially scavenge ROS/RNS to stop radical chain reactions, it is considered as primary chain-breaking antioxidants and free radical scavengers (FRS) (Boots and others 2007). We conducted three antioxidant capacity determination assays to evaluate the scavenging activity and reduction potential of samples, namely DPPH (1,1-Diphenyl-2- picrylhydrazyl) radical scavenging capacity assay, FRAP (Ferric reducing antioxidant potential) assay and ORAC (Oxygen radical absorbance capacity) assay. These methods are simple, inexpensive, and widespread in use and representing HAT and ET based methods.

2.1.1.1 DPPH (1,1-Diphenyl-2- picrylhydrazyl) radical scavenging capacity assay

The DPPH radical is long-lived organic nitrogen radical and has a deep purple color. It is commercially available and does not have to be generated before assay. In this assay, the purple chromogen radical is reduced by antioxidant/reducing compounds to the corresponding pale yellow hydrazine. The reducing ability of antioxidants

towards DPPH radical can be monitored by the absorbance decrease at 515–528 nm until the absorbance remains stable in organic media (Brand-Williams and others 1995). Although widely used for measuring and comparing the antioxidant status of phenolic compounds and foodstuffs, there are some drawbacks which limit its application. DPPH can only be dissolved in organic media (especially in alcoholic media), not in aqueous media, which is an important limitation when interpreting the role of hydrophilic antioxidants (Arnao 2000).

2.1.1.2 FRAP (Ferric reducing antioxidant potential) assay

It is based on the ability of phenolics to reduce yellow ferric tripyridyltriazine complex to blue ferrous complex by the action of electron-donating antioxidants (Benzie and others 1999). The resulting blue color measured spectrophotometrically at 593 nm is taken as linearly related to the total reducing capacity of electron-donating antioxidants. FRAP assay is carried out in acidic (nonphysiologically low pH value=3.6) conditions to maintain the iron solubility. One FRAP unit is defined as the reduction of 1 mol of Fe (III) to Fe(II) (Huang and others 2005)

2.1.1.3 ORAC (Oxygen radical absorbance capacity) assay

ORAC measures antioxidant inhibition of peroxyl-radical- induced oxidations and reflects classical radical chain- breaking antioxidant activity by H-atom transfer (Ou and others 2001). In the basic assay, the peroxyl radicals generated from thermal decomposition of AAPH (2,2′-azobis(2amidinopropane dihydro- chloride) radical in aqueous buffer (Cao and others 1997) react with a fluorescent probe, an oxidizable protein substrate, to form a nonfluorescent product.

In general, samples, controls, and standard (Trolox of four or five different concentrations for structuring the standard curve) are mixed with fluorescein solution and incubated at constant temperature (37 °C) before AAPH solution is added to initiate the reaction (MacDonald-Wicks and others 2006). In air-saturated solution, the generated AAPH radical reacts with O_2 rapidly to give a more stable peroxyl radical $ROO^{\cdot}$. The loss of fluorescence of the probe is an indication of the extent of damage from its reaction with the peroxyl radical. The fluorescence intensity [485 nm (ex)/525 nm (em)] is measured every minute for a spesific time duration at ambient conditions (pH 7.4, 37 °C). In the presence of antioxidant, the fluorescence decay is prevented (Ou and others 2002). As originally designed, the

ORAC assay is limited to measurement of hydrophilic chain-breaking antioxidant capacity.

To solve these disadvantages, methylated β-cyclodextrin is used as a solubility enhancer for lipophilic components, which allows for the measurement of the antioxidant capacity of both hydrophilic and lipophilic components in a given sample separately using the same radical source (Huang and others 2002a)

2.2 Delivery Systems

Administration of active phytochemical components, nutraceuticals, into the human body requires the use of an appropriate vehicle for bringing an effective amount of the active component intact to the desired site in the body. The desired site varies and it may be the blood stream, organs, and cells, and so on (Huang and others 2010). The enhancement of oral bioavailability of poorly soluble drugs as well as functional food and nutraceutical ingredients remains one of the most challenging aspects of nutraceutical development. For example, after being received quercetin aglycone orally, only in a relatively few studies it can be detected in plasma and urine. From the urinary excretion data, it cannot be concluded that <3% of quercetin is bioavailable (Erlund 2004).

Majority of phytochemicals, such as polyphenols and carotenoids, are either poorly soluble or lipophilic compounds. It is known that the delivery of these phytochemicals is significantly influenced by their physicochemical properties, such as water solubility, partition coefficient, lipophilicity, and crystallinity, and so on (Huang and others 2010). Most nutraceutical ingredients are poorly water soluble and a limiting factor to the in vivo performance of poorly water soluble neutraceticals after oral administration is their inadequate ability to be wetted by and dissolved into the fluid in the gastrointestinal (GI) tract. Therefore, the use of those nutraceutical ingredients in food formulations and has been a challenging problem confronted by food scientists.

Nutraceutical dispersions can be formulated either as emulsions or suspensions (Jayant 2011) that will be explained in the following sections. Oil-in-water emulsions are used as delivery systems in many industries, including pharmaceuticals, petrochemicals, health care products, cosmetics, agrochemicals,

and foods (McClements and others 2009). Drug penetration was reported to be strongly enhanced by solubilisation in small droplets (below 0.2μm). In this context, it has also been reported that when using oil-in-water emulsions as vehicles, the pharmacological activity is correlated to emulsion droplet size. Oil-in- water nano-emulsions can be administered orally to increase the bioavailability of poorly water-soluble drugs due to an enhancement of the intestinal absorption of the drug. It has been also found that the absorption in the gastrointestinal tract is improved by a small droplet size (Sadurní and others 2005).

2.2.1 Nanoemulsions

A simple emulsion consists of two immiscible liquids, typically oil and water, where one is dispersed as small spherical droplets within the other. The liquid that forms the droplets is known as the dispersed or internal phase and the liquid that surrounds the droplets is called the continuous or external phase (Karlene and Derick 2006). It is convenient to classify emulsions according to the relative organization of the oil and aqueous phases (Figure 2.3). When the oil droplets dispersed in an aqueous phase, it is called an O/W emulsion (e.g., milk, cream and mayonnaise) whereas water droplets dispersed in an oil phase, it is called a W/O emulsion (e.g., margarine, butter and spreads) (McClements and others 2009; McClements and others 2007). It is also possible to prepare multiple emulsions that consist of oil droplets contained in larger water droplets, which are themselves dispersed in an oil phase (O/W/O), or vice versa (W/O/W). In general, multiple emulsions are more difficult to prepare and control than simple emulsions, they are quite unstable, and rapidly separate into o/w or w/o emulsions (Malmsten 2002), they can be used for protecting certain ingredients, for controlling the release of ingredients, or for creating low-fat products (McClements and Weiss 2005).A number of different terms are commonly used to describe different kinds of emulsions depending on droplet size, and it is important to clarify what these terms mean **(**Table 2.2**)** (McClements 2011). Conventional emulsions tend to be optically turbid or opaque because the droplets have similar dimensions to the wavelength of light ($r \approx \lambda$) and thus, they scatter light strongly provided that the refractive index contrast between the droplets and surrounding liquid is not close to zero and the droplet concentration is not too low.

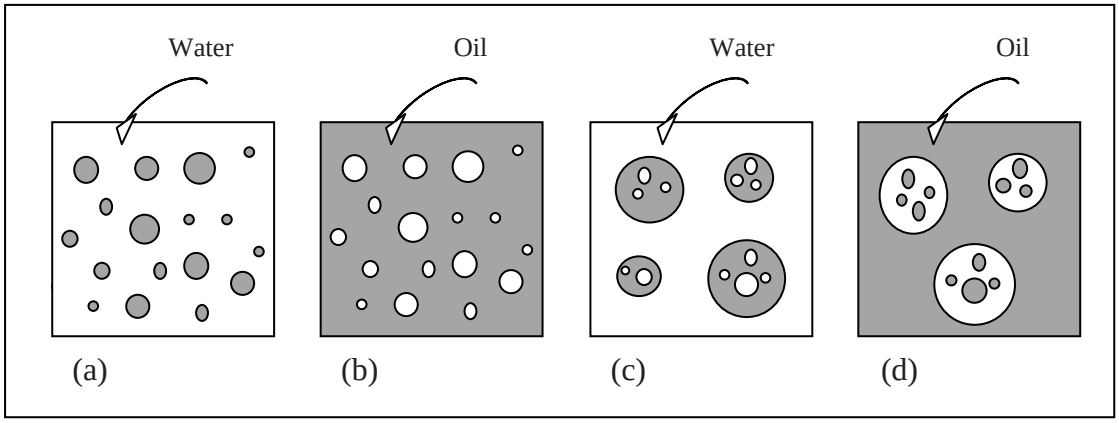

Figure 2. 3: Depiction of (a) oil-in-water (O/W), (b) water-in-oil (W/O), (c) water-in-oil-in-water (W/O/W) emulsions and (d) oil-in-water-in-oil (O/W/O) (McClements 2011).

Nanoemulsions, that can be considered to be a type of conventional emulsion, are a class of extremely small droplet emulsions in the nanometric scale typically in the range 50–200 nm of diameter but much smaller than the range (from 1 to 100 μm) for conventional emulsions (Solans and others 2005). Evidently the size range may vary depending on the authors. Some authors consider 500 nm as the upper limit (Gutiérrez and others 2008; Jafari and others 2008).

Table 2. 2: Comparison of thermodynamic stability and physicochemical properties of colloidal dispersions prepared from oil, water and emulsifier (McClements and Rao 2011; McClements 2011; Jafari and others 2008).

Property	*Macroemulsion*	*Nanoemulsion*	*Microemulsion*
Appearance	Milky/opaque	Transparent to milky	Transparent
Radius range	100nm -100μm	10-100 nm	2 - 50 nm
Surface to mass ratio m^2g^{-1}	0.07-70	70-330	130-1300
Thermodynamic stability	Unstable	Unstable; kinetically stable	Stable
Surfactant load	Fairly low	Medium (~<10%)	Fairly high (>20%)

Nanoemulsions appear to be transparent or sligtly turbid (similar to microemulsions) due to their relatively small droplet size compared to the wavelength of light ($r << \lambda$) so that they only scatter light waves weakly (McClements 2011; McClements and Rao 2011).Unlike microemulsions (which are also transparent or translucent and thermodynamically stable) nano-emulsions are only kinetically stable, the long-term physical stability of nano-emulsions (with no apparent flocculation or coalescence) make them unique and they are sometimes referred to as 'Approaching Thermodynamic Stability' (Tadros and others 2004).

Conventional emulsions are often prone to gravitational separation and droplet aggregation because of the relatively large size of the droplets. On the other hand, nanoemulsions are usually highly stable to gravitational separation because the relatively small droplet size means that the Brownian motion (the random movement of particles in a liquid due to the bombardment by the molecules that surround them) is larger than the small creaming rate induced by gravity.

In addition, nanoemulsions tend to have better stability against droplet aggregation than conventional emulsions because the strength of the net attractive forces acting between droplets usually decreases with decreasing droplet size, whereas the strength of the repulsive steric forces is less dependent on size. However, these systems will tend to breakdown by time due to a variety of physicochemical mechanisms, including gravitational separation, flocculation, coalescence, and/or Ostwald ripening (Huang and others 2010).

2.2.1.1 Nanoemulsion Composition

Before separate oil and aqueous phases are converted to an emulsion, it is usually necessary to disperse the various ingredients into the phase in which they are most soluble. Oil-soluble ingredients, such as certain vitamins, coloring agents, antioxidants, and surfactants, are mixed with the oil, whereas water-soluble ingredients, such as proteins, polysaccharides, sugars, salts, and some vitamins, coloring agents, antioxidants, and surfactants, are mixed with the water (McClements 2008; McClements 2012b).

Parameters whose influence on nano-emulsion characteristics can be studied may be classified as composition or preparation variables. For emulsification by low-energy methods composition variables will have a much higher influence than preparation variables, however for shear emulsification, the influence of preparation variables will be determinant (Gutiérrez and others 2008).

Oil Phase:

The oil phase used to prepare nanoemulsions can be formulated from various non-polar components, including tri-, di- and monoacylglycerols, free fatty acids, flavor oils, essential oils, mineral oils, fat substitutes, waxes, oil-soluble vitamins, and various lipophilic nutraceuticals (such as carotenoids, curcumin, phytosterols, phytostanols, and Co-enzyme Q). The formation, stability, and properties of nanoemulsions often depend on the bulk physicochemical characteristics of the oil phase, e.g., polarity, water-solubility, interfacial tension, refractive index, viscosity, density, phase behavior, and chemical stability. For example, the creaming stability of emulsions depends on the density contrast between the oil and aqueous phases; or the interfacial tension of an oil–water interface may also influence the size of the droplets produced during homogenization, since droplet disruption usually becomes easier as the interfacial tension decreases; oil polarity may also influence the partitioning of functional constituents (such as flavors, antioxidants, preservatives, or colors) between the oil and aqueous phases, which may alter the physicochemical or sensory properties of the system; the usage of oils of different refractive index or color may lead to differences in emulsion turbidity. In the food industry, it is often desirable to prepare nanoemulsions using triacylglycerol oils due to their low cost, abundance, and functional or nutritional attributes, e.g., corn, soybean, sunflower, safflower, olive, flaxseed, algae, or fish oils (McClements and Rao 2011; McClements 2005c).

Aqueous Phase:

Careful control of the aqueous phase composition can be used to optimize the formation or improve the stability of nanoemulsions.The aqueous phase may also contain a variety of components, including co-solvents (such as simple alcohols and polyols), carbohydrates, proteins, minerals, acids, and bases. Some methods of forming nanoemulsions using low-energy methods require the presence of cosurfactants (such as short- and medium-chain alcohols) or cosolvents (such as

polyols like propylene glycol, glycerol, and sorbitol). Cosolvents are highly polar molecules that are not particularly surface active themselves, but that may alter the physicochemical properties of the emulsifier molecules, such as their surface-activity, oil-water partition coefficient, and the ability to form colloidal structures (McClements and Rao 2011; McClements 2011).

Stabilizers:

The summary of the examples of some common stabilizers that can be used in the food industry to formulate nanoemulsions is given in Table 2.3. A conventional emulsion is thermodynamically unstable and always has a tendency to breakdown over time. Oil and water do not coexist comfortably because of the surface energy (Gibbs free energy) of the oil–water interface; the free energy of the separated oil and water phases is lower than that of the emulsion itself and the sysyem will always revert to this lowest energy configuration at thermodynamic equilibrium. Because of the interfacial tension (σ) between oil and water, any emulsion will seek to minimize the interfacial energy by making the interfacial area between oil and water as small as possible. Thus emulsions tend to reduce the surface area between the two immiscible liquids and when it is left to stand for long enough it will revert to a state in which the oil and water phases are completely separated (McClements 2008; Douglas 2003). In order to make a long-lived emulsion which is kinetically stable for a reasonable period of time, it is necessary to add a ‘surfactant’ or ‘emulsifier’ before homogenization (Figure 2.4).

Surface-active compounds operate through a hydrophilic head group that is attracted to the aqueous phase, and an often-larger lipophilic tail that prefers to be in the oil phase (Hasenhuettl 2008).

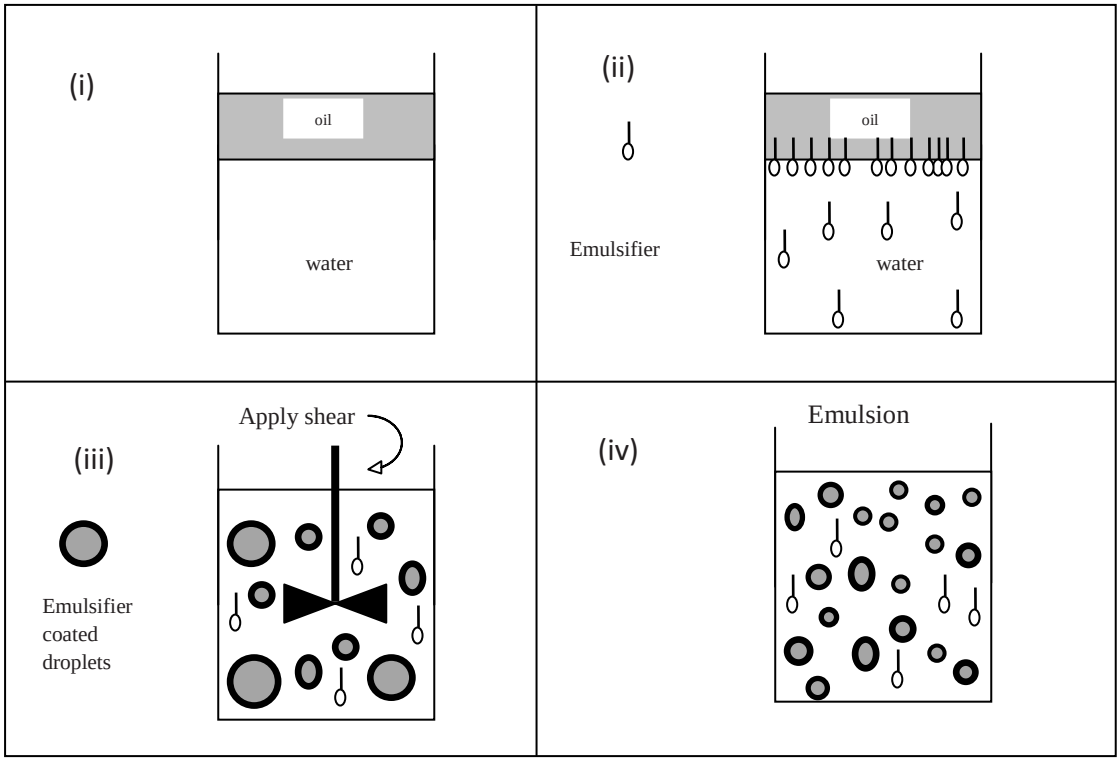

Two immiscible liquids, such as oil and water, will phase separate an oil layer (lower density) on top of a water layer (higher density) with a flat interface to minimize the interfacial and gravitational energies (ii) An emulsifier, generally soluble in the continuous phase, preferentially adsorbs on the oil–water interface. In this example, the surfactant is soluble in the water phase (iii) Shear is applied to the system, causing the oil to break up into droplets that are coated with surfactant and are inhibited from coalescing due to the interfacial repulsion. As the emulsion is sheared, larger oil droplets are stretched and rupture into smaller droplets. (iv) After the shear has been stopped, the emulsion can persist for a reasonable of time (Mason and others 2006).

Figure 2. 4 : Emulsion formation.

Table 2. 3: Examples of some common stabilizers that can be used in the food industry to formulate nanoemulsions (McClements 2011).

Stabilizer	Function	Examples
Emulsifier	Surface-active substances that adsorb to oil–water interfaces and form protective coatings around droplets that prevent droplet aggregation	Small molecule surfactants (e.g., Tweens, Spans), phospholipids (egg, soy or dairy lecithin), amphiphilic proteins (e.g., WPI, caseinate), amphiphilic polysaccharides (e.g., gum Arabic, modified starch)
Texture modifier	Substances that increase the viscosity or gel the aqueous phase. Thickening enhances the texture and organoleptic properties of the final product, and improves stabilization against gravitional separation processes	Sugars (e.g., sucrose, HFCS), polyols (e.g., glycerol, sorbitol), polysaccharides (e.g., xanthan, pectin, carrageenan, alginate, guar gum) and proteins (e.g., gelatin, WPI, SPI)
Weighting agent	Added to oil droplets to reduce the density contrast between the oil droplets and the surrounding aqueous phase, thereby reducing the driving force for gravitational separation.	Dense lipophilic materials (e.g., BVO, SAIB, Ester Gums) .Often used in beverage emulsions to increase their creaming stability
Ripening retarder	Highly hydrophobic materials that slow down or prevent Ostwald ripening when incorporated within oil droplets. They are soluble in the oil phase but highly insoluble in water	Lipophilic materials with very low water-solubility (e.g., LCT, mineral oils, esters gums)

Abbreviations: BVO= brominated vegetable oil; LCT= long chain triglycerides; WPI= whey protein isolate; SPI= soy protein isolate; SAIB = Sucrose-acetate isobutyrate

Emulsifiers generally play two roles in emulsion kinetic stability: (1) They lower interfacial tension between the oil and water phases and thereafter reduce the amount of work required to overcome surface energy in order to disperse one system into the other meaning lowering energy required for breaking up emulsion droplets during homogenization (Karlene and Derick 2006; Garti 2002) (2) to adsorb and form a mechanically, cohesive interfacial film around freshly formed droplets during homogenization and to prevent their fast reflocculation or coalescence during the emulsification process by steric or electrostatic interactions (Garti 2000, 2002)

Food emulsifiers are generally put into two categories: (1) synthetic surfactants permitted for food applications are mostly derived from fatty acids or alcohols, and esters of the fatty chains and hydrophilic functional groups like polyol, glycol, sorbitol, sucrose, acetic, lactic, succinic, tartaric, citric, and polyethyleneglycols (2) naturally occurring surfactants, including proteins (from vegetable, marine, and animal sources), chemically and enzymatically modified proteins, glycolipids, polysaccharide hydrocolloids (from various sources), and naturally occurring small molecular weight surfactants (like lecithins, monoglycerides, and saponins). Some naturally occuring emulsifiers such as proteins behave differently from the small molecule surfactans. Although some proteins are excellent emulsifiers, not all proteins can adsorb strongly to an o/w interface, either because their side chains are strongly hydrophilic or because they possess rigid structures that do not allow the protein to adapt to the interface. Examples of such proteins are gelatin, which forms poor emulsions because it has a hydrophilic character and is a large, rather rigid, molecule, and lysozyme, which although it does adsorb to O/W interfaces, tends to be a poor emulsifier (presumably because of its relatively inflexible structure). A few polysaccharides do appear to interact with emulsion droplets. Of these, the best known example is carrageenan, which will have very strong steric stabilization because the carrageenan molecules may protrude far into the solution from the emulsion interface (Douglas 2003).There is no single classification available to categorize all types of surfactants. Nevertheless, there are a few characteristics that can be used for their classification. A valuable classification tool is hydrophile - lipophile balance (HLB). It is a measure of the ratio of the hydrophilic head group to the lipophilic tail.

In general a surfactant with a low HLB number (3–6) is predominantly hydrophobic, oil-soluble and can stabilize W/O emulsions, and forms reverse micelles in oil. A surfactant with a high HLB number (8-15) is predominantly hydrophilic, preferentially soluble in water, can stabilize O/W emulsions, and forms micelles in water. Extreme high or low values are not functioned as emulsifiers since almost all of the molecule will be solubilized in the continuous phase. They would, however, be very useful for full solubilization of another ingredient, such as a flavor oil or vitamin, in the continuous phase. A surfactant with an intermediate HLB number (7–9) has no particular preference for either oil or water, and therefore tend to gather in high concentration at the interface, considered a good "wetting agent." Table 2.4 illustrates the ranges of HLB values that are most suited for a particular application (McClements and Weiss 2005; Karlene and Derick 2006).

One of the major drawbacks of the HLB concept is that it does not take into account the fact that the functional properties of a surfactant molecule are altered significantly by changes in temperature or solution conditions. Thus, a surfactant may be capable of stabilizing O/W emulsions at one temperature, but W/O emulsions at another temperature, even though it has exactly the same chemical structure. Another limitation is that the optimum HLB number required for a surfactant to create a stable emulsion often depends on the oil type (McClements 2005d; Garti 2000; Karlene and Derick 2006).Another important parameter is the charge of the head group and they can be classified as ionic, non-ionic, and zwitterionic surfactants.

Nonionic Surfactants:

Nonionic surfactants have been widely used to form nanoemulsions due to their low toxicity, lack of irritability, and the capacity to easily form nanoemulsions by both high-energy and low-energy approaches. They have several advantages over ionic surfactants, such as covering a wide range of HLB values, being more environmentally friendly and easily biodegradable. Examples include sugar ester surfactants (e.g., sorbitanmonooleate, sucrose monopalmitate), polyoxyethylene ether (POE) sur- factants (e.g., Brij 97), and ethoxylated sorbitan esters (e.g., Tweens and Spans) (McClements and Rao 2011; McClements 2005c).

Table 2. 4: HLB values and applications (McClements and Weiss 2005).

HLB range	Application
<3	Surface films
3-6	W/O emulsions
7-9	Wetting agents
8-15	O/W emulsions
13-15	Detergents
15-18	Solubilizers

Ionic Surfactants:

Anionic surfactants make about 75% of all the consumption of surface-active material. They are rarely encountered in the preparation of an actual food. Their utilization is very limited even small doses of anionic surfactants can cause allergic reactions and nausea. Examples include such as CITREM, DATEM, and sodium dodecylsulfate or SDS. Ionic surfactants may be used to form nanoemulsions by various low-energy and high-energy approaches. Cationic surfactants, i.e. lauric alginate, are primarily recognized because of their strong bacteriostatic properties (McClements and Weiss 2005; McClements and Rao 2011).

Zwitterionic surfactants:

Zwitterionic surfactants have two or more oppositely charged ionizable groups on the same molecule. Consequently, they can have a net negative, neutral, or positive charge depending on solution pH. Phospholipids are common zwitterionic surfactants that have GRAS status, which permits their use in food, e.g., lecithin (McClements and Rao 2011; McClements 2011).

The type of emulsifier used has a major impact on the type of homogenization approach that can be used to form a nanoemulsion. Many small molecule surfactants are highly effective at producing nanoemulsions using both high- and low-energy methods. On the other hand, proteins and polysaccharides are not typically suitable for producing nanoemulsions using low-energy methods, and are not usually as

effective as surfactants at forming nanoemulsions with small droplet sizes using high-energy methods. The formation and stability of nanoemulsions can also often be improved by using combinations of emulsifiers, rather than using a single emulsifier. For example, employing a lipophilic and hydrophilic surfactant in conjunction can facilitate the formation of small particles using both low-energy and high-energy approaches. On the other hand, using mixed-emulsifier systems can often improve the stability of nanoemulsions to particle aggregation after formation.

2.1.1.2 Preparation methods

In addition to water, oil and emulsifier, energy is also needed to make an emulsion. To produce nanoemulsions, either a large amount of energy or surfactant or the combination of both is required. Nanoemulsions can be fabricated using a variety of approaches, which are typically categorized as either high-energy or low- energy approaches (Tadros and others 2004; Solans and others 2005; McClements and Rao 2011; McClements 2011; Mason and others 2006; McClements 2005c; McClements and Li 2010). High-energy methods utilize mechanical devices capable of generating intense disruptive forces that mix and disrupt oil and water phases leading to the formation of tiny oil droplets. In contrast, low energy methods rely on the spontaneous formation of emulsions under specific system compositions or environmental conditions as a result of changes in interfacial properties.

A-High-energy approaches

At present, high-energy approaches are the most common method used to prepare nanoemulsions in industrial food operations because they are capable of large-scale production. In general, the particle size produced by high-energy approaches is governed by a balance between two opposing processes occurring within the homogenizer: droplet disruption and droplet coalescence (Jafari and others 2008).

The mechanical energy required for emulsification exceeds the interfacial energy by several orders of magnitude (Tadros and others 2004). The reason such intense energy levels are needed is that generated disruptive forces must exceed the restorative forces holding the droplets into spherical shapes. These restorative forces are determined by the Laplace pressure: $\Delta P = \gamma/2r$, which increases with decreasing droplet radius (r) and increasing interfacial tension (γ). Thus, as the droplet radius becomes increasingly smaller within a homogenizer, it becomes increasingly

difficult to break them up further (Jafari, Assadpoor and others 2008; Tadros and others 2004; Solans and others 2005; McClements and Rao 2011; McClements 2011; Mason and others 2006; McClements 2005c; McClements and Li 2010).

The smallest size of the droplets that can be produced using a high-energy approach depends on the homogenizer type, homogenizer operating conditions (e.g., energy intensity, duration, and temperature), sample composition (e.g., oil type, emulsifier type, relative concentrations), and the physicochemical properties of the component phases (e.g., interfacial tension and viscosity)(McClements and Rao 2011). The most well-known mechanical devices which are capable of producing the tiny droplets present in nanoemulsions are high-pressure homogenizers, microfluidizers, and ultrasonic devices.

A.1 High pressure homogenizers (HPHs):

HPHs are currently the most popular method of creating fine emulsions in the food industry (Figure 2.5). A coarse emulsion premix is usually produced using high speed mixers. The disruption of droplets in a high speed mixer occurs mainly due to the existence of a turbulent flow situation. The energy input per unit volume is unevenly distributed in the apparatus. This results in a broad droplet size distribution. The major droplet disruption occurs in the immediate vicinity of the rotating blades where shear forces are highest. The effectiveness of droplet disruption depends on the geometry of the mixer and the rotational speed of the blades (McClements and Weiss 2005). Then this coarse emulsion is fed through a narrow orifice of high pressure homogenizer. The homogenizer has a pump that pulls the coarse emulsion into a chamber on its backstroke and then forces it through a narrow valve at the end of the chamber on its forward stroke.

As the coarse emulsion passes through the valve it experiences a combination of intense disruptive stresses (e.g. turbulence, shear and cavitation) that cause the larger droplets to be broken down into smaller ones (Jafari and others 2008).

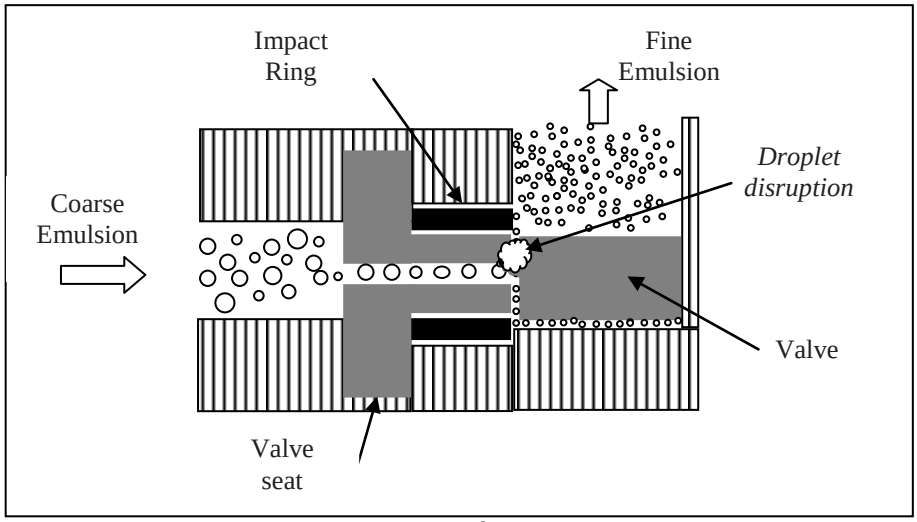

Figure 2. 5: Schematic representation of high-pressure valve homogenizers.

The homogenization valve can have various geometries with externally adjustable gap sizes. The average residence time of the premix in the valve is less than a few milliseconds. Due to the fast acceleration of the liquid in the annulus (more than 200 m/s), the hydrostatic pressure in the annulus can drop below the vapor pressure of the liquid. Consequently, steam bubbles are formed. The bubble formation is transient and they collapse in the rear part of the annulus where pressure and temperature increase again. The collapse of these bubbles (cavitation) is the primary source of the mechanical energy that causes oil droplet disruption. The effectiveness of the droplet disruption can be directly related to the applicable pressure difference (McClements and Weiss 2005). It also depends on the viscosity ratio of the two phases (usually oil and water). Small droplets can only usually be produced when the disperse-to-continuous phase viscosity ratio falls within a certain range ($0.05<\eta D/\eta C<5$). Finally, it is important to use sufficient amount of an emulsifier that can rapidly adsorb to the new droplet surfaces to prevent re-coalescence. It is usually necessary to operate at extremely high pressures and to use multiple passes through the homogenizer. Even then, it is only possible under certain circumstances to obtain droplets less than 100 nm in radius (McClements and Rao 2011; McClements 2011).

A.2 Microfluidizer:

In some design respects microfluidizers are similar with high pressure valve homogenizers, since they use a pump to force a coarse emulsion through a narrow orifice at high pressures to facilitate droplet disruption. Nevertheless, the design of the channels through which the coarse emulsion is made to flow within the device is different (Figure 2.6) (McClements and Rao 2011).

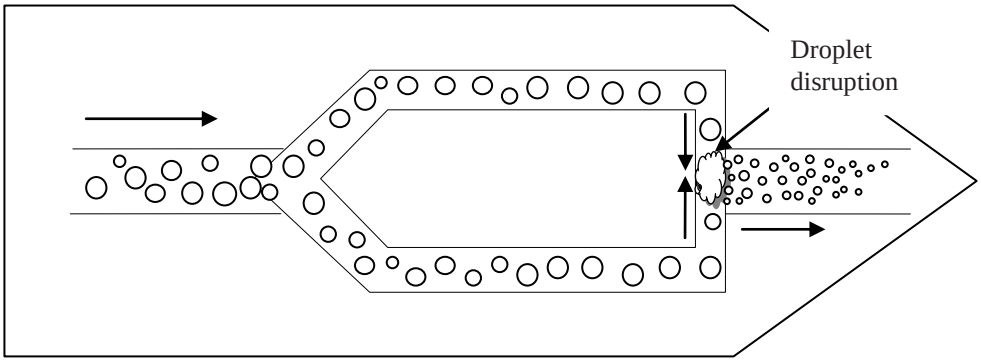

Figure 2. 6: Schematic representation of microfluidizers.

Microfluidization produces a tighter particle size distribution than that of traditional valve homogenization (Ping-Chung, 2010). In the interaction chamber of the "microfluidizer" that is the heart of this device; two jets of crude emulsion from two opposite channels collide with one another at high velocity (Jafari and others 2007a). Forcing the flow stream by high pressure through microchannels toward an impingement area creates a tremendous shearing action, which cause the fluids to intermingle and can provide an exceptionally fine emulsion. In general, inertial forces in turbulent flow along with cavitation are predominantly responsible for droplet disruption in microfluidizer (Jafari and others 2008; Jafari and others 2007b;McClements 2005c). Like high pressure valve homogenizers, the droplet size produced tends to decrease with increasing homogenization pressure, number of passes, and emulsifier concentration. In addition, the disperse-to-continuous phase viscosity ratio should be within a certain range to facilitate the formation of small droplets (McClements 2011; Chen and others 2011).

A.3 Ultrasonic homogenizers:

This type of homogenizer uses high-intensity ultrasonic waves (frequency > 20 kHz) that generate intense shear and pressure gradients within a material that disrupt the droplets mainly due to cavitational and turbulent effects (McClements 2011) (Figure 2.7). These devices consist of an ultrasonic probe that contains a piezoelectric crystal. When a high-intensity electrical wave is applied to the transducer, which causes the piezoelectric crystal inside it to rapidly oscillate and generate an ultrasonic wave. The ultrasonic wave is directed toward the tip of the transducer where it radiates into the surrounding liquids and generates intense pressure and shears gradients (mainly due to cavitational effects) that cause the liquids to be broken up into smaller fragments and intermingled with one another (McClements 2005c). Cavitation is the formation and collapse of vapor cavities in a flowing liquid. The collapse of these cavities causes powerful shock waves to radiate throughout the solution in proximity to the radiating face of the tip, thereby breaking the dispersed droplets (Jafari and others 2008).

To create a stable emulsion it is usually necessary to irradiate a sample for periods ranging from a few seconds to a few minutes and prolonged exposure of certain food components to high-intensity ultrasound can promote degradation, for example, oxidation of lipids, depolymerization of polysaccharides, or denaturation of proteins (McClements 2005c).

B- Low energy approaches:

Low-energy approaches take the advantage of the intrinsic physicochemical properties of the system ingredients mainly surfactants, co-surfactants and excipients in the formulation, leading to the generation of emulsion droplets in the nanometric range (Anton and Vandamme 2009). Low-energy approaches are often more effective at producing small droplet sizes than high- energy approaches, but the types of oils and emulsifiers that can be used are limited. For example, it is currently not possible to use proteins or polysaccharides as emulsifiers in most of the low-energy approaches used to form nanoemulsions. Instead, it is often necessary to utilize relatively high concentrations of synthetic surfactants to form nanoemulsions by these approaches, which may limit their use for many food applications (McClements and Rao 2011). For example to produce the similar sized droplets ($d<160$ nm) the surfactant to oil ratio is higher than 70% when low energy method is

applied and this ratio is around 10% when high energy methods utilized (Ostertag and others 2012). The two commonly reported low-energy nano-emulsification methods are the spontaneous emulsification method and the phase inversion methods (Anton and others 2008).

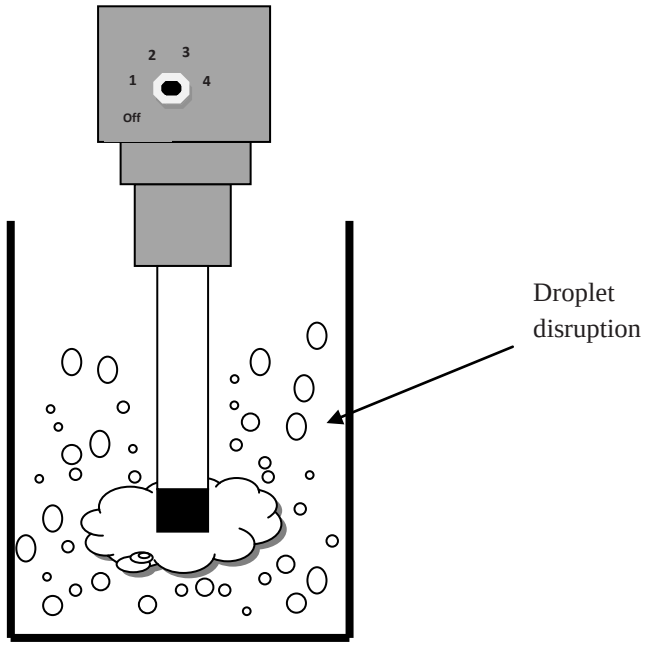

Figure 2.7: Schematic representation of ultrasonic probe homogenizer.

B.1. Spontaneous emulsification:

It has been proposed that the general principles and mechanism governing the formation of nanoemulsions using this method is the solvent displacement from the oily to the aqueous phase meaning the movement of a water-miscible component (either solvent or surfactant) from the organic phase into the aqueous phase (Anton and Vandamme 2009; Anton and others 2008; McClements 2011). This movement creates a large interfacial turbulent force at the oil–water interface, which cause an increase in oil-water interfacial area, turbulence, and spontaneous formation of oil droplets surrounded by aqueous phase through a budding process (Figure 2.8) (McClements and Rao 2011; McClements 2011).

To prepare very small droplets, it is usually necessary to use a high ratio of water-miscible solvent-to-oil (e.g. tiny percentage of oil in the organic phase before mixture). Practically, this method can be carried out in a number of different ways—the compositions of the two phases can be varied; the environmental conditions can be varied (e.g., temperature, pH, and ionic strength); and/or, the mixing conditions

can be varied (e.g., stirring speed, rate of addition, and order of addition) (Anton and Vandamme 2009; McClements and Rao 2011; Anton and others 2008). The droplet size will be depending on oil type, surfactant type, surfactant to oil concentration, surfactant location (initially in water or in oil).

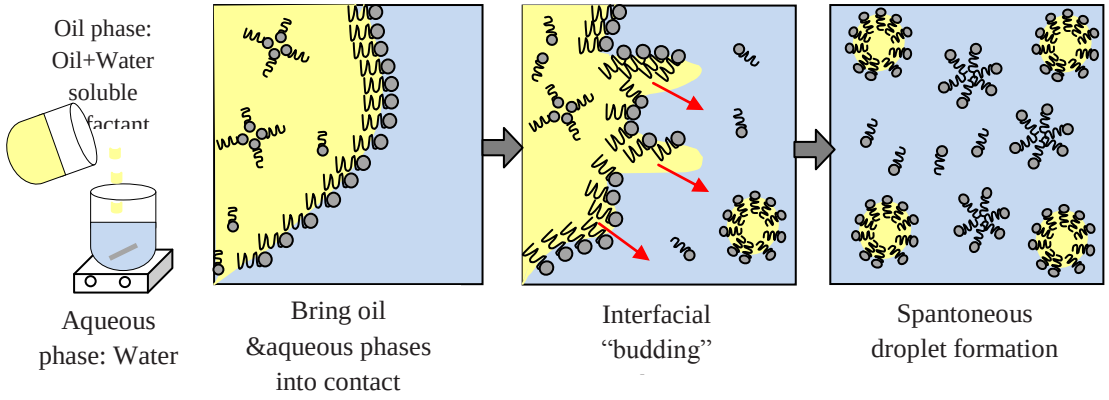

Figure 2.8: Schematic representation of proposed mechanism for spontaneous emulsification (McClements and Rao 2011).

A practical example of spontaneous emulsification is the cloudiness that occurs when water is added to certain anise-flavored spirits, e.g., Ouzo or Pastis. These well-known anise-flavored alcoholic beverages are nano-emulsions produced when a large amount of water is added to a three-component homogeneous solution composed of water (about 55%), alcohol (e.g. ethanol, about 45%) and an anise-flavored "oil" (about 0.1%), which is soluble in ethanol, but insoluble in water. While diluting with water, some of the alcohol molecules move out of the organic phase into the aqueous phase, which causes the flavour oils to be no longer soluble, and small oil droplets spontaneously form in the solution and that scatter light and mixture turns into a cloudy white colour (Solans and Solé 2012; McClements 2011).

B.2. Phase inversion methods:

A number of methods have been developed to formulate nanoemulsions that depend on inducing a phase inversion in emulsions from a W/O to O/W form (or vice versa), e.g., phase-inversion temperature (PIT), phase-inversion composition (PIC), and emulsion-inversion point (EIP) methods.

B.2.1.Phase inversion temperature (PIT):

PIT method includes the spontaneous emulsion formation by varying the temperature profile of certain mixtures of oil, water, and polyoxyethylene type of non-ionic surfactant (Tadros and others 2004). The temperature at which an oil–water–surfactant system changes from an O/W emulsion to a W/O emulsion is known as the phase inversion temperature (PIT). At temperatures well below PIT (~T < PIT -30°C), these surfactans are hydrophilic. The surfactant monolayer has a large positive spontaneous curvature forming oil-swollen micelles (or O/W microemulsions) and these micelles coexist with excess oil phase. At high temperatures sufficiently greater than the PIT (T > PIT + 20 °C), the polyoxyethylene chains are dehydrated and the spontaneous curvature becomes negative and these surfactants become more and more lipophilic. Then water-swollen reverse micelles (or W/O microemulsions) appear and coexist with excess water phase. At intermediate temperatures, the Hydrophile-Lipophile Balance (HLB) temperature, surfactant affinity for water and oil phases is balanced. Then, the spontaneous curvature becomes close to zero and a thermodynamically stable planar structure with zero curvature, appears which can be a bicontinuous microemulsion, or a lamellar liquid crystal, depending on the concentration of the surfactant and the system. A nanoemulsion can be formed spontaneously by rapidly cooling an emulsion from a temperature at or slightly above the PIT to a temperature well below the PIT with continuous stirring (Figure 2.9) (Conxita and others 2009; McClements 2011). At the HLB temperature, although emulsification in very small droplets is favored due to extremely low interfacial tensions, the emulsions are very unstable.

Therefore, to produce kinetically stable nano-emulsions, the temperature has to be quickly moved away from the HLB temperature by a rapid cooling or heating (by about 25–30 °C) (obtaining O/W or W/O emulsions, respectively). If the cooling or heating process is not fast, coalescence predominates and polydisperse coarse emulsions are formed (Solans and others 2005; Solans and Solé 2012).

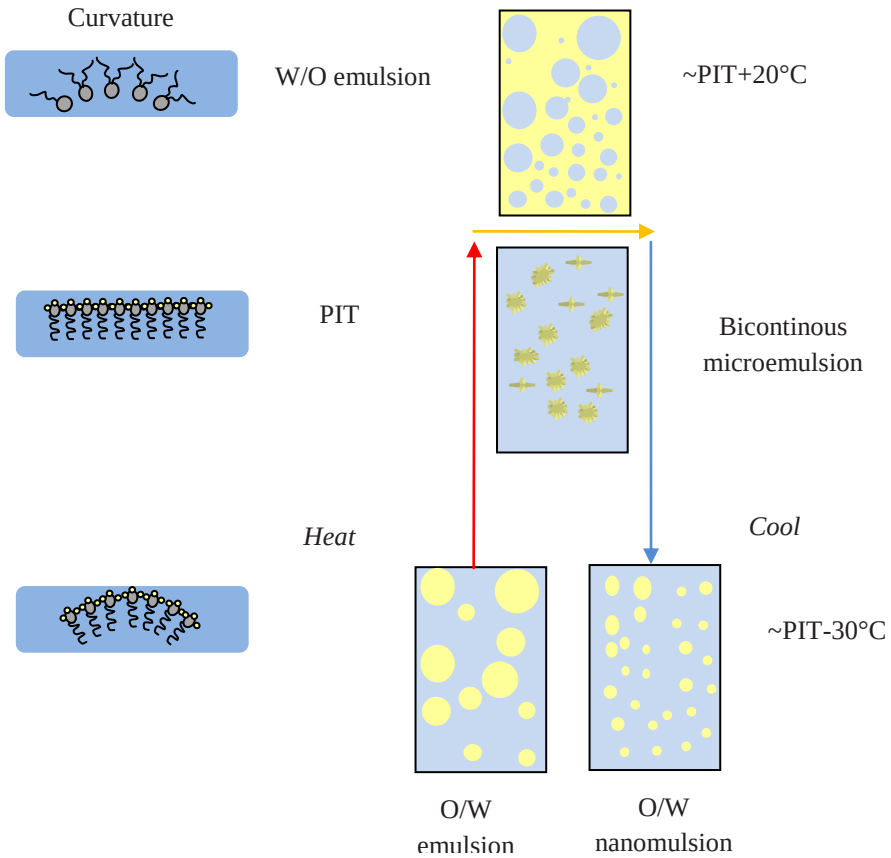

Figure 2.9 : Schematic diagram of the temperature-dependence of the spontaneous curvature of surfactant monolayers (McClements and Rao 2011; McClements 2011).

B.2.2. Phase inversion composition (PIC)

PIC method is somewhat similar to the PIT method, but the optimum curvature of the surfactant is changed by altering the composition of the system, rather than the temperature, that is a phase inversion can be induced by a change in composition (Solans and others 2009). For example, an O/W emulsion stabilized by an ionic surfactant can be made to phase invert to a W/O emulsion by adding salt. Another way to prepare nanoemulsions using the PIC method is by changing the pH to alter the electrical charge and stability of emulsions. Fatty acids may stabilizeW/O emulsions at low pH (pH<pKa) because the carboxyl groups are uncharged so they have a relatively high oil solubility. However, they may stabilize O/W emulsions at high pH values because the carboxyl group becomes ionized so they become more water-soluble. Conse- quently, nanoemulsions can be formed by increasing the pH of a fatty acid-oil-water mixture from below to above the pKa value of the carboxyl groups (McClements and Rao 2011).

B.2.3. Emulsion inversion point (EIP):

In this method, the change from one type of an emulsion to another is through a catastrophic-phase inversion.Practically, catastrophic-phase inversion is usually induced by either increasing (or decreasing) the volume fraction of the dispersed phase in an emulsion above (or below) some critical level (Figure 2.10) (Ostertag and others 2012).

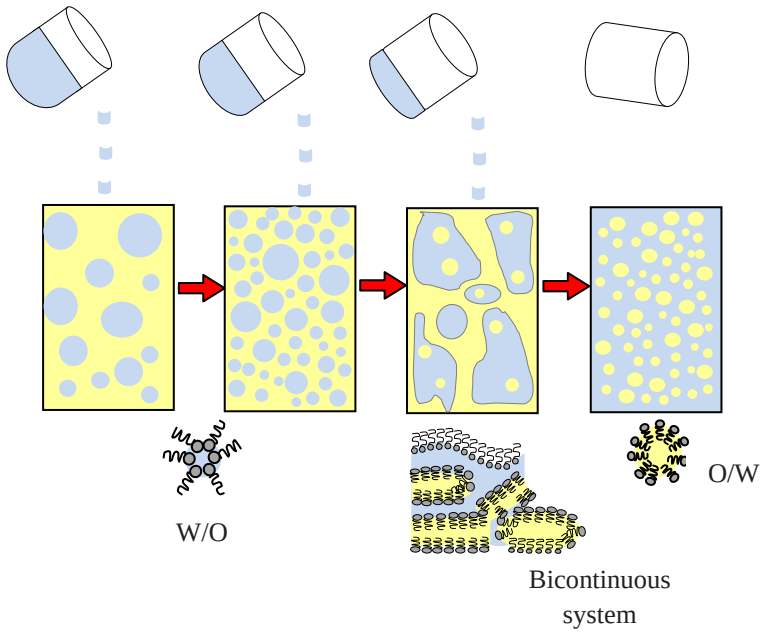

Figure 2.10 : Schematic representation of the proposed mechanism for low-intensity emulsification by the catastrophic phase inversion (CPI) method (McClements and Rao 2011; McClements 2011)

For example, a W/O emulsion consisting of water droplets dispersed in oil is initially formed using a particular surfactant, and then increasing amounts of water are added to the system with continued stirring. At low amounts of added water, additional water droplets are formed within the oil phase. However, once a critical water content is exceeded, the coalescence rate of water droplets exceeds the coalescence rate of oil droplets, and so phase inversion occurs from a W/O to an O/W system. The value of the critical concentration where phase inversion occurs, as well as the size of the oil droplets produced, depends on process variables, such as the stirring speed, the rate of water addition, and the emulsifier concentration (Ostertag and others 2012; McClements and Rao 2011).

2.2.2 Liposomes/Nanoliposomes

When amphiphilic molecules such as phospholipids are placed in an aqueous environment, they form aggregated complexes in an attempt to shield their hydrophobic sections from the water molecules while still maintaining contact with the aqueous phase via the hydrophilic head groups. If a sufficient amount of energy is provided to the aggregated phospholipids, they can arrange themselves in the form of organized, closed bilayer vesicles (i.e., liposomes or nanoliposomes). During this process, liposomes can entrap hydrophilic solutes that are present in the hydration media. Lipophilic molecules, or lipid-soluble compounds such as certain vitamins, nutrients, and drugs, can also be incorporated into liposomal bilayers by dissolving these molecules together with the lipids (da Silva Malheiros and others 2010; Mozafari and others 2008b; Mozafari and others 2008a).

Nanoliposomes possess the same physical, structural and thermodynamic properties as the liposomes (Mozafari and others 2006). The underlying mechanism of liposome/nanoliposome formation is basically based on the unfavorable interactions occurring between phospholipids and water molecules, where the polar headgroups of phospholipids are exposed to the aqueous phases (inner and outer), and the hydrophobic hydrocarbon tails are forced to face each other in a bilayer (da Silva Malheiros and others 2010).

Liposomes can be divided into three corresponding to their lamellarity: multilamellar vesicles (MLV) composed of a number of concentric bilayers, separated by aqueous regions; multivesicular vesicles (MVV) composed of many small non-concentric vesicles encapsulated within a single lipid bilayer; unilamellar vesicles (ULV) constituted of a single bilayer. ULV can be classified depending upon size: vesicles whose diameters ranging from 20 nm to 100 nm are named small unilamellar vesicles (SUV); those size chaging from 100 nm to 1000 nm are referred to as large unilameller vesicles (LUV); and large unilamellar vesicles possesing higher diameters than 1000 nm are known as giant unilamellar vesicles (GUV) (Taylor and others 2005; Mozafari and others 2008b; Quemeneur and others 2007).

Liposomes have attracted considerable attention in the biomedical, food and agricultural industries in recent years because they are biocompatible, biodegradable, nontoxic, and have the ability to act as targeted release-on-demand carrier systems for both water and oil-soluble functional compounds such as

antimicrobials, flavors, antioxidants and bioactive compounds. Typical sources of phospholipids being soy or egg lecithins have been used to prepare liposomes in the field of food applications. Such lecithins have long been used as emulsifiers and texture modifiers in foods and are generally recognized as safe (Keller 2001; Taylor and others 2005; Gibis and others 2012).

2.2.2.1 Preparation methods

There are several methods that may be used to produce liposomes. Manufacture of both liposomes and nanoliposomes requires input of energy to a dispersion of lipid/phospholipid molecules in an aqueous medium (da Silva Malheiros and others 2010; Mozafari and others 2008b).

Depending on which type of liposome is produced, the required energy input can greatly vary. MLVs form readily when bilayer-forming polar lipids are dispersed in aqueous media under mild agitation. To generate unilamellar vesicles, substantial energy inputs are required that are sufficient to disrupt multilameller structures. Generally, similar to emulsions, liposomes are only stable for a defined period of time; i.e. they are said to be "kinetically stable". Because of this, many of the principles of emulsion formation also apply to the formation of liposomes and the techniques used to produce emulsions may often be used to produce liposomes. The most commonly applied techniques are based on the input of mechanical energy in the system e.g., high-intensity ultrasonication, high-pressure homogenization, membrane extrusion, and membrane homogenization. Non-mechanical methods include, thin-film hydration, reverse phase evaporation, removal of detergents from mixed detergent/lipid micelles and freeze-drying followed by rehydration. *Freeze drying-rehydration* and *freeze–thawing* techniques are used more to refine preformed liposomes and improve their properties rather than produce them (Taylor and others 2005).

The standard non-mechanical preparation procedure is through *thin-film hydration* method. A thin film produced by the evaporation of a chloroform/methanol solution of phospholipid, cholesterol, and other hydrophobic compounds. After that, an aqueous phase and hydrophilic compounds added by input of sufficient amount of mechanical or thermal energy, causes bilayer sheets of the hydrophobic components to separate from the bulk and form liposomes (Mozafari and others 2008b).

The *reverse-phase evaporation (REV)* method, involves the preparation of water-in-oil emulsions, where the lipid is solubilized in the organic phase with a low boiling point and the aqueous phase contains the solute to be entrapped. Followed that the system is briefly homogenized (vortex or low energy sonicator) to form an emulsion. Upon evaporation of the solvent under reduced pressure, the system is converted to an aqueous dispersion of vesicles (Taylor and others 2005; Yuan-Peng and others 2001).

The *detergent dialysis* method dialysis involves the solubilization of lipids (and proteins) in nonionic or ionic detergents. Liposomes form gradually during the process of detergent removal either by passing the sample through a gel filtration column or by dialysis in a large volume of solution. As surfactant that was present in excessive amount compared to the lipid in the system is removed from the aqueous phase, surfactant molecules in the mixed micelle will be gradually removed. Consequently, the mixed micelle is first converted into a mixed surfactant-polar lipid vesicle and after complete removal of the surfactan it will transfer into a surfactant free liposome (Taylor and others 2005; Yuan-Peng and others 2001).

Non-mechanical preparation methods of liposomes/nanoliposomes generally involve utilisation of non-food-grade solvents and detergents. The presence of solvents has a risk of remaining in the final formulation, thus contributing to toxicity and influencing the stability of the liposomal system. Since no toxic solvents utilisation included in mechanical methods, they promise alternative liposome manufacturing methods in addition to allowing process of higher volume of samples. Homogenization and microfluidization are the easiest ways for the scale-up. The use of high-intensity ultrasonication, high-pressure homogenization, microfluidizer is explained above; here only brief information about membrane extrusion and homogenization will be given.

In *extrusion* and *membrane homogenization* method, the dispersed phase containing large liposomes is forced to pass through a membrane or a filter with a uniform pore size distribution allowing a homogeneous population of smaller vesicles. This forced passage exerts shear forces that cause a rupture of the membranes, followed by a rapid resealing. Substances that are entrapped in the larger vesicles prior to passage through the capillaries will leak out during the extraction process; therefore extrusion has to be performed in the presence of the substance that is to be

encapsulated. Extrusion and membrane homogenization is influenced by the temperature and extrinsic properties such as the size of the pores, the applied pressure across the membrane of filter and the flow rate (Taylor and others 2005).

2.2.3 Nanosuspensions

Nanosuspension is a carrier-free colloid drug delivery system, consisting of solid drug nanoparticles stabilized by polymer and/or surfactant with a mean particle size below 1 μm (i.e. in the nanometer range, typically somewhere between 200 and 500 nm (Gao and others 2011; Singare and others 2010; Keck and Müller 2006). Solubility problems of many newly developed high-potential drugs/neutraceuticals are a severe obstacle in formulation development, especially when they show poor solubility simultaneously in aqueous media. This leads, in many cases, to a poor and/or varying bioavailability after oral administration. Nanosuspensions are a promising strategy for improving the dissolution rate and oral bioavailability of poorly water soluble drugs by reducing the particle size and/or transforming drugs from a crystalline to an amorphous state.

2.2.3.1 Preparation methods

There are two main approaches for formulating a nanosuspension: top down approach and bottom up technology. However, the combination techniques, combining a pre-treatment with a subsequent size reduction step are also being employed (Shegokar and Müller 2010).

The *bottom up* technology involves dissolving drug in a solvent which is then added to non-solvent to build particles by precipitation of dissolved molecules (Chan and Kwok 2011). For precipitation technique the following prerequisites should be satisfied: (1) the drug should be soluble at least in one solvent (2) the solvent is miscible with a non-solvent (3) the solvents used in this techniques should be eliminated to an acceptable level in the end products (Gao and others 2008). The basic advantage of precipitation techniques is that they use relatively simple, low cost equipment. However, there are basic problems associated with precipitation techniques. The particles produced need to retain their size after precipitation, particle growth to microcrystals needs to be avoided, as well (Keck and Müller 2006).

The *top down approach* relies on mechanical attrition to convert large crystalline particles into nanoparticles .The 'Top down Technologies' include media milling (pearl/ball milling) and high pressure homogenization (Singare and others 2010; Van Eerdenbrugh and others 2008).

In *media milling process*, particle size reduction comprises mechanical attrition of suspended drug particles using milling media e.g. glass, zirconium oxide or special polymers such as hard polystyrene derivatives. Basically, the drug, surfactant and water are filled into the milling chamber charged with milling pearls (Figure 2.11); then the pearls are rotated at a high rate driven by the motor and the drug was processed into nanosized crystals by the high shear forces (Gao and others 2008).

Shear forces generated by the movement of the milling media lead to particle size reduction (Van Eerdenbrugh and others 2008; Keck and Müller 2006). Erosion from the milling material during the milling process is a common problem. The milling time mainly depends on the hardness of the drug, viscosity, temperature, energy input, size of the milling media and surfactant concentration used and requested particle size. The milling time can last from about 30 min to hours or several days (Shegokar and Müller 2010; Gao and others 2008). Routinely, the drug/surfactant slurry was milled to a final size of less than 400 nm and generally this could be achieved over a 4-day period. It was reported that the poorly water soluble drug, naproxen, was reduced in average particle size from 20–30 μm to 270 nm over 5 days of milling (Hu and others 2004).

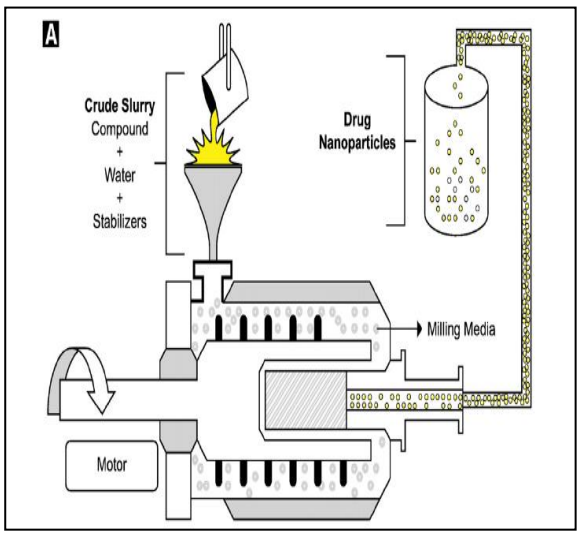

Figure 2.11: The schematic diagram of the nanosizing process using wet milling technology (Merisko-Liversidge and Liversidge 2011).

The two homogenisation principles/homogeniser types applied are: microfluidisation (Microfluidics, Inc.) and piston-gap homogenisers (e.g. APV Gaulin, Avestin, etc.). The size of the drug nanocrystals which can be achieved depends mainly on: (1) Power density of the homogeniser (2) Number of homogenisation cycles (3) Temperature (Keck and Müller 2006).

The microfluidizer technology is based on the jet stream principle and can generate small particles by a frontal collision of two fluid streams in a Y-type or Z-type chamber under pressures up to 1700 bar. The jet streams lead to particle collision, shear forces and cavitation forces. Often a relatively high number of cycles (50–100 passes) are necessary to obtain sufficient particle size reduction (Shegokar and Müller 2010).

In the process of piston-gap homogenization, the poorly water soluble drug is first dispersed in an aqueous surfactant solution by high speed stirring, and the suspension is then passed through a high pressure homogenizer applying a typical pressure of 1500 bar and three to 20 homogenization cycles (Hu and others 2004). A liquid suspension passes through a narrow channel or tiny gap inside a pipe. Due to the narrowness of the gap, the streaming velocity of the suspension and the dynamic fluid pressure increase. According to Bernoulli's equation, to maintain constant energy, this is compensated by a reduction in the static pressure below the boiling point of the aqueous phase at room temperature. In consequence, water starts boiling gas bubbles are formed. As the suspension leaves the gap, the pressure suddenly rises to normal pressure and the gas bubbles implode (cavitation) vigorously, and the breaking up the crystals is caused by cavitation, fluid shear, and particle collision against each other occurs. The principle of improving solubility is to increase the rate of dissolution by enlarging the surface area of the drug powder by means of particle size reduction or generation amorphous phases of drugs (Chan and Kwok 2011; Shegokar and Müller 2010; Gao and others 2008).

Nanosuspensions for oral route are mainly characterized by particle size distribution (PSD), zeta potential, crystalline status, and dissolution velocity and saturation solubility. A particle of less than 400nm is considered to be acceptable for a nanosuspension to be administered intravenously (Singare and others 2010; Sahoo and others 2011). In order to avoid particle growth during storage time and to prepare formulations for oral administration, nanosuspensions are converted into dry

forms by spray-drying or lyophilization. Dry product should redisperse well in water, with little increase in the size (i.e. little aggregates) (Shegokar and Müller 2010; Mitri and others 2011).

2.2.4 Stability

The term ‘‘stability’’ of a colloidal system describes the ability of a colloid to resist changes in its properties over time: the more stable the system, the more slowly its properties change. Table 2.5 lists some factors involved in determining the stability of colloidal systtems e.g., emulsions. Particles in an emulsion system always show Brownian motion and hence collide with each other frequently. The stability of droplet particles is thus determined by the interaction between the particles during such a collision. There are two basic interactions: one being attractive and the other repulsive. When attraction dominates, the particles will adhere with each other and aggregate and finally the entire dispersion may coalesce. When repulsion dominates, the system will be stable and remain in a dispersed state. Van der Waals forces are the primary source of attraction between colloidal particles. These forces are always present between particles of similar composition. Therefore, a colloidal dispersion is said to be stable only when a sufficiently strong repulsive force counteracts the van der Waals attraction(Miller 2010; McClements 2005e).

Stability can be obtained by surroundig colloidal particles mainly with an electrical double layer (electrostatic or charge stabilization) and with adsorbed or chemically attached polymeric molecules (steric stabilization). Some food emulsions are stabilized almost entirely by steric stabilization, whereas others are mainly stabilized by a combination of steric and electrostatic stabilization; these are said to be electrosterically stabilized (McClements 2005b; Schramm and Stasiuk 2005).

Table 2.5: Some factors related to emulsion stability (Schramm and Stasiuk 2005).

Low interfacial tension	easier to form and maintain large interfacial area
Electric double layer (EDL) repulsion	reduces the rates of aggregation and coalescence
Steric repulsion	reduces the rates of aggregation and coalescence
Surface viscosity	retards coalescenc
Small droplet size	may reduce the rate of aggregation
Small volume of dispersed phase	reduces the rate of aggregation
Bulk viscosity	reduces the rates of creaming and aggregation
Small density difference between phases	reduces the rates of creaming and aggregation
Dispersion force attraction	increases the rates of aggregation and coalescence

The droplets in most food emulsions might have an appreciable electrical charge depending on the type of emulsifier used to stabilize the emulsion, the concentration of the emulsifier at the interface, and the prevailing environmental conditions (e.g., pH, temperature, and ionic strength). The electrostatic interaction between similarly charged droplets is repulsive, and so electrostatic interactions play a major role in preventing droplets from coming close enough together to aggregate (McClements 2005b).

Steric interactions are one of the most important stabilizing mechanisms in emulsions. Unlike electrostatic interactions, they occur in almost every type of emulsion because most droplets are stabilized by a layer of adsorbed emulsifier molecules (Table 2.6).

Table 2.6: Comparison of steric and electrostatic stabilization mechanisms (McClements 2005b).

Steric Stabilization	*Electrostatic Stabilization*
Insensitive to pH changes	pH dependent-dramatically decreased when the electrical charge on the droplet surface is reduced e.g. by altering the pH
Insensitive to electrolyte	Aggregation tends to occur at high electrolyte concentrations due to electroscreening
Large amounts of emulsifier needed to cover droplet surface (because a thick interfacial layer is required)	Small amounts of emulsifier needed to cover droplet surface
Weak flocculation (easily reversible)	Strong flocculation (often irreversible)
Good freeze–thaw stability	Poor freeze–thaw stability

Another major difference is the fact that the electrostatic repulsion is usually weaker than the van der Waals attraction at short distances, whereas the steric stabilization is stronger. This means that emulsions stabilized entirely by electrostatic repulsion are prone to coalescence when the droplets approach sufficiently closely, whereas emulsions stabilized by steric interactions may flocculate, but they are unlikely to coalesce because of the extremely strong short-range repulsion (McClements 2005b). An emulsion may become unstable due to a number of different types of physical and chemical processes. *Creaming*, *sedimentation*, *flocculation*, *coalescence*, and *Ostwald ripening* are examples of physical instability, whereas oxidation and hydrolysis are common examples of chemical instability (Figure 2.12) (McClements and Weiss 2005).

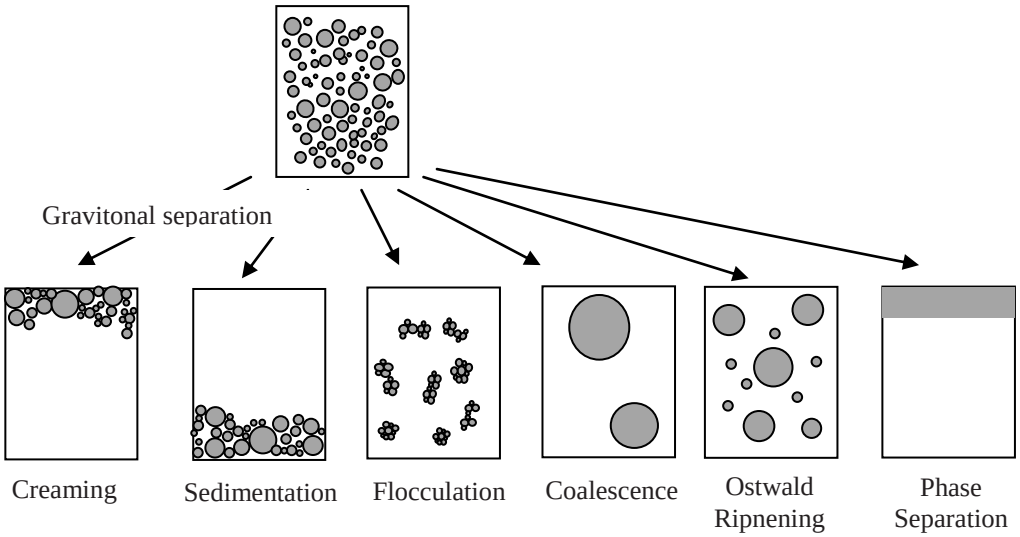

Figure 2.12: Food emulsions may become unstable through a variety of physical mechanisms, including creaming, sedimentation, flocculation, coalescence, and phase inversion (McClements 2007)

The stability of nanoemulsions is different from that of conventional emulsions prepared from similar components. Nanoemulsions are usually highly stable to gravitational separation because the relatively small droplet size means that Brownian motion dominate gravitational forces. In addition, nanoemulsions tend to have better stability against droplet aggregation than conventional emulsions because the strength of the net attractive forces acting between droplets usually decreases with decreasing droplet size, whereas the strength of the repulsive steric forces is less dependent on size (McClements and Li 2010). However, they tend to phase separation by some of the four destabilization mechanisms: sedimentation or creaming and flocculation, as reversible mechanisms, and coalescence and Ostwald ripening, as irreversible ones. An adequate selection of surfactant molecules can protect nanoemulsions from flocculation and coalescence.

Nanoemulsions may also be more susceptible to chemical degradation than conventional emulsions. Their very large specific surface areas may be promoted any chemical degradation reaction that occurs at the oil–water interface, such as lipid oxidation. Besides that, nanoemulsions are transparent and UV and visible light can penetrate into them easily, which may promote any light-sensitive chemical degradation reactions (McClements 2011; Solans and others 2009; Walstra 2002; Miller 2010).

2.2.4.1 Gravitational separation

Gravitational separation may result in either creaming or sedimentation, creaming is the upward movement of droplets due to the fact that their density is lower than that of the surrounding liquid, whereas sedimentation is the downwards movement of droplets due to the fact that they have a higher density than the surrounding liquid (Coupland 2005). Liquid edible oils normally have lower densities than water and, as a result, creaming is more prevalent in O/W emulsions, whereas sedimentation is more prevalent in W/O emulsions (McClements 2007; McClements 2005e). However, if an O/W emulsion contains crystalline lipids then they may be prone to sedimentation because the density of lipids usually increases when they crystallize (McClements and Rao 2011).

It should be possible to produce density-matched particles by controlling the oil-core size and the thickness of the adsorbed emulsifier layer. For core-shell particles the radius is given by $r_{particle} = r_{core} + \delta$, the shell layer usually has a higher density than the oil or aqueous phases, so that an increase in the volume fraction of the shell layer would increase the overall particle density. This may have important implications in preventing gravitational separation in emulsions since it will reduce the density contrast between the particles and surrounding fluid. In addition, very small particles may actually sediment rather than cream if they contain sufficiently thick and dense emulsifier layers. When the same composition used in protein stabilized emulsions, nanoemulsions (d= 66 nm) tend to sediment because the overall particle density is greater than water (the shell makes a large contribution to particle density) whereas conventional emulsions (d =325 nm) tend do cream because their overall density is less than water (the shell makes little contribution to particle density) (McClements and Rao 2011).

The velocity that an isolated rigid spherical particle moves upwards in an emulsion or nanoemulsion in an ideal (Newtonian) liquid due to gravitational separation is given by Stokes' law (2.1). The driving force is gravity, the resisting force is viscosity and is approximately proportional to the droplet velocity (McClements 2005e; Lesmes and McClements 2009; Schramm and Stasiuk 2005):

$$v_{stokes} = \frac{2gr^2(\rho_2 - \rho_1)}{9\eta_1} \quad \textbf{(2.1)}$$

υ_{stokes} is the velocity (positive for creaming; negative for sedimentation), r is the radius of particle, g is the the acceleration due to gravity, ρ is the density, η is the shear viscosity, and the subscripts 1 and 2 refer to the continuous and dispersed phases, respectively. As it can be seen from Stokes' law that creaming will occur faster when there is a larger density difference and when the droplets are larger. For example, droplets of an oil phase (ρ_2 =910 kgm^{-3}) suspended in an aqueous phase (η_1 = 1mPa s, ρ_1 = 1000 kg m^{-3}) will cream at rates of 0.17, 0.68, 4.3 and 17mm per day for r =0.1, 0.2, 0.5 and 1 μm (McClements 2007).

Stokes' law highlights a number of ways that gravitational separation can be retarded in an emulsion, e.g., by reducing the density contrast between the oil and water phases, by decreasing the size of the droplets, or by increasing the viscosity of the continuous phase, or by increasing the droplet concentration. The mathematical models are not currently sophisticated enough to take into account the inherent complexity of most food emulsions. For a more accurate prediction of the creaming stability of a food emulsion one needs to take into account a variety of other factors, including droplet fluidity, concentration, polydispersity, charge, and interactions; interfacial thickness; and, non-Newtonian fluid behavior of the continuous phase (McClements 2005e).

2.2.4.2 Flocculation

Flocculation is the process whereby two or more droplets come together to form an aggregates in which the droplets retain their individual integrity. It may be either advantageous or detrimental to emulsion quality depending on the nature of the food product. Flocculation accelerates the rate of gravitational separation in dilute emulsions, which is undesirable because it reduces their shelf life. It also causes a pronounced increase in emulsion viscosity and may even lead to the formation of a gel. Some food products are expected to have a low viscosity and therefore flocculation is detrimental. In other products, a controlled amount of flocculation may be advantageous because it leads to the creation of a desirable texture (McClements and Weiss 2005; McClements 2005e).

Flocculation destabilization of an emulsion takes place by two mechanisms: bridging flocculation and depletion flocculation (Somasundaran and others 2006)

Bridging flocculation occurs when a polyvalent ion (such as Ca^{+2}, Mg^{2+} or Al^{3+}) or high molecular weight biopolymers (e.g. polysaccharides or proteins) exist at insufficient amount and simultaneously binds to the surface of droplets that have an opposite charge by forming bridges between two or more droplets. At sufficiently high biopolymer concentrations the flocs may not form (or can easily be disrupted) because there is sufficient biopolymer present to completely cover all droplet surfaces, and so a single biopolymer does not link more than one droplet (McClements 2005b; McClements and Weiss 2005).

Depletion flocculation occurs in the presence of nonadsorbing colloidal particles, such as biopolymers or surfactant micelles, in the continuous phase of an emulsion. The concentration gradient of polymers between narrow region surrounding droplets and the bulk solution generates an osmotic force This attractive force increases as the concentration of colloidal particles increases, until eventually, it may become large enough to overcome the repulsive interactions between the droplets and cause them to flocculate. The lowest concnetration required to cause depletion flocculation is referred to as the CFC (critical flocculation concentration). The CFC decreases as the size of the emulsion droplets increases and the effective volume fraction of the colloidal particles (directly related to molecular weight of polymer) increases (McClements 2005b; McClements and Weiss 2005; Somasundaran and others 2006)

2.2.4.3 Coalescence

Coalescence is the process where two or more liquid droplets merge together to form a single larger droplet. In oil-in-water emulsions, coalescence eventually leads to the formation of a layer of oil on top of the material, which is referred to as oiling off. In water-in-oil emulsions, it leads to the accumulation of water at the bottom of the material (McClements 2007). Improving the stability of an emulsion to coalescence may be achieved by preventing droplet flocculation, preventing formation of a creamed layer, reducing the droplet concentration, and altering the rheological properties of the interfacial membrane to improve rupture resistance (McClements and Weiss 2005).

2.2.4.4 Ostwald ripening

Ostwald ripening is the process whereby large droplets grow at the expense of smaller ones, it arises from emulsion polydispersity and the difference in solubility between small and large droplets, is the main mechanism for nanoemulsion destabilization (Solans and others 2005; Coupland 2005).

The increase in solubility with decreasing droplet size means that there is a higher concentration of solute around a small droplet than around a larger one. The solute molecules therefore move from the smaller droplets to the larger droplets because of this concentration gradient. This process causes the smaller droplets to shrink, and the larger droplets to grow, leading to an overall net increase in the mean droplet size with time (Solans and others 2005; Tadros and others 2004). The solubility of oil in water is so low for most food oils that the rate of Ostwald ripening is usually negligible (Coupland 2005). Nevertheless, it is important in O/W emulsions that contain more water-soluble lipids (e.g., flavor oils or essential oils) or when the aqueous phase contains alcohol (e.g., cream liqueurs) (McClements 2007).

Several methods may be applied to reduce Ostwald ripening: Addition of a small amount of second oil with low solubility in the aqueous phase prior to homogenization. The mass transport of molecules from one droplet to another depends on the rate at which the molecules diffuse across the interfacial membrane. It may therefore be possible to retard Ostwald ripening by decreasing the diffusion coefficient of the dispersed phase in the membrane, or by increasing the thickness of the membrane (Solans and others 2005; Tadros and others 2004).

2.2.5 Layer by layer (LBL) depositioning technique

These systems typically consist of oil droplets (the core) surrounded by nanometer thick layers (the shell) comprised of different polyelectrolytes. This interfacial engineering technology would utilize food-grade ingredients (such as proteins, polysaccharides, and phospholipids) and processing operations (such as homogenization and mixing) that are already widely used in the manufacture of food emulsions (Weiss and others 2006).

Modifying and controlling interfacial layer coating of lipid droplets e.g. its composition, charge, thickness, rheology, environmental responsiveness may provide various advantages over conventional singe layered emulsions.

- Improved physical stability to environmental stresses such as pH, salt, heating, freeze–thaw cycling, drying and mechanical agitation. For example, thick and dense interfacial layers can be designed to increase the effective density of multilayer-coated oil droplets, thereby improving their stability to creaming. On the other hand, thick and highly charged interfacial layers can be designed to decrease the attractive and increase the repulsive colloidal interactions between multilayer-coated lipid droplets, thereby improving their stability to flocculation and coalescence. Finally, mechanically strong interfacial coatings can be designed to slow down Ostwald ripening in emulsions (Thanasukarn and others 2006; Aoki and others 2005; Ogawa and others 2004).
- Improved chemical stability to oxidation reactions, e.g. interactions between lipids and metal ions can be minimized by controlling the interfacial charge and thickness (Shaw and others 2007; Klinkesorn and others 2005).
- Ability to trigger release of functional agents in response to specific changes in environmental conditions, such as dilution, pH, or temperature. For example, it is possible to cause interfacial layers to detach from the droplet surfaces when the pH is altered (McClements and others 2007; McClements and Li 2010).

2.2.5.1 Preparation methods

The principle behind the formation of multilayer emulsions is the use of a layer-by-layer (LBL) electrostatic deposition approach. In this method, an ionic emulsifier that rapidly adsorbs to the surface of lipid droplets during homogenization is used to produce a "primary" emulsion containing small droplets, then an oppositely charged polyelectrolyte is added to the system that adsorbs to the droplet surfaces and produces a "secondary" emulsion containing droplets coated with a two-layer interface. This procedure can be repeated to form oil droplets coated by interfaces containing three or more layers (Figure 2.13) (McClements and Li 2010). A colloidal dispersion stable to flocculation can be formed only only within a narrow concentration range of $C_{sat} < C < C_{dep}$, where C_{sat} is the minimum concentration of polymer required to cover the oppositely charged particles and C_{dep} is the polymer concentration where depletion flocculation occurs. At low polyelectrolyte concentrations the particles should be susceptible to bridging flocculation because there is insufficient polyelectrolyte present to completely saturate the surface of all the particles ($C < C_{sat}$).

However, if the polyelectrolyte concentration is increased further so that C_{dep} is exceeded then the particles will be susceptible to depletion flocculation, and it will not be possible to make a stable multilayer system (Guzey and McClements 2006).

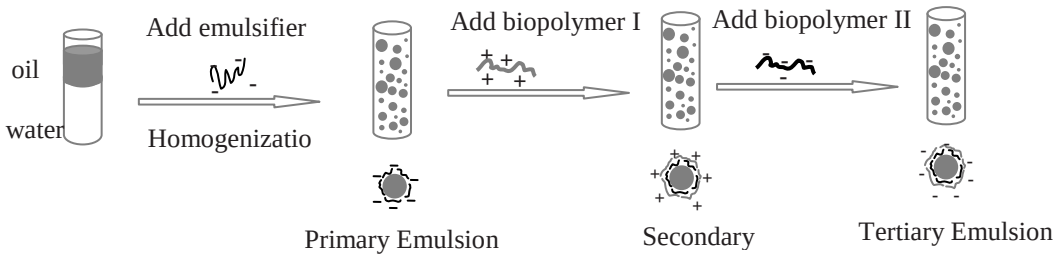

Figure 2.13: Schematic for formation of a number of nanolayers around particles.

For this reason, a washing step may be required between each electrostatic deposition step to remove any excess non-adsorbed polyelectrolyte remaining in the continuous phase. Otherwise, this free polyelectrolyte might interact with the next oppositely charged polyelectrolyte added to the system, thereby altering its tendency to adsorb to the droplet surfaces. Washing can be carried out by centrifugation or ultrafiltration of the emulsion after the coating procedure has been carried out. Alternatively, the solution conditions can be optimized so that there is little or no free polyelectrolyte remaining in the aqueous phase after the coating step. If necessary mechanical agitation is applied to the secondary emulsion to disrupt any flocs formed (McClements 2012a). It should be mentioned that in some systems it is possible to mix the colloidal particles and polyelectrolyte molecules together at a pH where they do not have opposite charges, and then adjust the pH to a value where they do have opposite charges so as to promote polyelectrolyte adsorption (Guzey and McClements 2006; Guzey and others 2004; Guzey and McClements 2007; McClements 2012a).It should be noted that the polyelectrolyte layers are held together by electrostatic attraction, and may therefore dissociate if the pH or ionic strength is changed. Dissociation can be prevented by covalently cross-linking the adsorbed layers after they have been formed around a lipid droplet, e.g., using enzymes, chemicals, or heating (McClements and others 2009; Zeeb and others 2012; Li and others 2012).

By manipulating the solution pH it is possible to control the degree of polyelectrolyte adsorption to the particle surfaces. Droplets stabilized by commercial polysaccharide emulsifiers tend to have a net negative charge (e.g., gum Arabic and

modified starch) due to the presence of anionic groups (e.g., sulfate or carboxyl) on the polymer chains. Droplets stabilized by proteins (e.g., whey protein, casein, soy proteins, egg proteins) have a net charge that depends on the solution pH relative to the isoelectric point (pI) of the adsorbed protein. Protein-coated droplets have a positive charge at pH<pI, are neutral at pH=pI, and a negative charge at pH>pI. Proteins with different isoelectric points can be selected for particular applications, e.g., β-lactoglobulin has a pI near 5, but lactoferrin has a pI near 8 (Guzey and McClements 2006; Guzey and others 2004; Guzey and McClements 2007; McClements 2012a).

The properties of multilayer emulsions can be manipulated by carefully controlling the ionic composition of the aqueous solution both during and after multilayer formation. The magnitude and range of electrostatic interactions between a polyelectrolyte and a droplet surface decrease as the ionic strength of the solution increases because of the accumulation of counter-ions around the surfaces, which is usually referred to as electrostatic screening. Electrostatic screening becomes stronger as the concentration and valency of the counter-ions in the solution increases. Multivalent counter-ions (e.g., Ca^{2+}, Fe^{2+}, Fe^{3+}) are much more effective at screening electrostatic interactions than monovalent counter-ions (e.g., Na^{+},Cl^{-},K^{+}). In the absence of salt or relatively low salt concentrations, polyelectrolytes tend to form relatively thin layers with the chains being flat against the surface. In solution, there is a strong electrostatic repulsion between different segments of the same polyelectrolyte chain, which causes the molecule to become highly extended (Figure 2.14). Consequently, when it first adsorbs to an oppositely charged surface it tends to lie flat and be spread out.

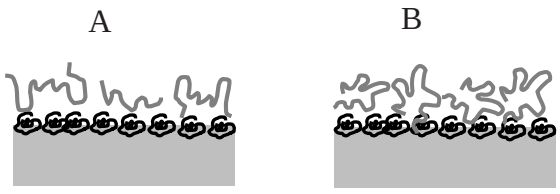

Figure 2.14: Effect of ionic strength on layer thickness and polymer orientation at the substrate surface; (A) at low ionic strength, and (B) at high ionic strength

On the other hand, in the presence of salt, polyelectrolytes often form thicker layers because they have a more compact chain conformation (ball-like conformation) in solution due to weaker intra-molecular repulsion. The interactions between segments of the polyelectrolyte chains and oppositely charged groups on the droplet surface will be weakened. For the same reasons, the total amount of polyelectrolyte adsorbed to the surface tends to be greater in the presence of salt than in its absence (Guzey and McClements 2006, 2007 Guzey and others 2004; McClements 2012a).

The characteristics of a polyelectrolyte multilayer may also be changed by adjustments in the ionic strength of solution after the polyelectrolyte layer has been formed. For example the permeability of a polyelectrolyte multilayer to small molecules can often be increased by increasing the ionic strength. At sufficiently high ionic strength one or more polyelectrolyte layers may become detached from the droplet surfaces because of the weakening in attractive electrostatic interactions (Guzey and McClements 2006, 2007; Guzey and others 2004; McClements 2012a).

2.3 Characterization Methods

In order to conduct a successful research about food dispersions, it is necessary to have access to a variety of analytical instruments that can provide detailed information about their properties.

2.3.1 Light scattering methods

The interaction of laser light with particles produces a scattering pattern due to reflection, refraction and/or diffraction phenomena. The basic assumption of laser diffraction, when determining particle size, is based on the fact that a particle passing through a laser beam will scatter light at an angle based on their size and the refractive index of the material under study (O'hagan and others 2005). The intensity of the scattered light can be affected by particle size, refractive index, number of particles, angle of observation as well as the wavelength of light. The higher the refractive index of the particles relative to the medium, the more light that will be scattered. There are two main techniques: (1) static light scattering and (2) dynamic light scattering

The static light scattering (also called laser diffraction) methods is based on the principle that a beam of light directed through a dispersion is scattered by the

particles in a well-defined manner (McClements 2005a). The technique of laser diffraction relies on the fact that particles passing through a laser beam scatter light at an angle that is inversely proportional to their size. Small particles scatter light at wide angles whereas large particles scatter light at small angles. That information is then passed to an algorithm designed to use Mie Scattering Theory which transforms the scattered light data into particle size information. The software finds the particle size distribution (PSD) that gives the best-fit between the measured scattering pattern and the theoretically predicted one, and then reports the data as a table or plot of particle concentration (number or volume) versus particle size (diameter or radius) (McClements 2007; Meeren and others 2004b).

The dynamic light scattering (DLS) also known as photon correlation spectroscopy (PCS) offers an alternative measurement and has been used for the size measurement of particles between about 3 nm and 5 μm in diameter. Instead of an array of detectors, a DLS analyzer captures light from one angle only (usually 90°). At any one angle, the intensity fluctuations occur over very short time periods when light is scattered by particles that change their relative spatial location due to random movement, Brownian motion, and then using a suitable mathematical model to convert the intensity fluctuations into a particle size distribution. The frequency of these intensity fluctuations depends on the speed at which the particles move, and hence on their size. Smaller particles move more rapidly than larger ones, and therefore give more rapid intensity fluctuations (McClements 2007; O'hagan and others 2005). The relationship between the size of a particle and its speed due to Brownian motion is defined in the **Stokes-Einstein** equation (2.2).

$$D = \frac{k_B T}{6\pi\eta R_H} \qquad \textbf{(2.2)}$$

Where D is diffusion coeffiecient of the particles, kB is the Boltzmann's constant, T is the temperature, η is the viscosity of the medium and RH is the hydrodynamic radius. This technique usually overemphasizes the contribution of larger particles to the size distribution.

This is partly because they tend to scatter more (i.e., have higher weighting factors), but also because of the nature of the correlation function itself, as the information about the small particles is contained only in the short-time part of the function, whereas information about the large particles is contained at all points (Dalgleish 2004).

Commercial light scattering instruments are capable of determining particle diameters within the range of below 100 nm to 1000 μm. In light scattering instruments it is usually assumed that the particles are spherical, homogeneous, and non-interacting. However, these assumptions may not be valid all the time, for example an emulsion containing flocs that are non-spherical and heterogeneous, and so the resulting particle sizing data should be treated with caution (Dalgleish 2004). These instruments normally require that the droplet concentration be relatively low (between 0.001 and 0.1 wt%) so as to be able to pass a light beam through and to avoid multiple scattering effects. Consequently, many food emulsions need to be diluted considerably prior to analysis (O'hagan and others 2005; McClements 2007). One must be aware that dilution and stirring of emulsions may cause appreciable alterations in particle size distribution, e.g. dilution and stirring are likely to disrupt any weakly flocculated droplets, but leave strongly flocculated droplets intact. In addition to that, when emulsion dilution is necessary prior to analysis, it is usually important to carry it out using a buffer solution that has the same properties as the continuous phase of the original emulsion, for example, pH and ionic strength (McClements 2005a). For that reason using only light scattering tehcniques may not be appropriate to understand the microstructure of emulsion, flocculates samples determined under microscope may not show increase in particle size when they measured by light scattering . Since dilution of emulsions where depletion flocculation is important may disrupt the flocs, the concentration of non-adsorbed polymer falls below the critical value required to promote droplet flocculation. Thus an emulsion that is highly flocculated in the original sample may appear non-flocculated after dilution (McClements 2007).

2.3.2 Microscopy

A number of microscopy techniques are available to provide information about the structure, dimensions, and organization of the components within food dispersions, for example, optical microscopy, electron microscopy, and atomic force microscopy

(AFM). Each microscopic technique works on different physicochemical principles and can be used to examine different levels and types of structural organization.

Nevertheless, each type of microscopy must have three qualities if it is going to be used to examine the structure of small objects: resolution, magnification and contrast. Most modern microscopes are attached to personal computers that can capture and store a digital version of the image, which can then be processed using various digital processing programs to obtain information about microstructure, e.g., particle size distribution, floc microstructure, floc size, fractal dimensions (McClements 2005a; McClements 2007).

2.3.2.1 Conventional optical microscopy

The main advantage of microscopy is that it is based on direct observation of the particles. In practice, it is difficult to obtain reliable measurements and it is said that light microscopy is applicable for particles larger than about 0.5 μm (Meeren and others 2004b; McClements 2005a). This is because of technical difficulties associated with the design and manufacture of the optical components with the microscope and because the Brownian motion of small particles causes images to appear blurred. The optical microscope therefore has limited application to food nanoedispersions because they contain structures with sizes below the lower limit of resolution. Nevertheless, it can provide valuable information about the size distribution of droplets in emulsions that contain larger droplets, and can often be used to distinguish between flocculation and coalescence, since only measurement of particle size may not be enough to differentiate (McClements 2005a; McClements 2007).

The natural contrast between the major components in food emulsions is often fairly poor (because they have similar refractive indices), which makes it difficult to reliably distinguish using conventional bright-field optical microscopy. For this reason, various types of chemical stain that bind to particular components within an emulsion (e.g., the proteins, polysaccharides, or lipids) or preferentially partition into either the oil or the aqueous phase has been used to enhance the contrast, improve the image quality, and provide more detailed information about the composition and microstructure of system. The contrast between different components can be improved without using chemical stains by modifying the design

of the optical microscope, e.g. by using *phase contrast* or *differential interference contrast (DIC)* microscopy. *Fluorescence microscopy* can be used to highlight particular structures within an emulsion by selecting fluorescent dyes that specifically bind to them. Certain food components either fluoresce naturally or can be made to fluoresce by adding fluorescent dyes that bind to them (McClements 2005a; McClements 2007).

2.3.2.2 Laser scanning confocal microscopy (LSCM)

LCSM can provide higher clarity images than conventional optical microscopy, and often allows the generation of three-dimensional images that can be used to determine the spatial location of the droplets in an emulsion. In the LCSM technique, sample components are scanned point by point with a focused laser beam. The reflected or emitted light (fluorescence) from the specimen is detected by two photomultipliers, digitized, and displayed on a monitor. The LSCM technique suffers from some of the same problems as conventional optical microscopy, but it has a better resolution and sensitivity, and the sample preparation is often less severe (McClements 2005a; McClements 2007).

2.3.2.3 Electron microscopes

Scanning or transmission electron microscopes use electron beams, rather than light photons to form a magnified image of the specimen (Bouchon and Aguilera 2008). Electron beams have much smaller wavelengths than light and so they can be used to examine much smaller objects. Two types of electron microscope are commonly used to examine the structure of food systems: transmission electron microscopy (TEM) and scanning electron microscopy (SEM). TEM normally produces a two-dimensional image of a thin slice of specimen, whereas SEM produces a more three-dimensional looking image of the topography of a specimen. The resolving power of SEM is about 3–4 nm, which is an order of magnitude worse than TEM, but about two or three orders of magnitude better than optical microscopy. Another major advantage of SEM over optical microscopy is the large depth of field, which means that images of relatively large structures are all in-focus (McClements 2005a). Traditionally, it was necessary to keep electron microscopes under high vacuum because electrons are easily scattered by atoms or molecules in a gas. This meant that the sample must undergo extensive preparation procedures (e.g., fixation,

dehydration) and not contain any ingredient that might evaporate under the intense energy of the electron beam. A method for overcoming these difficulties, which allows observation at atomic resolution while keeping the sample in a hydrated state, consists of rapidly freezing the sample in a cryogenic liquid. In order to alter minimally the specimen microstructure, extre mely high freezing rates must be achieved. This Cryogenic SEM or TEM technique involves quenching the sample in subcooled nitrogen or in liquid propane and then transfer to the vacuum chamber, where it can be fractured, etched, and heated to remove surface ice. Subsequently, the sample still will be in the frozen state. The prepared sample is then directly transferred to the cold stage of the microscope by an exchange air lock (Bouchon and Aguilera 2008).

2.3.2.4 Atomic force microscopy (AFM)

AFM creates an image by scanning a tiny probe (similar to the stylus of a record player, but only a few micrometers in size), across the surface of the specimen being analyzed. When the probe is held extremely close to the surface of a material it experiences a repulsive force, which causes the cantilever to which it is attached to be bent away from the surface. The extent of the bending is measured using an extremely sensitive optical system. By measuring the deflection of the probe as it is moved over the surface of the material it is possible to obtain an image of its structure (McClements 2005a).

2.3.3 Measurement of surface charge

The main purpose of surface charge analysis is to gain a better understanding of the physicochemical background such as creaming, flocculation, or thickening. Besides, surface charge analysis is one of the techniques that provide information about the interactions between the various food components, such as dispersed particles, surfactants, ions, and polyelectrolytes. The electrical characteristics of a particle are usually characterized in terms of its surface electrical potential (ψ), surface charge density (σ) and/or zeta-potential (ζ). Practically, the ζ -potential is often a better representation of the electrical characteristics of a particle in dispersions because it inherently accounts for the adsorption of any charged counter ions. In addition, the ζ -potential is much easier to measure than the electrical potential or the surface

charge density, and therefore droplet charges are usually characterized in terms of ζ. It is also an aid in predicting long-term stability (Meeren and others 2004a).

Zeta potential (ζ) is the potential difference between the dispersion medium and the stationary layer of fluid attached to the dispersed particle. The liquid layer surrounding the particle exists as two parts; an inner region (Stern layer) where the ions are strongly bound and an outer (diffuse) region where they are less firmly attached (Figure 2.15).

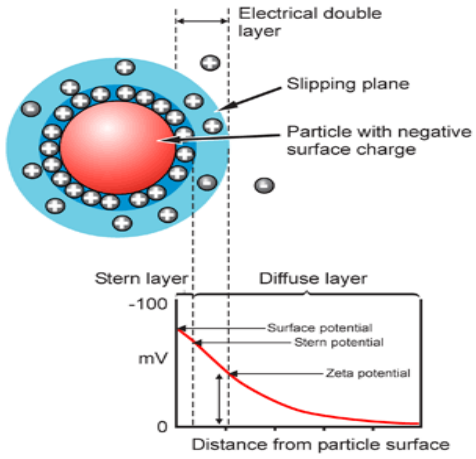

Figure 2.15: The Stern and diffuse layer.

For example, if the particle is negative, it causes some of the positive ions (often called *counter ions*) in solution to be attracted and firmly attached to a layer around the surface of the particle; this layer of counter ions is known as the *Stern layer*. Additional positive ions are still attracted by the negative particle, but now repelled by the Stern layer as well as by other positive ions that are trying to approach to the particle.

This dynamic equilibrium results in the formation of a *diffuse layer* of counterions. They have a high concentration near the surface which gradually decreases by distance, until it reaches the equilibrium with the counter-ion concentration in the solution.

In a similar, but opposite, there is a lack of negative ions in the neighborhood of the surface because they are repelled by the negative particle. Negative ions are called *co-ions* because they have the same charge as the particle. Their concentration will gradually increase with distance, as the repulsive forces of the particle are screened out by the positive ions, until equilibrium is again reached. The diffuse layer can be

visualized as a charged atmosphere surrounding the particle. The charge density at any distance from the surface is equal to the difference in concentration of positive and negative ions at that point. Charge density is greatest near the particle and gradually diminishes toward zero as the concentration of positive and negative ions merge together it reaches equilibrium. The attached counter-ions in the Stern layer and the charged atmosphere in the diffuse layer are referred to as the *double layer*.

The double layer is formed in order to neutralize the charged colloid and, in turn, causes an electrokinetic potential between the surface of the colloid and any point in the mass of the suspending liquid.This voltage difference is referred to as the surface potential. The magnitude of the surface potential is related to the surface charge and the thickness of the double layer. As we leave the surface, the potential drops off roughly linearly in the Stern layer and then exponentially through the diffuse layer, approaching zero at the imaginary boundary of the double layer. This boundary where Stern layer and diffuse layer meet is called the surface of hydrodynamic shear or slipping plane (Figure 2.15).

When a particle moves (e.g. due to gravity), ions within the boundary move with it, but any ions beyond the boundary do not travel with the particle and stay with the bulk dispersant. The potential at this boundary is known as the zeta potential (ζ).

The zeta potential cannot be measured directly; however, it can be calculated using theoretical models and from experimentally determined electrophoretic mobility data. When an electric field is applied across an electrolyte, charged particles move towards the electrode of opposite charge. Viscous forces acting on the particles tend to oppose this movement. When equilibrium is reached between these two opposing forces, the particles move with constant velocity.The velocity of the particle is dependent on the strength of electric field or voltage gradient; the dielectric constant of the medium; the viscosity of the medium and the zeta potential. The velocity of a particle in an electric field is commonly referred to as its Electrophoretic mobility. With this knowledge we can obtain the zeta potential of the particle by application of the **Henry equation** (2.3).

$$U_E = \frac{2\varepsilon\zeta f(ka)}{3\eta} \qquad \textbf{(2. 3)}$$

Where is U_E=electrophoretic mobility, ζ = zeta potenatial and ε = dielectric constant η = viscosity and f (*ka*)= Henry's function. The units of "k^{-1}" is taken a measure of electrical double layer thickness and the parameter "a" refers to the radius of particle size and therefore "ka" measures the ratio of the particle radius to the electrical double layer thickness. Electrophoretic determinations of zeta potential are most commonly done in aqueous media and moderate electrolyte concentrations. In this case F(ka) is 1.5 and this is referred to as the *Smoluchowski* approximation, for small particles in low dielectric constant media (eg non-aqueous media) it becomes 1.0 and is referred to as the *Huckel* approximation.

3. OPTIMIZATION OF CONDITIONS FOR THE PREPARATION OF QUERCETIN NANOEMULSIONS USING RESPONSE SURFACE METHODOLOGY

3.1 Introduction

Quercetin's low solubility in water (0.17-7.7 μg/ml), artificial gastric juice (5.5 μg/ml), and artificial intestinal juice (28.9 μg/ml) has limited its absorption upon oral administration (Gao Y and others 2009). After being received quercetin aglycone orally, only in a relatively few studies it can be detected in plasma and urine (Erlund 2004). Many approaches have been introduced to increase the water solubility and/or bioavailability of food bioactives by methods such as microemulsion (Gao Y and others 2009), incorporating into solid lipid nanoparticles (Li and others 2009), complexation with cyclodextrin (Lucas-Abellán and others 2007); (Zheng and Chow 2009), and liposome encapsulation (Zhang and others 2006). The combination of lipids and emulsifiers enhances the absorption of quercetin significantly which is strongly affected by its solubility in the vehicles used for the administration (Azuma K and others 2002). The enhancement of bioavailability by application of O/W microemulsions may be related to the better uptake of nanocarriers through to the gastrointestinal tract and also due to the decrease of degradation and/or metabolization of drugs. However, in spite of numerous advantages compared with other colloidal vehicles, such as thermodynamic stability, simple technology of sample preparation, optical transparency and low viscosity, microemulsions often require a higher oil or surfactant contents and the presence of cosurfactants (short- or medium chain alcohols) which is generally considered undesirable because of potential toxicity issues.(Rogerio and others 2010).

For food applications, the delivery vehicle must be prepared from only food-grade ingredients and this requirement limits the number of surfactants that can be used. Nonionic surfactants can be useful alternatives to design delivery systems and sorbitan esters (Tweens or Spans) for example due to their low toxicity, lack of irritability, and the capacity to easily form nanoemulsions (McClements and Rao

2011). Although they have been reported to have minimal toxicity, the biodegradability of many nonionic surfactants raises issues regard to long-term toxicity, especially in chronic use. For this reason, their concentration in delivery systems must be reduced (Lawrence and Rees 2000). In contrast to microemulsions, nanoemulsions can be prepared by reasonable surfactant concentrations (less than 10%), and posses very small droplet size and high kinetic stability. Therefore, one has to balance the benefits brought by the use of bioactives and potential side effects (e.g., obesity, cardiovascular diseases etc.) caused by the use of high amount of lipids and surfactants (Qingrong and others 2010).

Nanoemulsions provides high kinetic stability, they do not cream (or sediment) because the Brownian motion is larger than the small creaming rate induced by gravity. The internal phases of nanoemulsions supply an excellent reservoir for phytochemicals that need protection and transportation. Their small droplet sizes in the range of 50-200nm, much smaller than the range from 1 to 100 μm of conventional emulsions, enhance not only stability of the emulsions, but also the bioavailability of the encapsulated phytochemicals (Gutiérrez and others 2008; Huang and others 2010).

Different factors including process conditions and emulsion composition influence the physicochemical properties of the nanoemulsions. Response-surface methodology (RSM) is an effective technique for exploring the relationships between the responses and the independent variables, and optimizing the process conditions or product formulation (Yuan and others 2008; Anarjan and others 2010)

The aim of the present study is to prepare quercetin (QT) loaded nanoemulsions with food grade ingredients by using high pressure homogenization, and to optimize the pressure, emulsifier and oil concentration with the smallest particle size and greatest stability by using RSM.

3.2 Materials and Methods

3.2.1 Materials

Quercetin dihydrate (QT) (purity >90%) was obtained from Merck Chemicals. Food grade limonene oil and medium chain triacylglycerol (oil, MCT) were kindly provided by Florida Chemical Company (FL, USA) and by Stepan Company

(Northfield, IL), respectively. Polyoxyethylene (20) sorbitan monooleate (Tween 80; T80), Sorbitan monododecanoate (Span 20; S20), Ethanol, sodium azide (NaN_3) were purchased from Sigma-Aldrich Company (St. Luis, MO). Milli-Q water was used in all experiments.

3.2.2 Solubility of quercetin

The solubility of quercetin (QT) in limonene oil, MCT and oils mixed with emulsifiers (Span 20 and Tween 80) were investigated. An excess amount of QT was added to 3 g of oil and mixed at room temperature and 130 ºC for 30 min on a magnetic stirrer and filtered through 0.45 µm filter afterwards. The filtrate was diluted with ethanol and UV-Vis absorbance at 373 nm was measured with Cary UV–Vis spectrophotometer (Varian Instruments, Walnut Creek, CA) with 1 cm optical path. The quantity of QT was determined according to calibration curve of QT (R^2=0.997; y=0.074x-0.032) in ethanol in the concentration range of 2-15 ppm.

3.2.3 Screening of emulsion formulations by constructing of phase diagram

Nine different formulations were initially prepared by mixing oil and surfactant with different weight ratios changing from 1:9 to 9:1. After homogenization by high speed homogenizer (HSH; ULTRA–TURRAX T-25 basic , IKA Works Inc., Wilmington, USA) at 24 000 rpm for 5 min., some part of the sample was collected in a tube for stability investigation, while the other part was serially diluted in water and treated by HSH. The amount of aqueous phase added was varied to produce a water concentration in the range of 5% to 90% of total volume to generate the other points in the phase diagram. All samples stored at room temperature. After 24 h from preparation, the state of the emulsified systems was visually evaluated and classified as physically unstable or stable systems (Donsì and others 2010a).

3.2.4 Preparation of quercetin nanoemulsion

After determination of stable emulsion region in the pseudoternary phase diagram, experimental conditions determined by RSM were prepared as following: Quercetin (QT) was first dissolved in the mixture of limonene oil and Tween 80 at different concentrations and mixed 24 hours on a magnetic stirrer at room temperature to get complete solubilization, after that the oil phase mixed with Span 20 and water. The premix was homogenized using HSH at 24 000 rpm for 5 min to form a coarse

emulsion, followed by a high pressure homogenization (HPH, High pressure homogenizer, EmulsiFlex-C3, AVESTIN Inc., Ottawa, Canada) for 6 cycles at predetermined pressures. All formulations included NaN_3 as an antimicrobial agent at 0.01wt% in final concentration. The homogenization temperature was set at 25ºC. After homogenization, the emulsions were collected and stored at room temperature; their particle size and stability were analyzed.

3.2.5 Particle size analysis

The hydrodynamic diameter (z-average) of the emulsion droplets was measured using photon correlation spectroscopy (PCS)-based BIC 90 plus particle size analyzer equipped with a Brookhaven BI-9000AT digital correlator (Brookhaven Instrument Corporation, New York). The samples approximately diluted 100 times with Milli-Q water prior to the measurement to prevent multiple scattering and then placed in the cuvette holder, which was kept at temperature of 25.0 ± 0.1 °C. The light source of the particle size analyzer is a solid state laser operating at 658 nm with 30 mW power, and the signals were detected by a high sensitivity avalanche photodiode detector. The normalized field-field autocorrelation function g (q,t) is obtained from the intensity-intensity autocorrelation function, G(q,t), via the Sigert relation (Stepanek 1993; Wang and others 2008).

3.2.6 Stability of quercetin nanoemulsions

The stability of emulsions was defined in two terms, droplet growth ratio and stability of QT in nanoemulsion system. Since the QT emulsion in our system tends to aggregate by storage, the droplet size of emulsions at the bottom of test tubes by time (until day 12) was measured and the change in size compared to the day of preparation was defined as droplet growth ratio. QT stability of emulsion formulations was determined by taking samples from upper phase of test tubes at day 0, 4, 7 and 14 and UV-Vis absorbance at 373 nm was measured after diluted by ethanol. If the nanomulsions are not stable, the QT encapsulated will be released and the UV/Vis absorption of the sample will decrease by time (Wang and others 2008; Lin and others 2009)

$$\text{Droplet growth ratio} = \frac{\text{Particle size at day 12} - \text{Particle size at day 0}}{\text{Particle size at day 0}} \qquad \textbf{(3.1)}$$

$$\text{QT stability ratio} = \frac{\text{Absorbance at day 14}}{\text{Absorbance at day 0}} \quad \textbf{(3.2)}$$

3.2.7 Experimental design

After determination of stable emulsion region in the pseudoternary phase diagram**,** RSM was used to study the effect of the independent variables: pressure (X_1), concentration of emulsifier (X_2), concentration of oil (X_3) on the dependent variables: particle size (Y_1), droplet growth ratio (Y_2) and stability of QT (Y_3) in nanoemulsions. QT loading was set at 0.25% (w/w) for all formulations. The coded and uncoded independent variables used in the RSM design were listed in Table 3.1.

Table 3.1: Uncoded and coded independent variables used in RSM design

Independent variables	**Coded levels**					
	Symbol	**-α**	**-1**	**0**	**1**	**+α**
Pressure (MPa)	X_1	52	80	120	160	187
Emulsifier concentration (%)	X_2	4.95	7	10	13	15.05
Oil concentration (%)	X_3	9.95	12	15	18	20.05

α= 1.682 for 3 factor central composite design, number of run is 18 when the center point # is 4

A five-level central composite rotatable design was used for the RSM studies, and 18 experimental settings were generated with 3 factors as shown in Table 3.2. Individual experiments were carried out in randomized order. Optimization of the emulsion formulations in terms of pressure and oil and emulsifier concentrations was achieved by an evaluation of the contour plots. A second-order polynomial equation was used to express predicted responses (particle size: Y_1; droplet growth ratio: Y_2; stability of QT in emulsion: Y_3) as a function of the independent variables as follows:

$$Y_i = a_0 + a_1X_1 + a_2X_2 + a_3X_3 + a_{12}X_1X_2 + a_{13}X_1X_3 + a_{23}X_2X_3 + a_{11}{X_1}^2 + a_{22}{X_2}^2 + a_{33}{X_3}^2 \quad \textbf{(3.3)}$$

where X_i represents the independent variables, a_0 is a constant, a_i, a_{ii} and a_{ij} are the linear, quadratic and interactive coefficients, respectively. The significance of the estimated regression coefficient for each response variable was assessed at a

probability (*P*) of 0.05. The experimental design matrix, data analysis was performed using Statistica 8 (StatSoft, Inc., 2007).

3.2 Statistical analysis

Experimental data was analyzed by multiple regressions to fit the second order polynomial equation to all independent variables. The goodness of fit of the model was evaluated by the coefficient determination (R^2) and the analysis of variance (ANOVA).

To visualise the relationships between the responses and the independent variables, surface response and contour plots of the fitted polynomial regression equations were generated using Statistica 8 (StatSoft, Inc., 2007) software. The optimal conditions for the targeted responses were generated by the Modde 8.0 (Umetrics) software to validate the model.

3.3 Results and Discussion

3.3.1 Solubility of quercetin

The solubility of QT determined using two kinds of oil, limonene oil and medium chain triglyceride (MCT), and their combinations with emulsifiers, Tween 80 and Span 20, at room temperature and at 130°C. At room temperature, the solubility of QT in limonene oil was around two times higher than that of in MCT. When the oil was heated at 130 ºC at 30 min, the solubility of QT in both oils increased to the same levels. The solubility was drastically increased when limonene oil was mixed with Tween 80 depending on emulsifier concentration. Its solubility increases when T80 is mixed with limonene oil in different concentrations. Limonene oil and MCT were mixed with S20 at a ratio of 1:2 (w/w), the solubility values were considerably lower than that of limonene oil mixed with T80 (Table 3.3 and Figure 3.1).

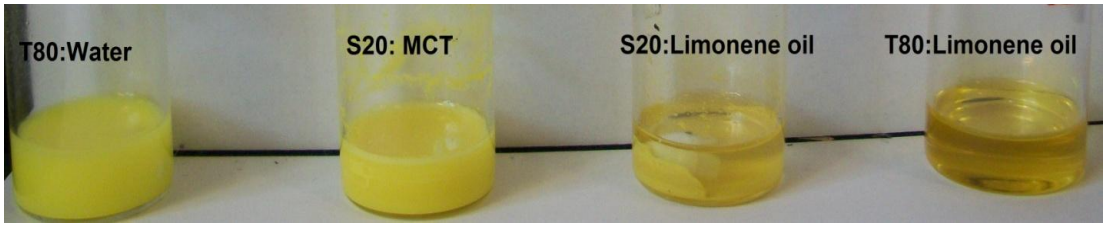

Figure 3.1: Solubility of QT in different environments at room temperature (T80: Water (1:16, w/w); S20: MCT (1:2, w/w); S20: Limonene oil (1:2, w/w) and T80: Limonene oil (1:2 w/w)).

Table 3.2: Experimental values of particle size and stability of QT nanoemulsions obtained from the central composite experimental design.

	Coded Values			**Decoded Values**			**Experimental values**		
Run#				X_1	X_2	X_3	Y1	Y_2	Y_3
1	-1	-1	-1	80	7	12	155.30	0.960	0.962
2	1	-1	-1	160	7	12	122.20	0.231	0.893
3	-1	1	-1	80	13	12	142.9	0.620	0.883
4	1	1	-1	160	13	12	106.25	0.802	0.744
5	-1	-1	1	80	7	18	123.60	0.915	0.742
6	1	-1	1	160	7	18	109.93	0.387	0.716
7	-1	1	1	80	13	18	117.60	0.341	0.887
8	1	1	1	160	13	18	99.70	0.242	0.834
9	**-α**	0	0	52	10	15	133.50	0.626	0.920
10	**+α**	0	0	187	10	15	116.00	0.060	0.860
11	0	**-α**	0	120	4.95	15	129.60	0.494	0.773
12	0	**+α**	0	120	15.05	15	108.10	0.290	0.976
13	0	0	**-α**	120	10	9.95	159.80	0.636	0.895
14	0	0	**+α**	120	10	20.05	108.70	0.331	0.800
15	0	0	0	120	10	15	111.30	0.388	0.927
16	0	0	0	120	10	15	112.30	0.432	0.842
17	0	0	0	120	10	15	103.07	0.621	0.852
18	0	0	0	120	10	15	110.73	0.511	0.845

X_1: Pressure, X_2: Emulsifier Concentration (%), X_3: Oil Concentration (%), Y_1: Particle size at day 0, Y_2: droplet drowth ratio at day 12, Y_3: QT stability ratio at day 14

Since the solubility of QT is highest at limonene oil mixed with Tween 80, the limonene oil was chosen as oil phase in the following formulations. A number of studies have shown that the solubility of highly hydrophobic compounds in oil phases can be increased by using mixtures of hydrophilic and lipophilic surfactants (Pouton and Porter 2008; Li and others 2012).

The ratio of hydrophilic (Tween 80 with a HLB value of ~18) to lipophilic surfactant (Span 20 with a HLB vlaue of ~6) was chosen as (1:1, w/w). Because it was found that, when the limonene oil was used as oil phase, the emulsion formulations prepared with the mixture of Tween 80 and Span 20 as emulsifiers had the smallest droplet size, having a HLB value of 12 (Kaufman and Garti 1984; Kourniatis and others 2010). In another study the stability and formation of orange oil/water nanoemulsions by high pressure homogenizer in the presence of mixtures of nonionic surfactants, having different HLB values, varying their type and concentration were evaluated. The results also showed that the optimal HLB range of the surfactant mixtures to obtain stable o/w nanoemulsions was around 12 (Kourniatis et al. 2010).

Table 3.3: Solubility of quercetin (mg/g) in limonene oil and medium chain triglyceride (MCT) and their combination with emulsifiers Tween 80 (T80) and Span 20 (S20).

Oil type	@ room temperature	@ 130°C	**Mixed with emulsifiers (w:w)**				
			T80:oil				S20:oil
			1:1	1:2	1:4	1:6	1:2
Limonene oil	0.62±0.09	2.29±0.5	39.47±6.4	27.24±3.6	19.82±1.4	13.16±2.7	1.23±0.1
MCT	0.28±0.06	2.09±0.5	*	*	*	*	1.98±0.4

Data represents the avarage of three measurements carried out in duplicate samples
*MCT and T80 does not mix

3.3.2 Screening of emulsion formulations by constructing of phase diagram

Nanoemulsions are prepared by application of high speed homogenization (HSH) to produce coarse emulsion and followed by high pressure homogenization (HPH) to produce the secondary nanoscale emulsions. The stability of the coarse emulsions was evaluated for different formulations in terms of emulsifier and oil content, and reported in the pseudoternary phase diagram, shown in Figure 3.2. Pseudoternary phase diagrams are frequently used, especially in the formulation of self emulsifying drug delivery systems, which are thermodynamically stable emulsions (Donsì and others 2010a). In the triangular phase diagram of Figure 3.2, the first axis represents the water, the second to limonene oil and the third represents the emulsifier mixture of Span 20 and Tween 80 at a fixed ratio (1:1, w/w).

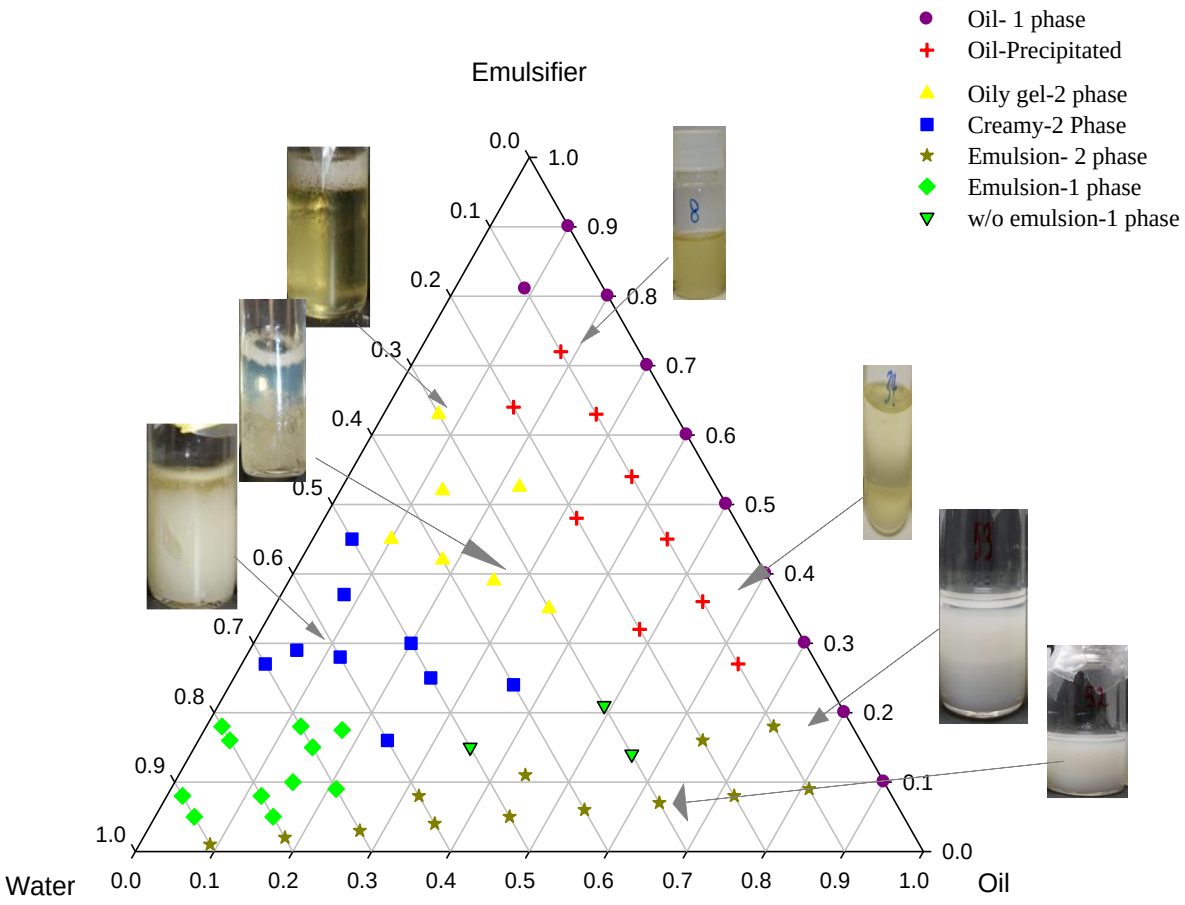

Figure 3.2: Pseudoternary phase diagram and stability of limonene oil-emulsifier (S20:T80 (1:1, w/w)-water system homogenized by HSH.

In the present study, we used the pseudoternary phase diagram as a compositional map for the identification of the optimal conditions to obtain kinetically stable emulsions, in terms of minimization of the amount of emulsifiers to be employed.

Nine different samples were initially prepared by mixing only the emulsifier and oil at different ratios (from 1:9 to 9:1), which on the diagram are located on the right side of the triangle, and homogenized by HSH. The other points reported in the diagram are generated by the serial water dilutions of the original nine mixtures. After 24h from preparation, the state of the emulsified system was visually evaluated and classified. By the addition of water into oil and emulsifier mixtures, precipitation of the bottom of the tube was observed when water content was 10-20% and oil content was 15-65%. Addition of more water until 50% and when the oil content was lower than 50% an oily gel phase occurred which had seperated after 24h from preparation.While the water content increased beyond 50% until 70% in the presence of emulsifier content higher than 25% and up to 30% of oil content, an unstable creamy phase observed which had shown two layers afterwards. When the oil content was between 35-55% and emulsifier content was 15-20%, the stable water in oil (w/o) emulsion region was observed, as well. Stable oil in water (o/w) emulsion phase occurred while the oil content was lower than ≤30% and emulsifier content was lower than < 20% (Figure3.2). The stable emulsion region found in pseudoternary phase diagram was further processed by HPH and the effect of independent variables (pressure, emulsifier and oil concentration) on particle size, droplet growth ratio and QT stability in nanoemulsion formulations was studied by using response surface methodology.

3.3.3 Analysis of response surface model

3.3.3.1 Fitting the models

The particle size and stability values of the QT nanoemulsions obtained from all the experiments are given in Table 3.2. The experimental data was used to calculate the coefficients of the quadratic polynomial equations, which were used to predict the values of particle size and stability of the emulsions. The particle size change belongs to day 12 was used in the response surface model, since the droplet growth showed highest value at day 12. Changes in QT stability of emulsions on day 14 were used in the experimental model. Analysis of variance (ANOVA) in Table 3.4 indicated that quadratic polynomial models were adequate for the prediction. The models showed no lack of fit because *p* values of particle size, emulsion droplet growth and QT stability (0.1355, 0.2760 and 0.2714) were higher than $p > 0.05$ and

coefficients of multiple determinations, R^2, being 0.9171, 0.8545, 0.7794, all indicate that models fit the experimental data points. For any of the terms in the models, a small *p*-value would indicate a more significant effect on the respective response variables. The linear term of oil concentration and homogenization pressure ($p < 0.01$), emulsifier concentration ($p < 0.05$), quadric term of oil concentration ($p < 0.01$), homogenization pressure ($p < 0.05$) and the interactive terms of pressure and oil concentration had a significant effect ($p < 0.05$) on the particle size of the nanoemulsions. The shear forces and turbulence, both of which are pressure dependent, produced during homogenization would affect the particle size and size distribution. Our results were agreed with other studies showing that increased emulsifier concentration and pressure resulted decrease in particle size (Yuan et al. 2008a; Anarjan et al. 2010; Jafari and others 2007; Yuan and others 2008c).

At constant oil content, increasing either emulsifier content or pressure had a tendency of producing smaller dropletsUpto a certain level of oil content, particle size became smaller at incresed pressures, beyond that level of oil concentration particle size change had not been affected by pressure change. This trend might be expected because increased pressure would cause larger oil droplets rupture into smaller droplets and there should be more amount of emulsifier present to cover freshly formed droplet surfaces during homogenization (Qian and McClements 2011) (Figure 3.3).

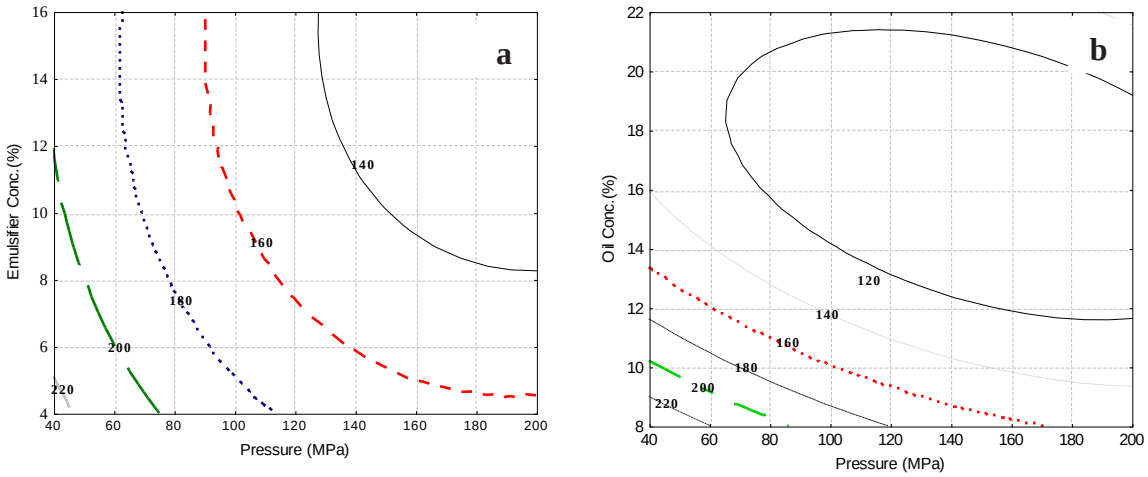

Figure 3.3: Contour plots of the particle size (nm) of the nanoemulsions as a function of pressure and emulsifier concentration % (a) at the oil concentration of 10%, and as a function of pressure and oil concentration% (b) at the emulsifier concentration of 10%.

Table 3.4: Analysis of variance of the regression coefficients of the fitted quadratic equations for the particle size, and stability (droplet growth ratio and quercetin stability) of nanoemulsions.

Dependent variable	Independent variable	Coefficient	*p* value	Model Fit
Particle size	Pressure	-1.4006	0.0036[b]	R^2=0.9171
	Pressure ^{2}	$2.71.10^{-3}$	0.0357[a]	
	Emulsifier conc.	-8.7067	0.0141[a]	
	Emulsifier conc.^{2}	$2.59.10^{-1}$	NS	
	Oil conc.	-36.324	0.0019[b]	
	Oil conc.^{2}	$8.64.10^{-1}$	0.0073[b]	
	Pressure X Emulsifier Conc.	$8.17.10^{-3}$	NS	
	Pressure X Oil Conc	$-3.98.10^{-2}$	0.0498[a]	
	Emulsifier Conc. X Oil Conc.	$1.68.10^{-1}$	NS	
	Constant	563.3528	0.0000[b]	
Lack of fit			0.1355	
Droplet growth ratio	Pressure	$-1.41.10^{-2}$	0.0110[a]	R^2=0.8545
	Pressure ^{2}	$-1.07.10^{-5}$	NS	
	Emulsifier conc.	$8.17.10^{-3}$	NS	
	Emulsifier conc.^{2}	$1.04.10^{-4}$	NS	
	Oil conc.	$1.19.10^{-3}$	0.0460[a]	
	Oil conc.^{2}	$3.68.10^{-3}$	NS	
	Pressure X Emulsifier Conc.	$1.39.10^{-3}$	0.0188[a]	
	Pressure X Oil Conc	$-8.30.10^{-5}$	NS	
	Emulsifier Conc. X Oil Conc.	$-1.32.10^{-2}$	0.0460[a]	
	Constant	1.8343	0.0025[b]	
Lack of fit			0.2760	
QT stability ratio	Pressure	$-1.62.10^{-3}$	NS	R^2=0.7795
	Pressure ^{2}	$-2.51.10^{-7}$	NS	
	Emulsifier conc.	$-7.01.10^{-2}$	NS	
	Emulsifier conc.^{2}	$-5.43.10^{-4}$	NS	
	Oil conc.	$-4.71.10^{-2}$	0.0471[a]	
	Oil conc.^{2}	$-1.61.10^{-3}$	NS	
	Pressure X Emulsifier Conc.	$-1.01.10^{-4}$	NS	
	Pressure X Oil Conc	$1.32.10^{-4}$	NS	
	Emulsifier Conc. X Oil Conc.	$6.82.10^{-3}$	0.0201[a]	
	Constant	1.7503	0.0000[b]	
Lack of fit			0.2714	

[a] Statistically significant at $p<0.05$; [b] Statistically significant at $p<0.01$; NS, not significant ($p>0.05$)

The linear term of oil concentration and homogenization pressure had a significant effect ($p < 0.05$) on the particle size stability of the nanoemulsions. Figure 3.4 shows the effect of oil and emulsifier concentration on the droplet growth ratio and quercetin stability in nanoemulsions. Interaction between these two componenets appeared as saddle surfaces, where particle size stability increased (smaller droplet growth ratio values) when emulsifier and oil content increased from ~10% and 15%, respectively and decreased (bigger droplet growth ratio values) when either emulsifier or oil content was lower. The relation between particle size stability and emulsifier content can be explained by the need of an interfacial emulsifier layer aound the droplets to prevent their flocculation or coalescence during storage. The interaction between emulsifier concentration and pressure, oil concentration had significant effect on droplet growth (p <0.05. The droplet growth ratio at the bottom of sample bottles was decreased by increased pressure meaning initially smaller particles were grown more slowly and this result was in agreement with the fnding of others (Yuan and others 2008b) (Table 3.4).

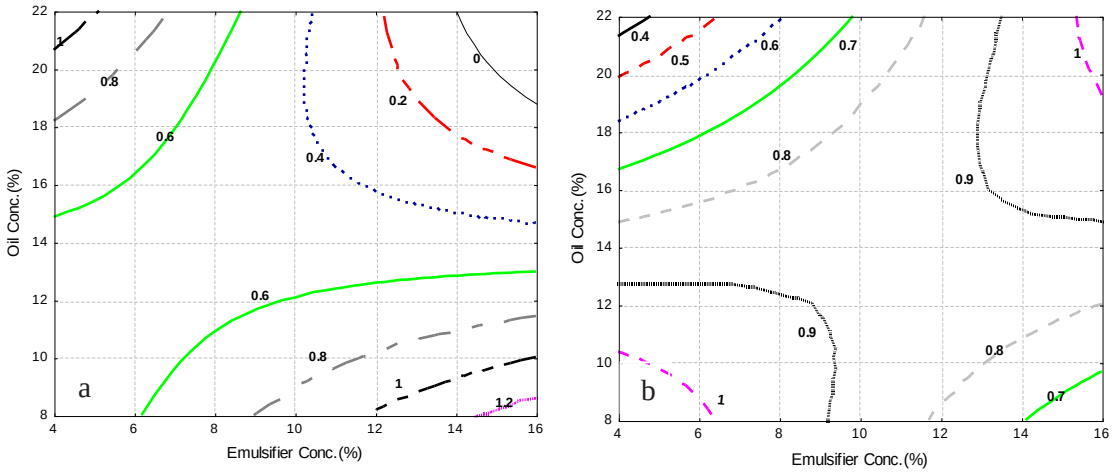

Figure 3.4: Contour plots of droplet growth ratio (a) and quercetin stability (b) of the nanoemulsions as a function of emulsifier and oil concentration % at the Pressure of 120 MPa.

To test the stability of quercetin in nanoemulsions, the samples were taken only from the upper level of the sample bottles for UV/Vis measurement. Linear term of oil concentration and the interaction of emulsifier and oil concentration had significant effect on QT stability (p <0.05) (Table 3.4). The model equations for the responses only with significant factors (independent variables) can be written as follow:

$$Y_1 = 563.35 - 1.40X_1 - 8.70X_2 - 36.32X_3 - 3.98.10^{-2}X_1X_3 + 2.71.10^{-3}X_1^2 + 0.86X_3^2 + 0.17X_2X_3$$

$$Y_2 = 1.83 - 0.14X_1 + 1.19.10^{-3}X_3 + 1.39.10^{-3}X_1X_2 - 1.32.10^{-2}X_2X_3$$

$$Y_3 = 1.75 - 4.71.10^{-2}X_3 + 6.82.10^{-3}X_2X_3$$

3.3.3.2 Verification of model and optimal conditions

The optimal conditions for the targeted responses were generated by the Modde 8.0 (Umetrics) software. Afterthat, at optimal conditions (Pressure 70 MPa; 13% emulsifier content; 17% oil content) nanoemulsions were prepared. The predicted values for responses are as follows 116.356 nm for particle size, 0.2966 for droplet growth ratio and 0.9075 for QT stability. At this condition, the experiments were carried out and particle size was measured as 119.733 nm, 0.3074 for droplet growth ratio and 0.8764 for QT stability, which were satisfactorily close to the values predicted by the model.

3.3 Quercetin Loading

Some emulsion formulations in the stable region of pseudoternary phase diagram were loaded with different amount of QT and their particle size was compared to the blank samples (Table 3.5). The process conditions applied for HSH was 3 min at 24.000 rpm and, 120 MPa and 6 cycles at 25°C for HPH.

For blank samples, when the emulsifier content was kept constant, the samples with higher oil content exhibited a bigger particle size (Table 5). More oil content indicates more oil/water interface to cover and the emulsifier content in the system could not be enough to cover the newly formed droplets which may cause an increase in the droplet size. This result was in agreement with previous studies (Floury and others 2002; Jafari et al. 2007). However, the samples loaded with QT did not follow the same trend. The particle size mostly depended on the oil concentration and amount of QT dissolved in the system. For the formulations including same amount of emulsifiers and loaded with same amount of QT, particle size became smaller by increasing oil content which was also verified by our RSM model study. When the oil/emulsifier ratio was low, the higher amounf of QT in the formulation resulted in bigger particle sizes. Although when the oil/emulsifier ratio

was high, change in the particle size may not depend on the amount of QT (Table 3.2). Increased concentration of the dispersed phase would result in more oil droplets for QT crystals to be accumulated in without affecting the droplet size. Otherwise, when there was less oil droplets, QT would accumulate in the available surfaces and expansion in size.

It has been shown that hydrophobic antioxidants in oil-in-water emulsions have a tendency to concentrate at the interfacial membrane where the oxidation was supposed to occur which increased their effectiveness against oxidation (Mickal Laguerre and others 2010). Quercetin, as a hydrophobic antioxidant, may accumulate in both oil phase and oil/water droplet interface.

Table 3.5: Particle sizes of emulsions loaded with different amount quercetin (QT).

Emulsifier conc. (%)	Oil conc. (%)	Particle Size (nm)				
		Blank samples	QT loaded samples (w/w)			
			0.1%	0.25 %	0.4 %	0.8 %
10	5	69.25±2.05	[b]	220.70±11.30	[b]	[a]
10	10	89.03±3.17	93.20 ± 0.42	168.90±12.60	196.50± 4.52	[a]
10	20	99.28±8.88	103.85±1.98	101.72±4.71	103.91 ±1.98	[a]
10	30	116.90±3.11	[b]	124.10±0.90	[b]	[a]
20	10	69.25±0.67	86..90±0.22	175.45±1.34	178.29±23.67	251.68±15.14

Data represents the avarage of three measurements carried out in duplicate samples

[a] Formulation was not prepared because the amount of QT cannot be loaded

[b] Experiment was not carried out

However, when the dispersed phase concentration was lower and there was less oil/water interfaces to be occupied by QT, it would accumulate on the available area and might make oil droplets larger and the interfacial layer thicker. The enhancement of quercetin absorption by solid nanoparticles was previously studied, and they also proposed that since the quercetin is mostly dissolved in the surfactants in their system, large amounts of surfactants arranged along the interface between water and lipid, the drug incorporation model should fit to the core-shell model with drug enriched shell (Li et al. 2009). In another study, QT was proven to interact with the micelles by means of hydrophobic interactions (Liu and Guo 2006). Above a critical concentration, addition of QT into an oil-in-water emulsion caused a significant decrease in interfacial area of droplets (Di Mattia and others 2009). They proposed that once all the micelles in the aqueous phase was saturated, QT might interact with

emulsifier molecules bounded to the oil droplet interface, thus favouring the partial coalescence of the newly formed oil droplets and leading to a subsequent decrease of the dispersion state (lower values of interfacial area & bigger droplet size).

Another interesting result was that when a formulation loaded with a smaller amount of QT, it was less stable than the one loaded with a greater amount of QT without depending on its initial particle size. When same formulation (oil: emulsifier: water, 10:10:80) was loaded with 0.1% and 0.4% QT, the emulsions loaded with less amount of QT which had particle size almost equal to the blank samples on the day of preparation showed clear phase separation on day 2. Whereas the emulsion loaded with 0.4% QT stayed stable with no change in the particle size (Figure 3.5).

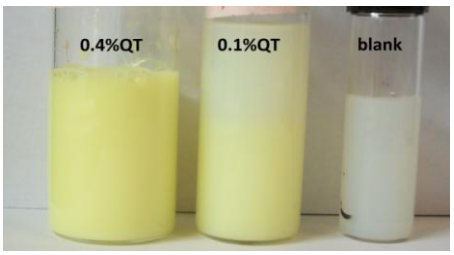

Figure 3.5: Stability of the emulsion with different quercetin content; 10:10:80 (oil: emulsifier: water) on day 2.

Stability of blank emulsion and the systems loaded with hydrophobic compounds would be different. It had been found that hydrophobic bioactive components may form crystals in emulsion- based delivery systems during storage, which sediment to the bottom of the system (Li et al. 2012; McClements 2012). In practice, due to supersaturation it is often possible to dissolve a greater amount of a crystalline material into a solvent than CS* (the equilibrium solubility), the material is fullly dissolved below this level, but forms crystals above it (McClements 2012).

Nevertheless, the system could persist in this metastable supersatutared state for some time before any crystallization is observed due to the presence of activation energies associated with nuclei formation that must be overcome. The height of the activation energy depends on the ability of crystal nuclei to be formed that are stable enough to grow into crystals. At present, little is understood about the origin of nucleation in oil-in-water emulsions, and of the consequences for the stability and functional performance of emulsion-based delivery systems. Once nuclei have been formed in a particular location within an emulsion they may grow into crystals. The

size, shape, and location of crystals in an emulsion will affect its physical stability and functional performance (Li et al. 2012; McClements 2012). In our system, similar to the study of Li and others (2012) we also observed the presence of a thin yellow layer at the bottom of the nanoemulsion by storage which might suggest that (i) nucleation and crystal growth occurred directly in the aqueous phase, or (ii) nucleation and crystal growth occurred in the oil phase or oil–water interface and then the crystals moved into the aqueous phase.

In our study the emulsions loaded with higher amount of QT showed increased stability which might be explained through the mechanism that crystals are unable to move to the droplet surface from the interior of the lipid droplet, because the crystal network formed in the droplet prevents their movement. An estimate of whether the crystals can reach the interface can be given by the ratio t_I/t_N:

$$\frac{t_I}{t_N} = \frac{6\Phi\pi r_c^2}{r_d^2} \qquad \textbf{(3.4)}$$

Here, t_I is the time required crystals to reach interface and t_N is the time required for network formation, r_c is the radius of the crystal, r_d is the radius of the lipid droplet..This equation highlights that the lower the crystal concentrations (ϕ) within the oil phase the more chance they have at reaching the droplet surface. In practice, there will also be a minimum crystal concentration required for network formation. If the crystal concentration is below this value, the crystals may aggregate but they may still be able to move to the droplet surface. This critical concentration will depend on the shape of the crystals and the strength of the attractive forces between them (McClements 2012).

In our system, the particle size of oil droplets loaded with more QT was larger and they were more stable to sedimentation of QT layer at the bottom compare to the system with smaller droplets loaded with less amount of QT. According to this equation, the formation of crystal network that prevents crystals moving to interface and eventually to the aqueous phase where they form larger crytals clusters requires a critical crystal concentration and crystals in the larger sized droplets more likely form the network than the smaller sized droplets.

Further work is clearly needed to better understand the influence of quercetin loading, particle size and the constituents of emulsion (e.g. oil type and concentration, surfactant type and concentration) on the crystal formation and stability of nanoemulsions. QT loading in this study could be as high as 0.8% for the formulation of 10:20:70 (oil: emulsifier: water). The QT loading into emulsion system in the literature was found as 0.043% (Rogerio and others 2010); 0.065% (Wu and others 2008); and in liposome system as 0.5% (Zhang and others 2006) where solvent mixtures were used to dissolve QT. 0.4%. QT loading was achieved in a microemulsion system where the initial concentration of oil (ethyl oleate): surfactant (tween 80): cosurfactant (dehydrated ethanol) concentration was 7:48:45 (Gao Y and others 2009).

3.4 Conclusion

In this study, stable QT nanoemulsions were prepared by using only food grade ingredients. The kinetically stable emulsion range was identified by using the pseudoternary phase diagram to minimize the amount of emulsifier. After that, in the range where stable coarse emulsion occurred, Response Surface Methodology (RSM) was applied to predict the responses of the changes in emulsifying conditions within the experimental ranges on the particle size and stability of QT emulsions. The lineer and quadric terms of homogenization pressure, oil concentration and interaction between pressure and oil concentration had a significant effect on the particle size of the nanoemulsions.

Concurrently, the independent variables of oil concentration and the interaction between oil and emulsifier concentration had significant effect on the stability of QT in nanoemulsions. This study also showed that, particle size of the droplets changes according to QT loading and the oil to emulsifier ratio in the formulation. When the oil/emulsifier ratio was low in the system, increasing QT loading resulted in increase the particle size. However when there was high amount of oil in the system, QT loading did not affect the particle size. When the emulsion formulation loaded with less amount of QT, it was less stable than the same emulsion formulation loaded with high amount of QT, regardless of the its initial particle size. We proposed that QT nanoemulsions in our system were sterically stabilized and they became unstable, if the thickness of the interfacial membrane is reduced.

4. PREPARATION OF QUERCETIN NANOSUSPENSIONS BY HIGH-PRESSURE HOMOGENIZATION

4.1 Introduction

An alternative procedure to improve the solubility of a drug is the use of physical processing methods which increase the surface area and wettability of drug particles by means of particle size reduction or generation of amorphous states of drugs. The rate of dissolution is proportional to the surface area. Owing to the increased surface to volume ratio of the nanocrystals, an increase in saturation solubility and very fast dissolution rate can be seen, especially for the particles those sizes lower than 1µm (Müller and Peters 1998). There are several physical processing methods such as jet or pearl mill micronization (Liu and others 2011; Gao and others 2008), precipitation (Rabinow 2004), spray drying, microfluidization (Verma and others 2011; Tan and Nakajima 2005), and high pressure homogenization (Krause and Müller 2001; Jacobs and others 2000). Although micronization techniques allow producing very fine suspensions, mostly they are not suitable for *in vivo* administration due to high polydispersity of products. The particle size should be in the nanometer range with little content of microparticles. Otherwise the large particles may lead to embolism if they exceed a critical administered dose when injected *in vivo* (Müller and Peters 1998; Donsì and others 2010b).

Among physical processing methods to produce nanosuspensions, high pressure homogenization (HPH) is a simple and highly recommended process with high efficiency, reproducibility, needless of organic solvents and the ease of scaling up this process in industry. In this process, a macrosuspension of drug particles is passed through a narrow homogenization gap at high pressure with a very high velocity. This technology can be applied to poorly water soluble drugs (Sahoo and others 2011; Donsì and others 2010b; Gao and others 2011; Gao and others 2008; Anarjan and others 2010).

The present work *aims* to utilize HPH for formulating quercetin as drug nanosuspension as a significant potential to enhance its water solubility/dispersity. The effect of pressure and the number of processing cycles on particle size and solubility/dispersity have been studied to achieve the optimized processing conditions. Quercetin powders prepared by a combination of HPH and the spray drying have been proven to be able to produce quercetin nanosuspensions with a higher dispersity and fast dissolution rate, and provide higher antioxidant activities.

4.2 Materials and Methods

4.2.1 Materials

Quercetin dihydrate (90%) was purchased from VWR Scientific (Seattle, WA), Polyoxyethylene (20) sorbitan monooleate (Tween80), Ethanol, Ferric Chloride ($FeCl_3.6H_2O$), Hydrochloric acid, AAPH (2,2'-Azobis (2-amidinopropane) dihydrochloride), Trolox (6-hydroxy-2,5,7,8-tetramethylchroman-2-carboxylic acid) and Methanol were purchased from Sigma-Aldrich Company (St. Luis, MO). Maltodextrin (Maltrin®M100) was provided from Grain Processing Corporation (Muscatine, IA). DPPH (1,1-Diphenyl-2- picrylhydrazyl), TPTZ (2, 4,6-tripyridyl-s-triazine) and Sodium Fluorescein were purchased from Fluka(Buchs, Switzerland). Milli-Q water (18.3 MΩ) was used in all experiments.

4.2.2 High pressure homogenization processing

Quercetin (0.5%, w/w) was dispersed in water or water-Tween80 mixtures and held on an oil bath for 20 min at 70°C. The suspensions were subjected to pre-milling treatments to reduce quercetin particle sizes to the micrometer range by high-speed homogenization, HSH (High-speed homogenizer, ULTRA–TURRAX T-25 basic, IKA Works Inc., Willmington, USA) at 24.000 rpm for 5 min. After filtration (Whatman grade 3, 6 µm mesh), the mixture was kept on a magnetic stirrer overnight at room temperature. On the next day, the water which was either evaoparated or lost during filtration was reconstitued and the samples were homogenized at 24.000 rpm 5 more minutes afterwards. The quercetin suspensions were further homogenized by high-pressure homogenizer, HPH (EmulsiFlex-C3, 90 AVESTIN Inc., Ottowa, Canada) at pressure levels ranging from 50 to 200 MPa and for up to 40 HPH cycles. The process temperature of HPH was kept constant at 25ºC.

4.2.3 Lyophilization

The quercetin nanosuspension was frozen at -20 ºC overnight and lyophilised using a Freezone 4.5 freeze-dry system (Labconco, Kansas City, MO).

4.2.4 Spray drying

Maltodextrin with a final concentration of 30% (w/w) was utilized as the carrier for quercetin and powder was retrieved by spray drying technique applied with Yamato Pulvis Mini-Spray GA32 (Yamato Scientific Co., Ltd, Tokyo, Japan). Quercetin suspensions were passed at a spray rate of 4 mL/min, with inlet temperature and outlet temperature fixed at 200°C and 120°C respectively. Dry air flow was set at 800 L/h, and the atomization pressure was set at 1.5 bars.

4.2.5 Particle size measurements

Particle sizes of quercetin dispersions were measured by photon correlation spectroscopy (PCS) – based BIC 90 plus particle size analyzer equipped with a Brookhaven BI-9000AT digital correlator (Brookhaven Instrument Corporation, New York, NY, USA). The light source of the particle size analyzer is a solid state laser operating at 658 nm with 30 mW power, and the signals were detected by a high sensitivity avalanche photodiode detector. All measurements were made at a fixed scattering angle of 90° and temperature of 25.0 ± 0.1 °C. The mean diameter, or z-diameter, was determined by Cumulant analysis of the intensity-intensity autocorrelation function, G (q,t) (Stepanek 1993; Donsì and others 2010b).

4.2.6 Solubility/Dispersity test

Saturation solubility/dispersity was measured through ultraviolet/visible (UV/vis) absorbance determination at 373 nm using Cary Eclipse UV/vis Spectrophotometer with 1cm optical path length. 25 milliliters of quercetin suspensions (initial quercetin solid content is 0.5%, w/w) prepared from quercetin in powder state, were centrifuged for 10 min at 10.000 rpm prior to analysis. After that the upper phase was exracted with ethanol. Quercetin concentration was determined by the calibration curve (R^2=0.999; y=0.069x-0.041) which was linear within the range of 2-15 ppm. It should be mentioned that the presence of residual fine solid particles, if not sedimented by the centrifugation method applied, may affect the UV/vis measurement.

Nevertheless, particle size measurements after centrifugation showed that the mean sizes of residual solid particles dispersed in the liquid were always lower than 300 nm for all tested samples.

4.2.7 Dissolution rate measurements

Dissolution rate shows how fast dried particles re-disperse into submicron suspensions upon rehydration. Dried powder of maltodextrin-entrapped quercetin was prepared for dissolution experiments with a typical formulation of 0.5 g of powder in 5 mL of distilled water. The samples held in independent flasks were agitated at 140 rpm on orbital shaker for different time periods. At definite times, a flask was collected from the shaker and the content was filtered through Whatman 4 and centrifuged at 10.000 rpm for 10 min and supernatant was assayed through UV/vis absorbance determination at 373 nm.

4.2.8 Atomic force microscopy (AFM)

Image of quercetin nanoparticles was collected by using a commercial Nanoscope IIIa Multi-Mode AFM (Veeco Instruments, CA) equipped with J scanner, which was operated in tapping mode using silicon cantilever. The quercetion nanosuspension sample for AFM imaging was prepared by treating the mixture of 0.5% quercetin in water with 20 cycle high pressure homogenization at 150 MPa. A drop of quercetin submicron suspension was deposited on a pre-cleaned silicon wafer surface, and evaporated naturally.

4.2.9 Differential scanning calorimetry (DSC) measurements

Thermal properties of HPH-treated quercetin powder were investigated in comparison to the thermal properties of pure quercetin, with DSC (model Q10, TA Instruments, New Castle, DE). Powder samples were placed in aluminum sealed pans at an amount of 5-10 mg. The thermal analyses were performed, with a temperature scanning range from 25 to 400 °C and a heating rate of 10 °C/min. Nitrogen was used as blanket gas.

4.2.10 Antioxidant activity assays

All samples (0.5 g HPH treated and non-treated spray dried powders) were dissolved in water (5 ml) and then centrifuged at 10.000 rpm for 10 min and supernatant was used for further antioxidant assays. Maltodextrin was used as blank.

4.2.10.1 DPPH free radical scavenging activity Assay

The DPPH assay was done according to the method of (Brand-Williams and others 1995) with little modifications. $6x10^{-5}$M DPPH solution was prepared in methanol. 2.9 ml of DPPH solution was mixed with 100µl of sample and reaction mixture was incubated in dark at room temperature for 30 min and the absorbance was taken at 517nm against blank solution. The radical scavenging activity was calculated using the following equation:

$$\text{Scavenging activity (\%)} = \left(\frac{A_{\text{blank at 517 nm}} - A_{\text{sample at 517 nm}}}{A_{\text{blank at 517 nm}}}\right) x100 \qquad \textbf{(4.1)}$$

4.2.10.2 Ferric reducing/antioxidant power (FRAP) assay

The FRAP assay was done according to (Benzie and Strain 1996) with little modifications. The working solution was prepared by mixing 25 ml of acetate buffer (pH=3.6), 2.5 ml of 10mM TPTZ solution in 40mM HCl, and 2.5 ml of 20mM Ferric Chloride solution. 3ml of working solution was mixed with 40µl sample. The increase in absorbance at 593 nm was measured after 4 min and higher absorbance values indicate higher reduction ability.

4.2.10.3 Oxygen radical antioxidant capacity (ORAC) assay

The ORAC procedure used an automated plate reader (Synergy™ HT Multi-Mode Microplate Reader; BioTek Instruments, Inc., Winooski, VT) with 96-well plates (Huang and others 2002b). Analyses were conducted in 75mM phosphate buffer pH 7.4 at 37 C. Peroxyl radical was generated using AAPH which was prepared fresh for each run. Fluorescein was used as the substrate. Fluorescence conditions were as follows: excitation was performed at 485 nm with a 20 nm bandpass and emission was measured at 520 nm with a 25 nm bandpass. The plate reader was controlled by Gen5™ Data Analysis software (BioTek Instruments, Inc., Winooski, VT).

The AUC and the Net AUC of the standards and samples were determined using Gen5 Data Analysis Software using equations 2 and 3 respectively.

$$\mathrm{AUC} = \left(\frac{R_1}{R_2}\right) + \left(\frac{R_2}{R_1}\right) + \left(\frac{R_3}{R_1}\right) + \cdots + \left(\frac{R_n}{R_1}\right) \quad \textbf{(4.2)}$$

Where R_1 is the fluorescence reading at the initiation of the reaction and R_n is the last measurement.

$$\mathrm{NetAUC} = \mathrm{AUC_{sample}} - \mathrm{AUC_{blank}} \quad \textbf{(4.3)}$$

The standard curve was obtained by plotting the Net AUC of different Trolox concentrations against their concentration. ORAC values of samples were then calculated automatically using the Gen5 software to interpolate the sample's Net AUC values against the Trolox standard curve. The standard curve was linear between 0 and 100 mM Trolox. Results are expressed as micromoles of Trolox equivalents (TE) per gram of powder (µmol TE/g).

Briefly AAPH (0.2069g) was dissolved in 5ml of 75mM phosphate buffer (pH 7.4), a fluorescein stock solution (4µM) was made in 75mM phosphate buffer (pH 7.4) and stored in foil at 4 °C. Immediately prior to use, the stock solution was diluted 1:50 with phosphate buffer. In all experimental wells, 150 µL of sodium fluorescein working solution was added. In addition, blank wells received 25 µL of 75 mM phosphate buffer (pH 7.4), while standards received 25 µL of Trolox dilution and samples received 25 µL of sample. The plate was then allowed to equilibrate by incubating for a minimum of 30 minutes at 37 °C. Reactions were initiated after pipetting each well with 25 µL of AAPH solution for a final reaction volume of 200 µL. The fluorescence was then monitored kinetically with data taken every minute for duration of 180 minutes.

4.2.11 Scanning electron microscopy (SEM)

The morphology of lyophilized HPH-treared crystals and pure non-treated crystals was observed using a scanning electron microscope (JSM-5410- SEM, Jeol Co., Japan). Prior to analysis, the samples were diluted with water to obtain a suitable concentration. Then, the samples were were mounted onto separate, adhesive-coated aluminum pin stubs, dried naturally and sputtered with gold. The SEM was operated

at high vacuum with an accelerating voltage of 10 kV. Images were taken at 3500 magnification.

4.2.12 Statistical analysis

All measurements were repeated at least three times using duplicate samples. Means and standard deviations were calculated from these measurements using Excel (Microsoft, Redmond, VA, USA).

4.3 Results and Discussion

4.3.1 Effect of high pressure conditions on particle size

Under pressure the suspension of quercetin, surfactant and water is forced through a valve having a narrow orifice. According to Bernoulli's equation, the flow volume of liquid in a closed system per cross-section is constant. That means that when the liquid is in the homogenizer gap, the reduction in the diameter leads to a tremendous increase in the dynamic pressure and simultaneous decrease in static pressure to maintain constant energy. A liquid boils when its vapour pressure is equal to the air/static pressure of the environment. In the gap, the static pressure falls below the vapor pressure of water causing the boiling of it at room temperature. This is followed by formation of gas bubbles, which implode vigorously and the cleavage along the drug crystal is caused by cavitation, fluid shear and particle collision against each other.

As the suspension leaves the gap, the pressure suddenly rises to normal air pressure again (Müller and Peters 1998; Gao and others 2008; Sahoo and others 2011; Keck and Müller 2006). Altough, the implosion forces in this instantaneous progress are sufficiently high to break down the drug microparticles into nanoparticles, the energy generated in such a short time (generally within miliseconds) is not sufficient to break down all particles into uniform nanocrystals even at the higher applied pressures, so more homogenization cycles are needed to be performed on the suspension to provide more energy to break down the crystalline structure. Therefore, homogenization often is performed in five, ten, or more cycles that depend on the hardness of the drug and the desired particle size (Jacobs and others 2000; Müller and Peters 1998).

Figure 4.1 shows the effect of number of cycles on the mean particle sizes, polydispersity of quercetin suspensions at a fixed operating pressure of 150 MPa and 25 °C inlet temperature.

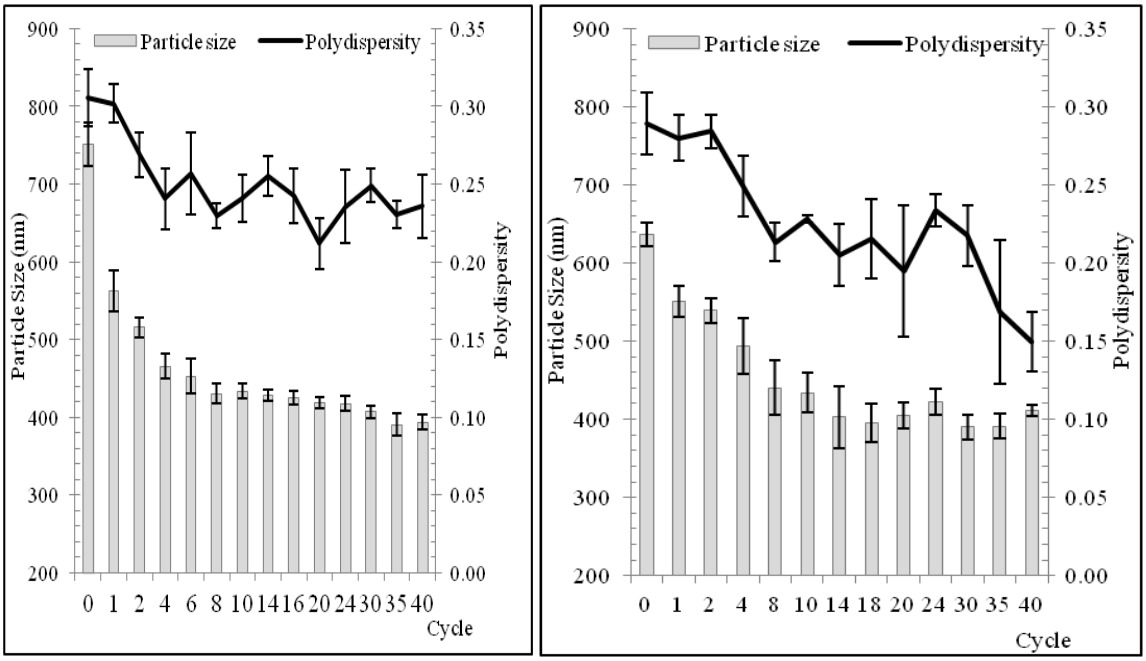

Figure 4.1: Change in particle size and polydispersity of quercetin in water (left) and in 1% Tween 80 (w/w) solution (right) as a function of HPH cylces. HPH pressure and processing temperature were fixed at 150 MPa and 25°C, respectively. Duplicate samples were prepared and the results are reported as the mean and standard deviation of three measurements made per sample.

The mean particle sizes of quercetin crystals in water and 1% T80 solution (w/w) exhibited ~30% reduction only after 2 cycles. Rate decreased with the following cycles and got a steady value (~430 nm) after 10 cycles. After that point, increasing the number of cycles did not change the particle size which was in agreement with previous studies (Sahoo and others 2011; Donsì and others 2010b). Polydispersity of samples reached a value of 0.2 for samples, but between cycles it showed fluctations which could indicate a slightly reversible formation of aggregates which were disaggregated in the next cycles (Figure 4.1). Generally the energy delivered into the system is proportional to the homogenization pressure, because higher pressure causes higher velocity of the fluid in the gap, as a result static pressure will drop to a larger extent leading to generation of more bubbles eventually to comminute the particles. Thus, it is anticipated that the higher the homogenization pressure, the smaller the particle size obtained as in observed in Figure 4.2.

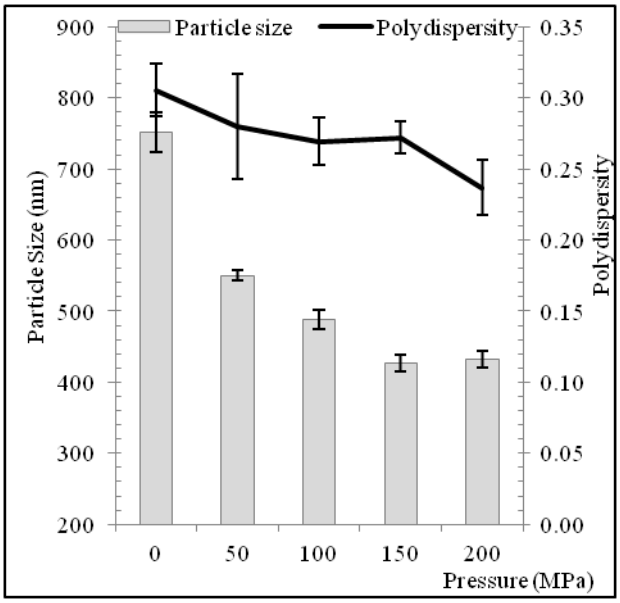

Figure 4.2: Change in particle size and polydispersity of quercetin in water as a function of homogenization pressure. HPH cycle and processing temperature were fixed at 20 and 25°C, respectively. Duplicate samples were prepared and the results are reported as the mean and standard deviation of three measurements made per sample.

However, it should be noted that there is no linear relationship between increase in pressure and decrease in size. Because HPH process breaks the particles/crystals preferentially at weaker points, i.e. imperfections and by decreasing the size, the number of imperfections is becoming less and remaining crystals are getting more perfect. If the force in the homogenizer is equal to the interaction forces in the crystal, the particles will not diminute further, even additional cycles are applied. The force required to break down the crystals seems to increase rather exponentially with decreasing particle size (Keck and Müller 2006).

The smallest particle size achieved at the end of 30 cycyle does not depend on concentration of stabilizer (Table 4.1), but the polydispersity index of the systems uses Tween 80 has lower values which indicate that having surfactant in the system provides fineness of particle by providing the agglomeration during HPH cycles (Figure 4.1). The role of surfactant in emulsion and suspension systems is theorotically different. In case of emulsions, the stabiliser/surfactant reduces the interfacial tension between the oil and the water phase. Consequently, the required energy to produce nanoemulsion decreases since the energy is equal to surface area X interfacial tension. On the other hand, in a suspension, the main energy is utilized

to break the crystal itself that means overcoming the binding forces in the crystal lattice (Keck and Müller 2006).

Nanosized quercetin particles were confirmed by an AFM height image, as shown in Figure 4.3.a. The AFM images suggested that most particles were mainly irregular shaped. Figure 4.3.b and c shows the SEM images of pure non-tretaed quercetin and lyophilized HPH treated samples. Pure quercetin showed lack of particle size uniformity and its size was relatively larger. On the other hand, HPH-treated samples exhibited particle size uniformity and lack of larger needle type crystalline structures

4.3.2 Effect of high pressure conditions on water dispersity

In general, water dispersity of a particle increases with a decrease of particle size because it causes a linear increase of the spesific surface area, which is in an inverse relationship with the particle diameter. The relationship between particle size and water dispersity can be explained by Ostwald- Freundlich theory (1) (Müller and Peters 1998; Gao and others 2008).

$$log \frac{C_s}{C_\infty} = \frac{2\sigma V}{2.303 RT\rho r} \qquad \textbf{(4.4)}$$

where C_s is the solubility, C_∞ is the solubility of the solid consisting of large particles, σ is interfacial tension, V is molar volume, R is gas constant, T is absolute temperature, ρ is density of the solid, r is radius. It is obvious that the solubility (C_s) of the the drug increases with a decrease of particle size (r). However, this effect is pronounced for materials that have mean particle size of less than 1µm (Müller and Peters 1998).

Another possible explanation for the enhancement in the solubility is the creation of high energy surfaces when disrupting the more or less drug microcrystals to nanoparticles. Hence by raising the interfacial area through particle size reduction, during which the transition among different polymorphic forms occurs (Donsì and others 2010b). The application of higher energy during HPH processing to the quercetin system caused more transitions from crystal to amorphous phase which can also explain the increase in water dispersity of quercetin (Figure 4.4 and 4.5). To further visualize the improved dispersity of quercetin nanosuspension after HPH, the photographic pictures of quercetin suspensions prepared in water and in 1% Tween

80 (w/w) solution treated by 40 cycles of HPH at 150 MPa as well as nontreated quercetin (insoluble parts were removed by filtration) were taken and presented in Figure 4.4.

The nontreated quercetin suspension in water was nearly colorless. In contrast, HPH treatment provided yellowish color. When Tween 80 was added to system color difference were more pronounced.The presence of Tween 80 in the solution increased the quercetin solubility in both HPH processed and non-processed suspensions depending on its concentration (Table 4.1). The utility of the surfactant systems in solubilization is well known. Due to its amphilphilic nature, Tween 80 can improve quercetin solubility by providing regions for hydrophobic interactions in solution (Narang and others 2007). As a surfactant, Tween 80 adsorbs onto surface and may decrease the interfacial tension between water and quercetin particles and thus water can penetrate in the pores of quercetin particle which would facilitate the dispersion of particles.

Table 4.1: Water dispersity of HPH treated quercetin nanosuspensions in T80 (w/w) concentrations for cycle 0 and 30 at 25°C and 150 MPa pressure.

Cycle	Tween 80 concentration % (w/w)	Quercetin dispersitiy in water (mg/ml)	Particle size (nm)	Polydispersity
0	0	2.4±0.1	751.1±28.3	0.31±0.02
	0.5	65.3±0.5	657.1±30.1	0.28±0.02
	1	135.5±6.8	662.6±27.2	0.24±0.01
	1.5	209.8±1.8	651.6±19.2	0.23±0.01
	2	270.5±13.2	664.7±18.1	0.27±0.04
30	0	7.3±0.03	426.6±11.8	0.27±0.01
	0.5	147.4±6.2	424.3 ± 9.2	0.21±0.02
	1	204.8±7.01	427.8±18.1	0.23±0.02
	1.5	304.3±3.8	430.6±4.5	0.23±0.02
	2	302.1±3.9	421.2±11.2	0.22±0.05

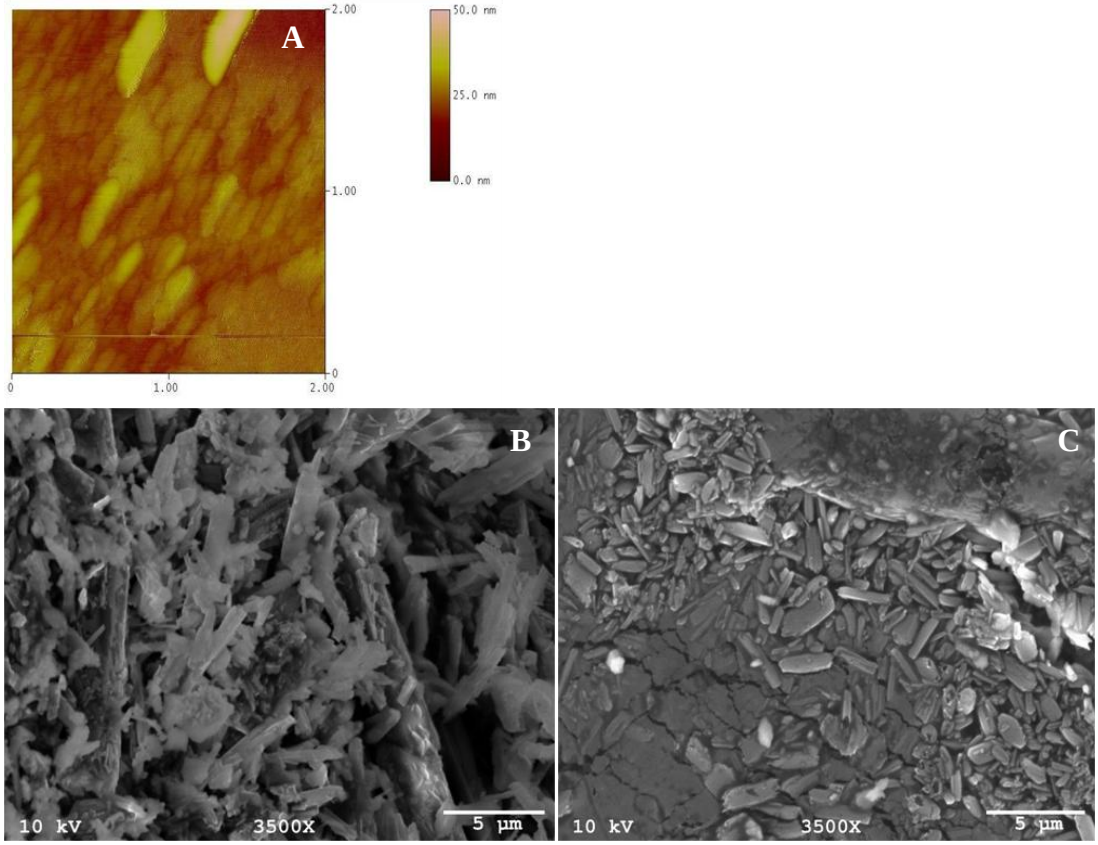

Figure 4.3*:* (A). AFM height image of HPH-treated quercetin nanosuspension deposited on a precleaned silicaon surface (B) SEM images of pure non-treated quercetin and (C) lyophilized HPH-treated quercetin nanosuspension. HPH was carried at 150 MPa for 20 cycles at 25°C. Pictures were taken at X3500 magnifications.

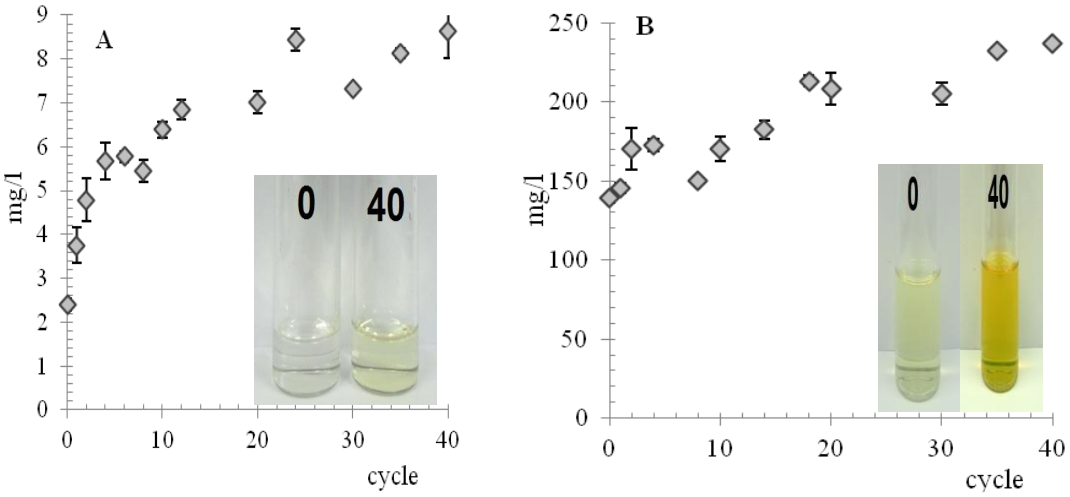

Figure 4.4: Water dispersity of quercetin nanosuspensions in water (A) and in 1% T80 (w/w) solution (B) as a function of cycle at 150 MPa and 25°C. Photographic pictures shows the quercetin nanosuspensions in water (left) and in 1% T80 (w/w) solution (right) for cycle 0 and 40 at 150 MPa and 25°C, insoluble part of quercetin was removed by ultracentrifugation.

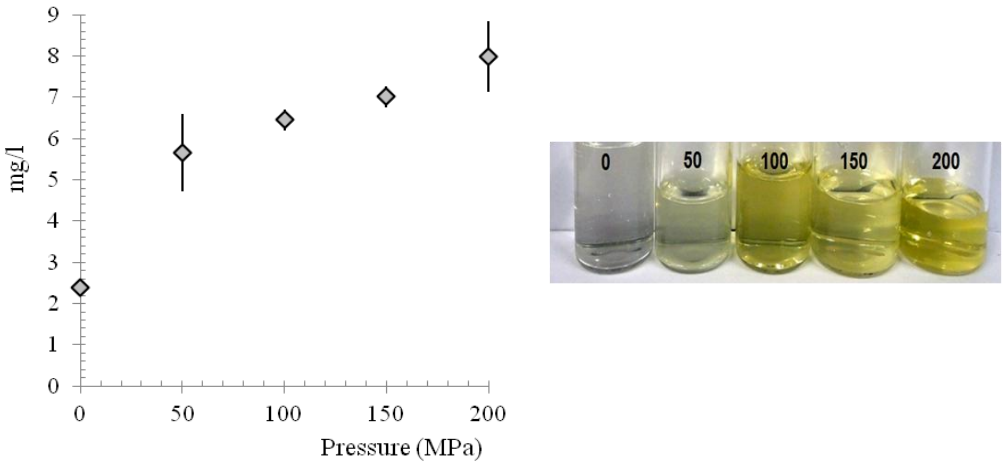

Figure 4.5: Water dispersity of HPH treated quercetin nanosuspensions in water at different pressures for cycle 20 at 25°C, insoluble part of quercetin was removed by ultracentrifugation.

4.3.3 Thermal properties of quercetin before and after HPH treatment

Thermograms of pure quercetin and lyophilized HPH-treated quercetin powders with scanning temperatures ranging from 25 to 400 °C was presented in Figure 4. 6. The curve of the quercetin showed two endothermic peaks: a broad endotherm peak centered at around 120°C corresponds to the loss of bounded water; the other was a sharp endothermic peak at 325°C indicating the melting point. This result was consistent with others reports (Gao and others 2011; Sahoo and others 2011). Melting peak of HPH treated quercetin suspensions shifted to lower temperature values which are the indication of a certain loss of crystallinity. Entalpy of fusion (integrated area under the curve) of pure quercetin was higher than HPH treated samples. Entalpy of fusion is proportional to the amount of crystallinity in the samples which shows that HPH treatment had a significant effect on the loss of crystallinity.

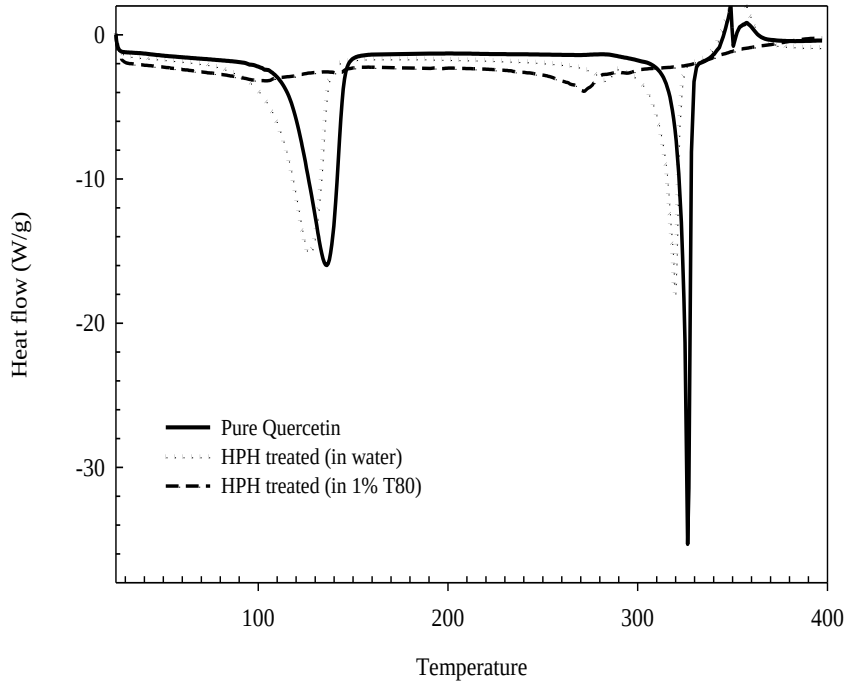

Figure 4.6: DSC thermograms of pure quercetin and lyophilized quercetin HPH-treated nanosuspensions prepared in water and in 1% T80(w/w). HPH was carried at 150 MPa for 20 cycles at 25°C.

4.3.4 Dissolution Rate

HPH-treated (at 150 MPa for 20 cycles at 25°C) quercetin suspensions in the presence of carrier matrix of maltodextrin (30%, w/w) were obtained by the spray-drying technique. The obtained powder is convenient for handling and storage and is ready for redispersion in water. Figure 4 7 shows the plot of the water dispersity of HPH-treated quercetin powders as a function of the agitation time. The dissolution times (time to reach the concentration plateau) for spray-dried samples were nearly the same within a 10 min period. The effect of spray drying on water dispersity can be evaluated by comparing the final values of water dispersity after complete powder dissolution to the dispersity of the original quercetin suspension. For the HPH-treated sample prepared in water, spray drying causes a certain increase of water dispersity, from 9 to around 15 mg/L. The effect of spray drying on the increasing water dispersity of quercetin can be attributed to the reduced crystallinity of the quercetin powder through the incorporation of maltodextrins (Vogt and others 2008; Chaubal and Popescu 2008)

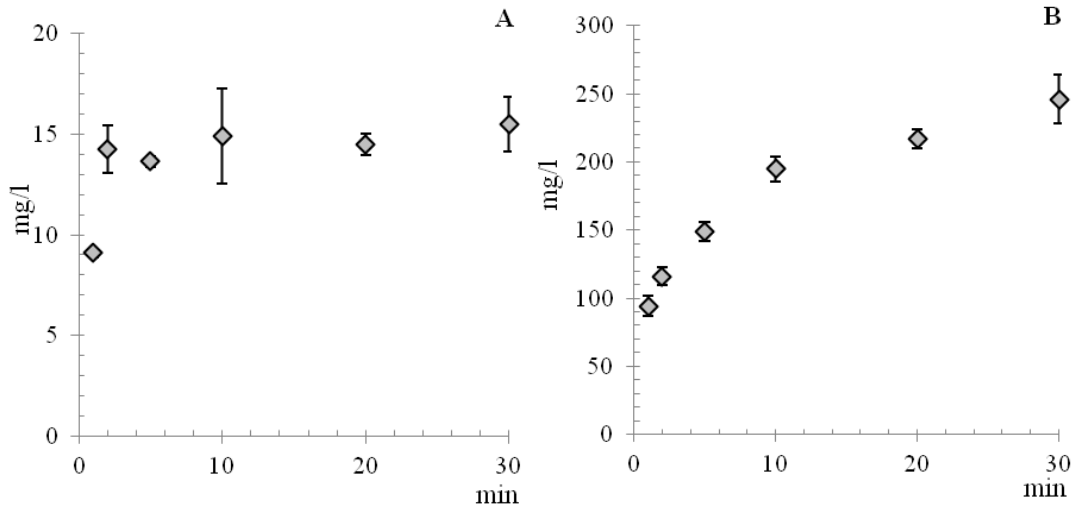

Figure 4.7: Dissolution of HPH-treated quercetin powder as a function of the agitation time. Predried suspension prepared in water (A) and in 1% T80 (w/w) solution (B). HPH was carried at 150 MPa for 20 cycles at 25°C.

4.3.5 Antioxidant assays

2, 2-diphenyl-1-picrylhydrazyl hydrate (DPPH) radical scavenging assay is routinely practiced for the assessment of antioxidant activity of single compounds and their mixtures. DPPH radical is stable at room temperature and produces a deep purple solution in organic solvents. The method is based on the discoloration due to reaction occurred between radical and antioxidant which can be determined spectrophotometrically (Karadag and others 2009).

FRAP assay is based on the ability of phenolics to reduce yellow ferric tripyridyltriazine complex (Fe(III)-TPTZ) to blue ferrous complex (Fe(II)-TPTZ) by the action of electron-donating antioxidants. The resulting blue color measured spectrophotometrically at 593 nm is taken as linearly related to the total reducing capacity of electron-donating antioxidants (Karadag and others 2009).

In our study samples first dissolved in water and followed by the removal of undissolved portion by ultracentrifugation, after that the supernatant was extracted with methanol. The radical scavenging activities and reducing abilities of spray dried HPH treated and non-treated quercetin powders were exhibited in Figure 4.8. In consistent with increased water solubility of quercetin by the application of high pressure, the HPH-treated samples scavenged more DPPH radical in the reaction medium and showed higher reducing power.

ORAC assay as originally designed is limited to measurement of hydrophilic chain-breaking antioxidant capacity. To solve this disadvantage, the method is modified by using solubility enhancers i.e., methylated β-cyclodextrin (Karadag and others 2009). In our study, ORAC assay was done as originally designed altough quercetin is a hydropohobic antioxidant and has very poor water solubility. Since one of the goals in our study was the enhancement of water solubility of quercetin, we expected an increase in ORAC values depending on HPH treatment which was also presented in Figure 4.8.

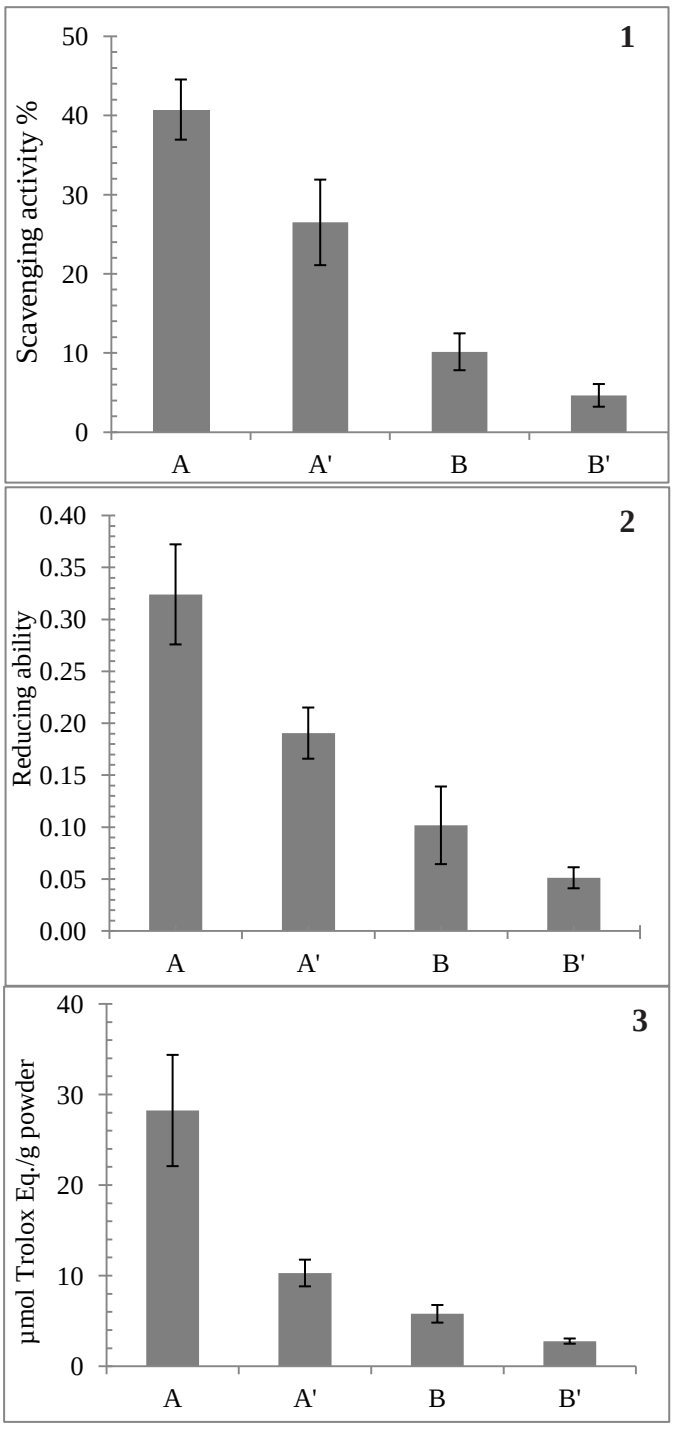

Figure 4.8: The scavenging activities (1), reducing abilities (2) and oxygen radical absorbing capacities (3) of spray dried quercetin suspension powders prepared in 1%T80 (w/w): (A) HPH treated samples (A') non-treated samples ; and prepared in water: (B) HPH treated samples (B') non-treated samples.

4.4.Conclusion

High pressure homogenization was used to increase the water dispersity of quercetin crystals and very fine suspensions in the nanometric range (around 400 nm) were produced. The effect of pressure and number of cycles, and concentration of stabilizer (Tween 80) on particle size, water dispersity and structure was examined. Particle size reduction rate was decreased by increasing the number of cycles and got a steady value (~430 nm) after 10 cycles. The force required to break down the crystals seemed to increase rather exponentially with decreasing particle size. The smallest particle size achieved did not depend on concentration of stabilizer, but the polydispersity index of the systems uses Tween 80 has lower values which indicate that having surfactant in the system provides fineness of particle by providing the agglomeration during HPH cycles. Furthermore, the formation of nanosized particles was confirmed by AFM and SEM images. DSC thermograms also showed the loss of crystallinity through shifting to lower melting temperature and enthalpy of fusion values of HPH-treated samples. Easily water redispersible powders were fabricated by using spray drying process when the maltodextrin was used as a carrier agent. HPH-treated spray dried powders showed higher antioxidant activity than non-treated samples through increased water dispersity in terms of radical scavenging activity, reducing ability and oxygen radical absorbance capacity determinations. HPH has been proven to be a mature method to create readily dispersible quercetin powders with high water dispersity, which is of vital importance for the enhancement of the oral bioavailability.

5. PRESENCE OF ELECTROSTATICALLY ADSORBED POLYSACCHARIDES IMPROVES SPRAY DRYING OF LIPOSOMES

5.1 Introduction

Liposomes are spherical bilayer vesicles formed from aqueous dispersions of phospholipids with typical sources of phospholipids being soy or egg lecithins. Such lecithins have long been used as emulsifiers and texture modifiers in foods and are generally recognized as safe. Liposomes have attracted considerable attention in the biomedical, food and agricultural industries in recent years because they are biocompatible, biodegradable, nontoxic, and have the ability to act as targeted release-on-demand carrier systems for both water and oil-soluble functional compounds such as antimicrobials, flavors, antioxidants and bioactive compounds (Keller 2001; Taylor and others 2005; Mozafari and others 2008b; Malheiros and others 2010; Gibis and others 2012).

However, liposomes are generally unstable when suspended in aqueous systems for prolonged periods. They can undergo physical degradation processes, including vesicle fusion, aggregation, and leakage of entrapped material over time. Since much deterioration processes take place in an aqueous environment, one possible approach may be the removal of water to generate dry powders. A few drying technologies are available, namely freeze-drying, spray-drying, spray-freeze drying technology. Freeze-drying is the most widely applied technology to produce dried liposomal dispersions and the structural changes brought about by freeze drying processes have been thoroughly investigated (Chen and others 2010; Harrigan and others 1990; Ingvarsson and others 2011). In comparison to freeze drying, spray drying is a less expensive, time- and energy consuming process. However, there are much fewer studies available that report results of spray drying of liposomes (Goldbach and others 1993a; Goldbach and others 1993b; Lo and others 2004; Wessman and others 2010).

Wessman and others (2010) studied the structural changes of liposomes resulted by freeze- and spray drying. They choose DSPC (distearylphosphatidylcholin) and cholosterol for lipid structure and lactose as carrier, due to its ability to form amorphous particles with a high glass transition temperature (Tg) and stability. The solid-state properties of the spray-dried powders were characterized by differential scanning calorimetry (DSC), the lipid aggregates present in the dispersions before drying and after reconstitution from spray- and freeze-dried solids were characterized by dynamic light scattering (DLS) and cryo-TEM (cryo-transmisson electron microscopy). Cryo-TEM and DLS results revealed that significant change in aggregate size and structure can be induced after both spray- and freeze-drying of the liposomes. After redispersing of dried liposomes, they are either totally collapsed or rearrenged into liposomes with thick walls consisting of two or several bilayers. In addition, the appearance of peanut shaped liposomes, envelopes two smaller liposomes, was frequently observed.

Goldbach and others (1993a) prepared dried liposome powders constitued of soybean phosphatidylcholine (SPC) by using lactose as carrier material with an inlet temperatre of 110°C and an outlet temperature of 75-80°C. When they entrapped hydrophilic drug, atropine sulphate, in liposomes constituted of SPC and SPC: Cholesterol (1:1 molar ratio), an important leakage (65-80%) occurred during spray drying.

Monosaccharides and more frequently disaccharides are utilized as stabilizing excipients during drying (Koster and others 2000; Koster and others 2003).When aqueous dispersions of liposomes were dehydrated in the absence of additives, the result would be the fusion of liposomes, formation of aggregates and leakage of encapsulated materials on rehydration. Therefore, several excipients have been identified and are commonly applied as stabilizers in dry liposomal formulations. Monosaccharides and more frequently disaccharides are utilized as stabilizing excipients during drying (Koster and others 2000; Koster and others 2003).

Recently, a method referred to as the layer-by-layer (LBL) depositioning method has been utilized to increase the stability of liposomes (Quemeneur and others 2007; Laye and others 2008; Chuah and others 2009; Mady and Darwish 2010; Quemeneur and others 2010; Gibis and others 2012). This method is based on the adsorption of different oppositely charged biopolymers such as proteins and carbohydrates on the

liposomal interfaces. This approach has been proven to provide better thermal as well as environmental (pH and ionic strength) stability in liposomes and emulsions (Ogawa and others 2003; Guzey and McClements 2007; Shaw and others 2007; Chun and others 2013; Klinkesorn and McClements 2009). However, to date, little is known as to how these layers may be used to create better food structures that have superior performances in the dried state.

We *hypothesize* that the LBL method may be an important tool to allow for the generation of dry powders that may yield much of the original liposomal dispersion back upon rehydration. The *objective* of this study was thus to test this hypothesis by using both adsorbing and non-adsorbing polymers in combination with liposomes followed by spray drying. Specifically, the influence of addition of chitosan and maltodextrin with different molecular weights to liposomes was examined in the liquid, dried and rehydrated states.

5.2 Materials and Methods

5.2.1 Materials

Chitosans were donated by Primex (Siglufjordur, Iceland) and had different molecular weights and degrees of deacetylation (Table 5.1). Lecithin, (Soybean phospholipids, 70% phosphatidylcholine) was provided by the American Lecithin Company (Oxford, Connecticut, USA). Maltodextrins DE 2 and 21 were donated by Roquette-frères SA, (Lestrem, France). Sodium acetate and acetic acid was purchased from Merck GmbH (Darmstadt, Germany) and Carl Roth GmbH & Co. KG (Karlsruhe, Germany) and used without further purification. 0.8µm isopore membrane filters were obtained from Millipore GmbH (#ATTP14250, Billerica, MA). Double distilled water was used in the preparation of all samples.

Table 5. 1: Molecular characteristics of chitosan used in this study**.**

Chitosan Type	Degree of Deacylation (%)*	$\bar{M}$ (Average Molecular Weight, kDa) Huggins Equation	M (Average Calculated Molecular Weight, kDa) Kraemer Equation
HMW-C	79	877	932
LMW-C	81	532	589

*As for manufacturer specification

5.2.2 Solution preparation

An acetate buffer solution (pH = 3.5 ± 0.1; 0.1 M) was prepared with 0.6 g/l sodium acetate and 5.75 ml/l acetic acid. A lecithin stock dispersion was prepared by dispersing 2% (w/v) lecithin powder in acetate buffer. Chitosan stock solutions were prepared by dispersing 1.5% (w/v) into buffer solution, and the solution was stirred overnight to ensure complete hydration. Maltodextrins were dissolved in acetate buffer to generate stock solutions with varying concentrations.

5.2.3 Chitosan molecular weight determination

The shear viscosity of serially diluted chitosan solutions in acetic acid was measured using a rotational rheometer (MCR 300, Anton Paar, Stuttgart, Germany) equipped with a double cylindrical system (DG-26.7/TEZ 150 P-C). The intrinsic viscosities of chitosan in 0.2M CH_3COOH/0.1 M CH_3COONa solution were calculated using the Huggins and Kraemer equation (Kasaai and others 2000; Wang and others 1991). The reduced viscosity η_r was calculated as:

$$\eta_r = \frac{\left(\frac{\eta}{\eta_0} - 1\right)}{c} \qquad \textbf{(5.1)}$$

where η_r is the viscosity of the chitosan solution at the polymer concentration of c and η_0 is the viscosity of liquid phase. The inherent viscosity was calculated as:

$$\eta_i = \frac{\ln\left(\frac{n}{n_0}\right)}{c} \quad \textbf{(5.2)}$$

The intrinsic viscosity (η) of chitosan solution was obtained from the intercept of a η_r and η_i versus c plot when c was approaching zero. Finally, avarage molecular weights of chitosan were calculated from the intrinsic viscosities using Mark–Houwink equation (Baxter and others 2005; Kasaai and others 2000; Pa and Yu 2001; Wang and others 1991).

$$[\eta] = K \cdot M_w{}^a \quad \textbf{(5.3)}$$

where η is intrinsic viscosity, K was a constant (1.424×10^{-3} mlg^{-1}) and a was a constant (0.96) (Wang and others 1991; Knaul and others 1998).

5.2.4 Preparation of uncoated and coated liposomes

Fine-disperse lecithin liposomes with average particle diameters of approximately 400 nm were manufactured by homogenizing lecithin solutions with a high shear disperser (DI-25 Yellowline, IKA) for 10 min at 9,500 rpm, and 3 min at 13,500 rpm. Thereafter the dispersion was filtered five times through 0.8 µm Isopore membrane filters (Millipore GmbH). Coated liposomes were produced by electrostatic deposition of positively charged chitosan layer onto the surface of negatively charged liposomes. To this purpose, liposome suspensions (2% w/v) were added to chitosan solutions (0.002% to 1.5% (w/v) chitosan) at room temperature and stirred overnight.

5.2.5 Particle size distribution and mean size

The particle size distribution of samples was measured using a laser light diffraction particle size analyzer (LA-950, Horiba, Japan). The instrument finds the particle size distribution that gives the best fit between experimental measurements and predictions made using light scattering theory (Mie Theory). A refractive index for lecithin of 1.44 and 1.33 for the aqueous phase was used to calculate particle size distributions.

Laser diffraction results were displayed as volume based distributions, and the volume mean diameter ($\bar{d}_{4,3}$) was used to report average particle diameters. The volume mean diameter can be calculated as:

$$\bar{d}_{4,3} = \frac{\sum n_i . d_i^4}{\sum n_i d_i^4} \qquad \textbf{(5.4)}$$

where n_i is the number of droplets of diameter d_i. All particle size measurements were made on at least two freshly prepared samples with three readings made per sample.

5.2.6 ζ –Potential measurement

Liposomal dispersions were diluted to a particle concentration of approximately 0.005% (w/v) with acetate buffer. Diluted dispersions were then loaded into a cuvette of a particle electrophoresis instrument (Nano ZS, Malvern Instruments, Malvern, UK), and the ζ -potential was determined by measuring the direction and velocity that the liposomes moved in the applied electric field. The ζ -potential measurements are reported as the average and standard deviation of measurements made from two freshly prepared samples, with 3 readings made per sample.

5.2.7 Optical microscopy

Samples were gently shaken before analysis using a vortexer to ensure homogeneity. One drop of sample containing liposomes was placed on an objective slide and then covered with a cover slip. Light microscopy images were taken with an axial mounted Canon Powershot G10 digital camera (Canon, Tokyo, Japan) mounted on an Axio Scope optical microscope (A1, Carl Zeiss Microimaging GmbH, Göttingen, Germany).

5.2.8 Spray drying

Uncoated and coated liposomal dispersions were mixed with stock maltodextrin solutions to obtain mixtures containing 20 % (w/v) MD, 0.5 % (w/v) lecithin and 0.175 % (w/v) chitosan. Samples were stirred overnight (12–15 h) prior to spray drying to ensure homogeneity. The dispersions were dried at a feed rate of 2.5 cm^3/min. at an inlet temperature of 160°C resulting in an outlet temp of 90°C, and 0.67 m^3/min. air flow using a laboratory scale spray-drier equipped with a 1.5-mm

nozzle atomizer operatorated at an atomizing air flow of 5 cm^3/min. (Mini spray-dryer B-290, BUCHI, Switzerland). Dried powders were collected and stored in airtight containers and placed in a desiccator (~3 % RH) at room temperature. All analysis was completed within a week after the spray drying process.

5.2.9 Moisture content

A Karl Fischer system of Metrohm (Metrohm, Switzerland), equipped with a Titrino KF 841 and 20 ml burette was used to determine the residual moisture content of powders. A two-component system containing Hydranal-Solvent and Hydranal-Titrant 5 (both Sigma-Aldrich Laborchemikalien, Germany) was used for measurement.

5.2.10 Water activity

The water activity of samples was measured using an AW Sprint TH500 Water Activity Meter (Novasina, Switzerland) at 25 °C.

5.2.11 Powder yield

Following the subtraction of moisture content in the spray dried powders, the yield was calculated as the ratio of the total weight of powder obtained at the end of spray drying process and the mass of initial solids (lecithin, chitosan and maltodextrin) fed into the system:

$$\text{Yield (\%)} = \frac{\text{total weight of powder after spray drying x (1-moisture content of powder)}}{\text{total dry weight of lecithin, chitosan and maltodextrin added initially}} \text{x100} \quad \textbf{(5.5)}$$

5.2.12 Particle size distribution of reconstituted liposomes

The powder was reconstituted to 10 g solids/100 g reconstituted liposomal dispersion by dissolving 0.5 g powder in 4.5 ml of acetate buffer (pH=3.5). The particle diameter was analyzed after overnight reconstitution using the above mentioned static light scattering method (Horiba LA-950, Japan).

5.2.13 Scanning electron microscopy (SEM)

Spray-dried powders were mounted onto separate, adhesive-coated aluminum pin stubs. Excess powder was removed by tapping the stubs sharply and then blowing dry air across. The stubs were sputter coated with a thin layer of gold in a Leica

vacuum coating unit at 40 mA for 100 seconds 3 times, at a working distance of 50 mm by using an argon gas purge. The samples were examined using a NeoScope JCM-5000 SEM. The SEM was operated at high vacuum with an accelerating voltage of 10 kV. Images were taken at 1000 and 4000 magnifications.

5.3 Statistical Analysis

All measurements were repeated at least three times using duplicate samples. Means and standard deviations were calculated from these measurements using Excel (Microsoft, Redmond, VA, USA). One way analysis of variance (ANOVA) was conducted using the Statistica 8 software (Stat Soft Inc., Tulsa, USA). Differences were analyzed using Duncan's Multiple Range Test comparisons and p value of <0.05 were chosen to determine significant differences.

5.4 Results and Discussion

5.4.1 Influence of chitosan addition on the properties of liposomes

The influence of chitosan molecular weight and concentration on liposome charge and particle diameter was monitored to determine the conditions where coated liposomes could be generated (Figure 5.1). The surface charge on liposomes changed from negative to positive when chitosan was added to liposomal dispersions. For both high and low molecular weight chitosan, the surface charge of the initially anionic liposomes (0.5 w/v %) increased from -32 mV to ~+56 mV with addition of chitosan (0-0.75 w/v %). Regardless of chitosan molecular weight, the net surface charge on the particles became zero after the addition of approximately 0.008 (w/v %) chitosan suggesting that at this chitosan concentration charge neutralization occurred. When the chitosan concentration exceeded 0.05 (w/v %), the ζ- potential became constant at ~+50 mV, indicating that the vesicles' surfaces had been fully covered with chitosan. The mean diameter of particles depended on the chitosan concentration added. The particle diameter of uncoated liposomes was ~0.4 μm and increased to around 50 μm after addition of low amounts of chitosan (0.0025 to 0.01, [w/v %]). Formation of aggregated structures could be observed under the microscope, and these were eventually followed by phase separation and formation of a supernatant and a sediment layer at the bottom of test tube after a few hours

(Figure 5.2). The surface charge of particles where large aggregates were formed corresponded to the range where surface charges went through a net negative to a net positive change (ζ = -15 mV - +25 mV). Previous studies have similarly indicated an increased likelihood for bridging flocculation to occur when charges transition from one regime to another (Laye and others 2008). This has been explained by the fact that insufficient amount of polymer is present causing polymers to attach simultaneously to two or more liposomes thereby destabilizing the vesicles' structures. The mean diameter of aggregates that were formed at low chitosan concentrations decreased with increasing chitosan concentration above 0.025 (w/v %). The mean diameter was lowest (0.5 μm) at a biopolymer concentration of ~0.4 (w/v %), where the ζ-potential had reached a constant value. There, microscopic images were void of any aggregated structures and no phase separation was visible in test tubes. Further addition of chitosan to the system induced depletion flocculation, due to presence of free polyelectrolytes in the continuous phase. The concentration gradient of polymers in the immediate vicinity of liposomes and the bulk solution generates an osmotic force which is strong enough to overcome the various repulsive forces thus favoring particle aggregation (McClements 2005e). In our study, the formation of flocs was visible in the microscopic images on the day of preparation but was not visible when inspecting the test tubes. Photographic images of test tubes taken after 2 weeks of storage however showed formation of a sedimentation layer in the bottom of the tubes (Figure 5.1 and 5.2). Our results are in agreement with literature. (Blijdenstein and others 2004). For example it was suggested that flocs formed by bridging flocculation are relatively strong and irreversible and grow to relatively large sizes, whereas flocs formed by weak depletion interactions are typically smaller in size and may be disassembled into single particles by application of mild mechanical forces (e.g. stirring)(Blijdenstein and others 2004).

It was also reported that depletion flocculation occurred in the presence of excessive chitosan concentration, but that the process was reversible and that aggregated liposomes dissociated upon dilution, stirring or mild sonication (Laye and others 2008). Depletion flocculation becomes more prevalent for polymers with higher molecular weights and at increased polymer concentrations. This is because the strength of the interaction increases as the concentration of free polymer increases

and because the range of the interaction increases as the radius of gyration of the polymers increases (McClements 2000).

Mun and others (2006) proposed that emulsion droplet aggregation through a depletion mechanism increased with increasing chitosan molecular weight. Similarly in our study, high molecular weight chitosan promoted depletion flocculation at lower chitosan concentrations. Optical microscopy images showed that at 0.5 % (w/v) chitosan, samples prepared with high molecular weight chitosan had flocs in them, whereas with low molecular weight chitosan flocculation did not occur until a chitosan concentration of approximately 0.75 % (w/v) (Figure 5.2). Thus, stable chitosan-coated liposomes could be formed only within a narrow concentration range of $C_{sat} < C < C_{dep}$, where C_{sat} is the minimum concentration of polymer required to cover the oppositely charged particles and C_{dep} is the polymer concentration where depletion flocculation occurs. In this concentration range, surfaces are completely saturated with polyelectrolyte, and there is not yet sufficient free polyelectrolyte in the continuous phase to promote depletion flocculation (Guzey and McClements 2006).

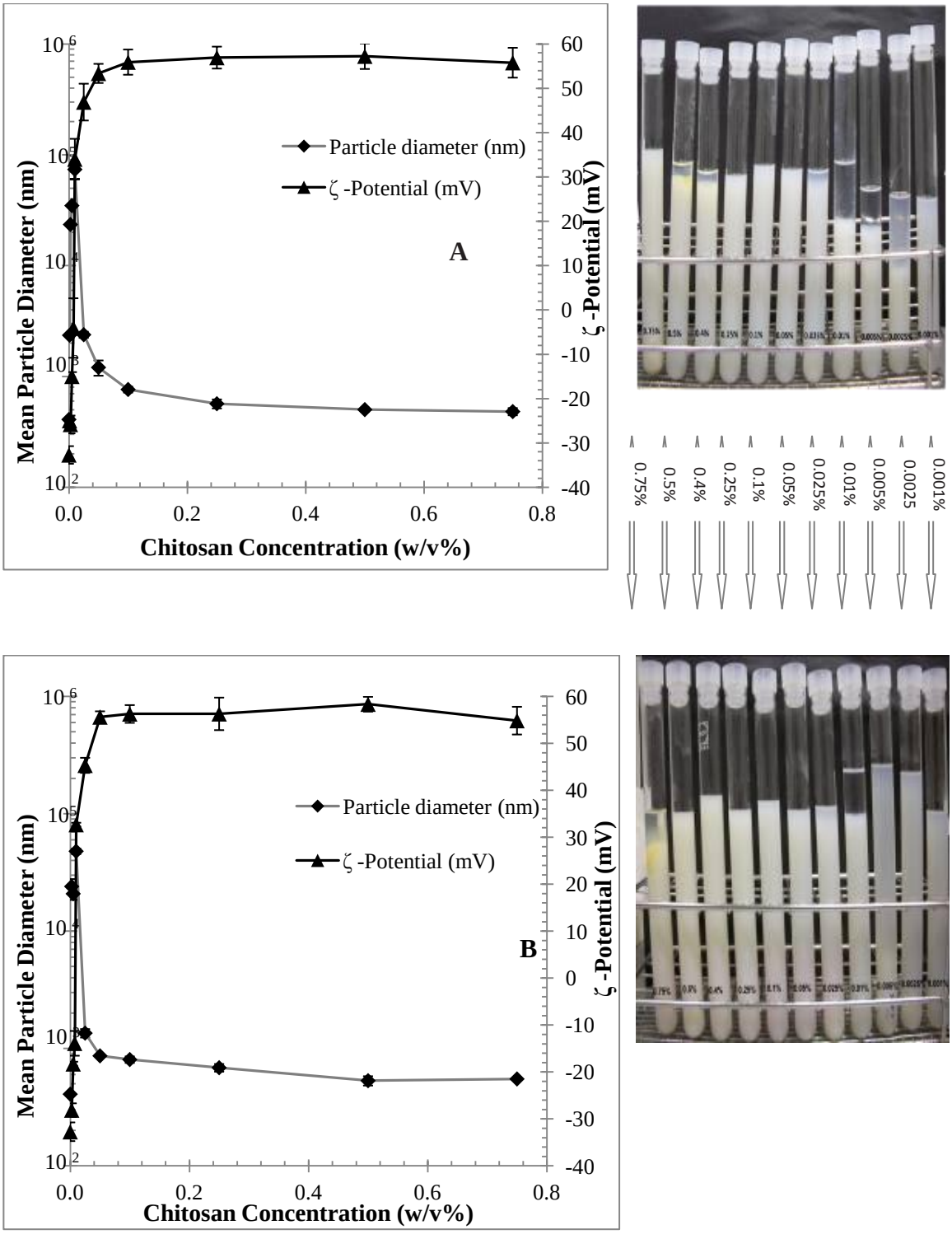

Figure 5. 1: Change in ζ-potential and mean particle diameter after addition of 0 to 0.75, w/v % chitosan to liposomes (0.5, w/v%) for (A) HMW-C and (B) LMW-C. Photographic images of dispersions (chitosan concentration increasing from 0.001-0.75% from left to right) were taken after 2 weeks of storage at room temperature.

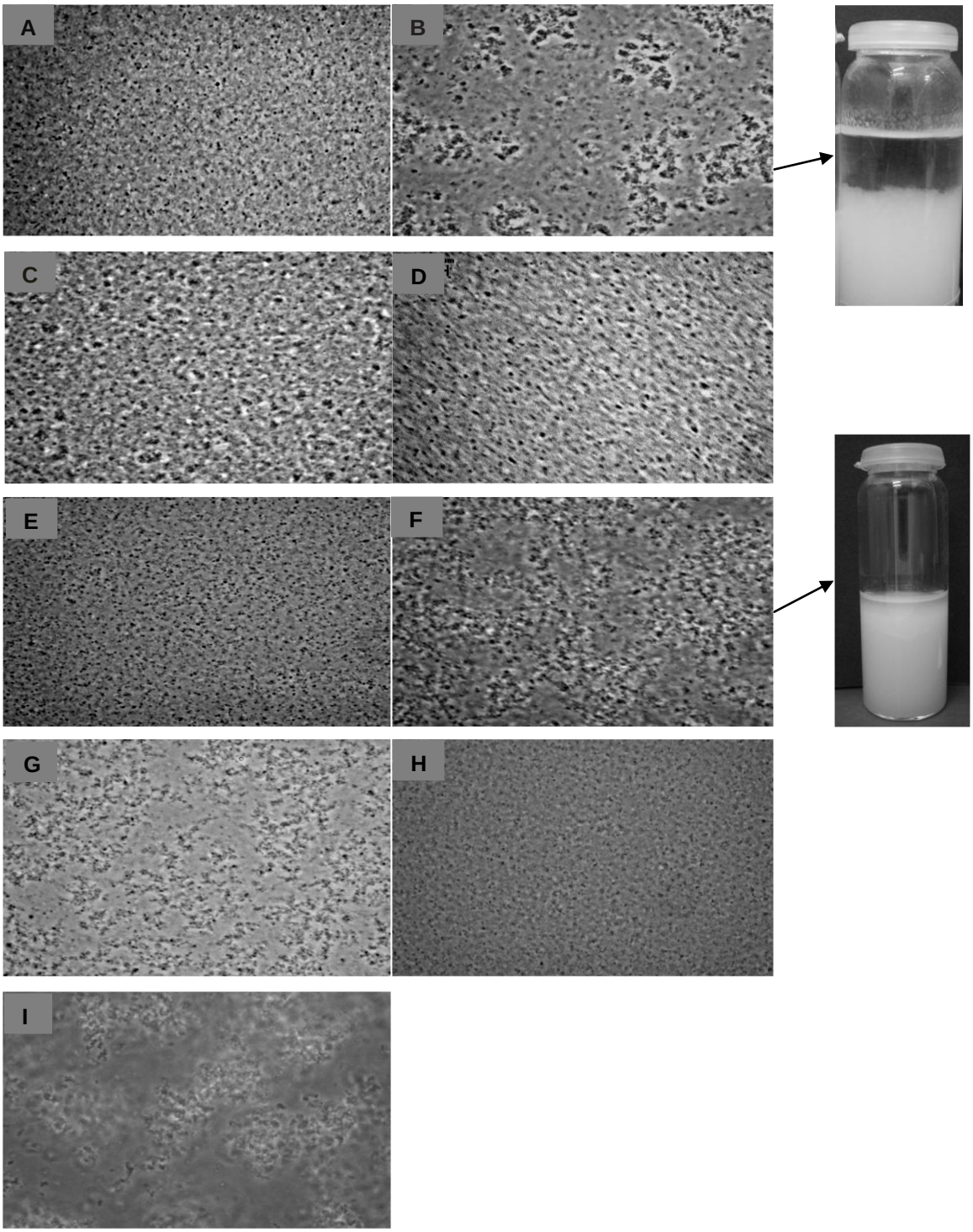

Figure 5.2: Microscopic images at x100 magnification, A: Liposome (1%) with initial size of ~0.4µm; B-G: After addition of high molecular weight chitosans, B: 0.01%, C: 0.05%, D: 0.1%, E: 0.25%, F: 0.5%, G: 0.75%; H and I : After addition of low molecular weight chitosans, H:0.5% and I: 0.75%.

The saturation concentration C_{sat} can be estimated by an empirical model via the change of the ζ-potential:

$$\frac{\Delta\zeta(c)}{\Delta\zeta_{sat}} = \frac{\zeta(c)-\zeta_{sat}}{\zeta_0-\zeta_{sat}} \approx \exp\left(-\frac{c}{c^*}\right) \approx \exp\left(-\frac{3c}{c_{sat}}\right) \quad \textbf{(5.6)}$$

where $\zeta\ (c)$ is the potential of liposomes at a chitosan concentration of c and ζ_0 and ζ_{sat} are the potentials in the absence of chitosan and when liposomes are fully saturated with chitosan. c^* is the polysaccharide concentration where the change in ζ-potential is *1/e* of the total change in ζ-potential at saturation: $\Delta\zeta = \Delta\zeta_{sat}/e$. The variable c_{sat} can be estimated by determining the polymer concentration at which the ζ-potential has increased or decreased by 95%. $c_{sat} = -c^*ln(0.05)$ or $c_{sat} \approx 3c^*$ (Guzey and McClements 2007).

Based on this information, we calculated a saturation concentration of 0.036 (w/v %) for low molecular weight chitosan and 0.027 (w/v %) for high molecular weight chitosan. This concentration corresponded to the polymer concentration where particle diameters started to become smaller after having become aggregated.

The surface coverage at the point of saturation Γ_{sat} can be calculated by considering the structure of liposomes. For phosphatidylcholine vesicles with a single bilayer, a shell thickness of approximately 5 nm has been reported (Xu and others 2012). The total surface area of liposomes is:

$$A = 4\pi r^2 n \quad \textbf{(5.7)}$$

where n is the number of liposomes; and n can be calculated from the concentration of lecithin:

$$n = \frac{C_{lecithin,total}}{C_{lecithin,liposome}} = \frac{C_{lecithin,total}V_{solution}}{\frac{4}{3}\pi(r^3-(r-\Delta r)^3).\rho_{lecithin}} \quad \textbf{(5.8)}$$

where $C_{lecithin,liposome}$ is the lecithin concentration needed to form an individual vesicle, r is the mean radius of the liposomes (200 nm), ρ is the density of lecithin (1.015 g/cm^3 at T = 25°C) and Δr is the thickness of the liposomal membrane (5 nm). The surface coverage Γ can then be calculated as:

$$\Gamma_{sat} = \frac{C_{sat}}{A} \quad \textbf{(5.9)}$$

For LMW-C and HMW-C, a mean surface coverage of 0.185 and 0.139 mg/m^2 was calculated for our ~400 nm liposomes. This value is similar to values reported previously where surface loads of biopolymers adsorbed to the surfaces of colloidal particles had been calculated (Helgason and others 2009; Li and others 2010).

5.4.5 Effect of maltodextrin addition on the properties of uncoated and coated liposomes

5.4.2.1 Uncoated liposomes

In our study, high and low molecular weight maltodextrins were added as carriers to facilitate spray drying of uncoated and coated liposomes. Lecithin and maltodextrin concentrations of 0.5 and 20 (w/v %) were used, respectively. Regardless of molecular weight, addition of maltodextrin to uncoated liposomes immediately caused extensive flocculation and a complete breakdown of the system (Figure 5.3).

Figure 5.4 shows a "phase diagram" illustrating at which liposome-maltodextrin concentrations this breakdown occurred. Excessive concentration of maltodextrin in the bulk solution appeared to cause depletion aggregation, albeit this time due to addition of maltodextrin. Depletion flocculation begins to occur at a defined minimum polymer concentration, the so-called critical flocculation concentration, which depends on the volume fraction of liposomes and the molecular weight of polymer. The region where flocculation occurred was larger for high molecular weight maltodextrin than for low molecular weight maltodextrin.

When low molecular weight maltodextrin was added to liposomes at large polymer concentrations, the particle diameter decreased between 40 and 90 nm (Table 5.2). At higher concentrations, flocculation occurred and particles aggregated which was visible under the microscope (Figure 5.4).

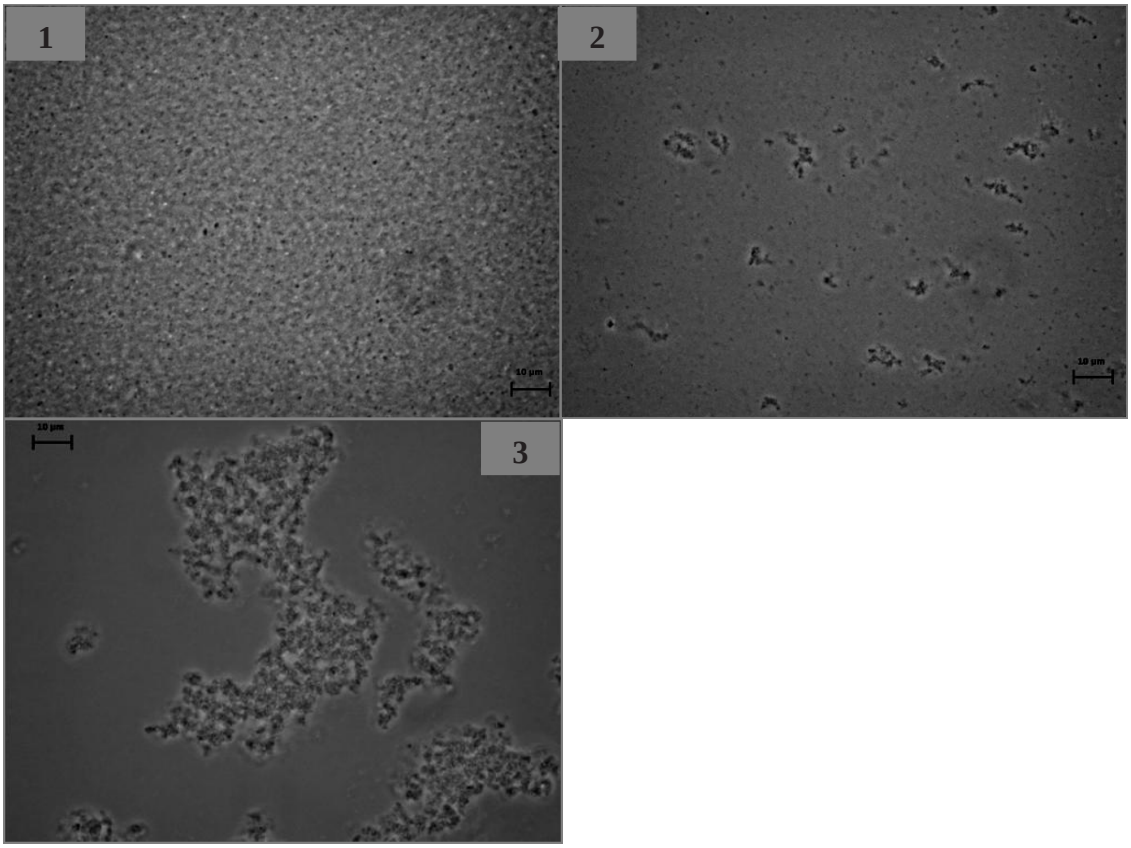

Figure 5.3: Microscopic images (x100 magnification) of dispersions after addition of LMW-MD and HMW-MD to uncoated liposomes (0.5 w/v %). 1: uncoated liposomes; 2: addition of LMW-MD (20 w/v %), 3: addition of HMW-MD (20 w/v %). The scale bar denotes a length 10µm

In contrast, liposomes mixed with concentrations of high molecular weight maltodextrin below the flocculation cut-off, (2 w/v% lecithin, and 2. 5w/v% HMW-MD) did not change in size (415.0 ± 11.2 nm) compared to uncoated ones (427.4 ± 2.8 nm). Liposomes are vesicles composed of an aqueous core surrounded by a phospholipid bilayer membrane. When these structures are immersed in a solution containing low molecular weight compounds with an appreciative potential to reduce water activity such as salts or sugars, water will migrate from the core to decrease the concentration gradient between the inside and the outside of the liposomes. Such an osmotic driving force may explain the size reduction observed.

Table 5.2:. The particle size change of uncoated liposomal dispersions by the addition of low molecular weight maltodextrin (LMW-MD)

Liposome Conc. (w/v %)	LMW-MD Conc. (w/v %)	Particle Diameter (nm)
Initial Diameter		427.4±2.8
2	5	358.2±1.6
	10	333.2±3.6
4	5	384.6±2.0
	10	350.0±3.6
	15	335.5±1.2
6	10	354.0±2.6
	15	336.4±2.4

Upon the addition of maltodextrin (20% w/v), uncoated liposomes broke down in the presence of both low and high molecular weight maltodextrin due to extensive flocculation. The results led us to the conclusion that uncoated liposomes combined with high concentrations of maltodextrin may not be suitable for spay drying (Figure 5.3 and 5.6). The addition of high molecular weight maltodextrin slightly reduced ζ-potential values ($p<0.05$), whereas low molecular weight maltodextrin addition had no effect on the electrical charge of uncoated liposomes (Table 5.3).

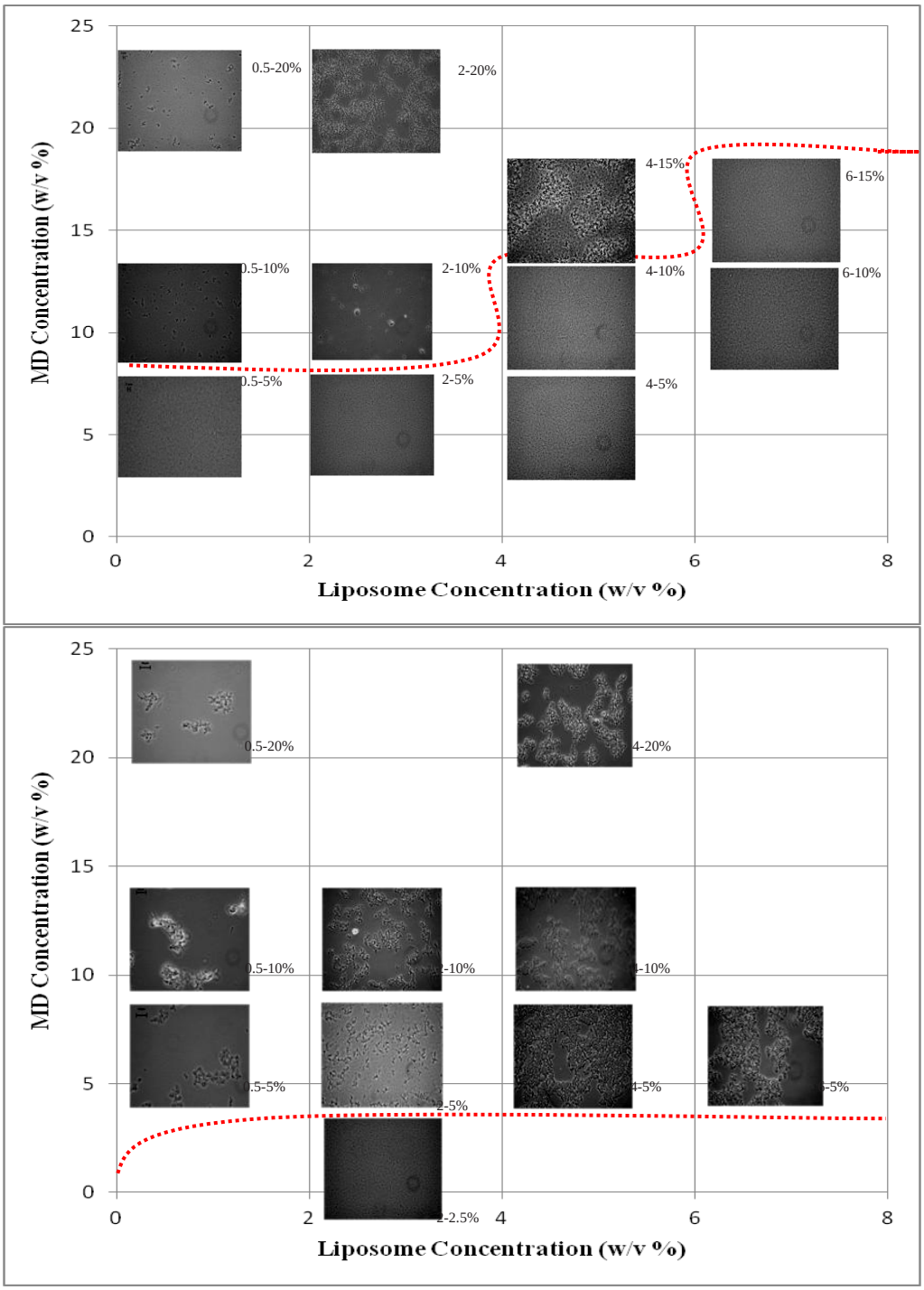

Figure 5.4: Optical microscopic images (at x100 magnification) of uncoated liposomal dispersions containing at various maltodextrin molecular weights and concentrations. The region below the dotted line shows the concentrations where dispersions did not flocculate.

Maltodextrin is a hydrophilic nonionic polysaccharide and as such no effect of its addition on electrical charge of liposomes is to be expected. However, it was observed that a slight decrease in ζ-potential of emulsions when maltodextrin concentrations increased; particularly so, if maltodextrins had a certain degree of polymerization (DE) (Klinkesorn and others 2004). They proposed that maltodextrin may have become attached to droplet surfaces due to hydrophobic interactions thereby reducing the negative charge of droplets. On the other hand high molecular weight maltodextrin addition caused after a few hours depletion flocculation which may also have contributed to the observed decrease in ζ-potential.

Table 5.3: ζ-Potential of uncoated and HMW-C and LMW-C (0.175 w/v%) coated liposomes (0.5 w/v%), droplets mixed with LMW-MD and HMW-MD (20 w/v%) prior to spray drying and reconstituted coated liposomes after spray drying**.**

	Initial ζ-Potential (mV)	MD Type [1]	ζ-Potential of Pre-dried Dispersions (mV)	ζ-Potential of Reconstituted Dispersions
Uncoated	-31.5±1.41	LMW-MD	-28.7±0.55	[2]
		HMW-MD	-26.0±1.94 [3]	
HMW-C [1]	56.0±0.92	LMW-MD	55.0±1.38	52.4±1.10
		HMW-MD	50.5±1.80	44.8±1.04
LMW-C [1]	55.8±1.61	LMW-MD	54.7±1.05	51.9±1.66
		HMW-MD	51.0±1.53	48.0±2.04

[1]Abbreviations: HMW-C: High molecular weight chitosan; LMW-C: Low molecular weight chitosan; HMW-MD: High molecular weight maltodextrin; LMW-MD: Low molecular weight maltodextrin

[2] Spray drying conducted only for chitosan coated liposomal dispersions.

[3] Phase separation was observed after a few hours. The measurement was done after the sample had been mixed using a vortexer prior to analysis.

5.4.2.2 Coated liposomes

Liposomes coated with 0.35 (w/v %) high and low molecular weight chitosan were used to prepare spray dried powders, since at this concentration neither depletion nor bridging flocculation had been observed. In contrast to uncoated liposomes that had

broken down after maltodextrin addition (Figure 5.4), the structure of chitosan-coated liposomal dispersions did not change after maltodextrin addition (Figure.5.5). This suggests that the presence of a "protective coat" of an adsorbed biopolymer decreased susceptibility against subsequent depletion flocculation by a second non-adsorbing polymer. The adsorption of chitosan to the liposomal surfaces increases the thickness of the interfacial layer and alters its charge. In consequence, there may be an increased steric and electrostatic repulsion between different liposomes which would reduce the extent of flocculation (Dickinson 2009). Many researchers have studied the increased stability of emulsions after adsorption of a polysaccharide layer (Wollenweber and others 2000; Payet and Terentjev 2008).

As mentioned above, a ~100 nm decrease in diameter of liposomes (Figure 5.7) was observed due to the previously mentioned osmotic effect after addition of low molecular weight maltodextrin to high and low molecular weight chitosan coated liposomes.

In contrast upon the addition of high molecular weight maltodextrin, the dispersions still showed unimodal particle size distribution but increased in particle size (Figure 5.7), e.g. the diameter of high molecular weight chitosan coated liposomes increased from ~0.5 µm to 1 µm while the diameter of LMW-C coated liposomes increased to 2 µm (Table 5.4).

The differences in particle size compared to their initial size before maltodextrin addition was significant ($p<0.05$). Since a high molecular weight chitosan layer on the particle surface can be expected to be thicker, liposomes coated with HMW-C appear to be less susceptible to depletion interaction upon addition of maltodextrin (Figure 5.5).

Finally, similar to uncoated liposomes, addition of low molecular weight maltodextrin to coated liposomes had no significant effect on ζ-potential values, whereas high molecular weight maltodextrin addition slightly decreased the ζ-potential ($p<0.05$) (Table 5.4).

Table 5.4: Particle diameter of HMW-C and LMW-C (0.175 w/v%) coated liposomes (0.5 w/v%), coated liposomes mixed with LMW-MD and HMW-MD (20 w/v%) prior to spray drying and reconstituted coated liposomes after spray drying (0.5 (w/v%) liposome; 0.175 (w/v%) chitosan; 20 (w/v%) maltodextrin).

	Initial Diameter (nm)	MD Type [(1)]	Mean Diameter of Pre-dried Dispersions (nm)	Mean Diameter of Reconstituted Dispersions (nm)
Uncoated	427±3			
HMW-C [(1)]	483±23	LMW-MD	381±15	367±22
		HMW-MD	1040±132	1255±159
LMW-C [(1)]	532±18	LMW-MD	409±24	366±16
		HMW-MD	2054±235	32302±6652

[(1)]Abbreviations: HMW-C: High molecular weight chitosan; LMW-C: Low molecular weight chitosan; HMW-MD: High molecular weight maltodextrin; LMW-MD: Low molecular weight maltodextrin

5.4.3 Moisture content and water activity of spray dried liposomal powders

The different liposomal preparations containing maltodextrin were then spray dried. The moisture content and water activity values of powders are listed in Table 5.5. Since the spray drying process parameters were kept constant, moisture content and water activity depended mainly on the feed solution properties. Indeed, there was no significant difference among samples ($p<0.05$) in terms of moisture content and water activity.

Similar results had been obtained by Goula and Adamopoulos (2008) and Gharsallaoui and others (2011), who both stated that the final moisture content of the spray-dried powders, at constant conditions, is mainly determined by the nature of the matrix material. Due to the more viscous nature of the low DE maltodextrin, and therefore coarser droplets we expected a somewhat lower evaporation rate. In our study however, no significant differences were found between powders containing different molecular weight maltodextrins while the powder yield of all samples varied somewhat (58 - 65 %).

Table 5.5: Yield, moisture content and water activity of chitosan coated liposome powders.

MD Type [(1)]	Chitosan Type [(1)]	Yield (%)	Moisture content (%)	Water activity
LMW-MD	LMW-C	64.7 ± 7.00	4.1 ± 0.62	0.09 ± 0.04
	HMW-C	61.7± 4.60	4.4 ± 0.35	0.09 ± 0.03
HMW-MD	LMW-C	57.4± 6.33	3.8 ± 0.45	0.08 ± 0.03
	HMW-C	57.3 ± 2.41	3.7 ± 0.82	0.08 ±0.03

[(1)]Abbreviations: HMW-C: High molecular weight chitosan; LMW-C: Low molecular weight chitosan; HMW-MD: High molecular weight maltodextrin; LMW-MD: Low molecular weight maltodextrin

Similar results had been obtained by Goula and Adamopoulos (2008) and Gharsallaoui and others (2011), who both stated that the final moisture content of the spray-dried powders, at constant conditions, is mainly determined by the nature of the matrix material. Due to the more viscous nature of the low DE maltodextrin, and therefore coarser droplets we expected a somewhat lower evaporation rate. In our study however, no significant differences were found between powders containing different molecular weight maltodextrins while the powder yield of all samples varied somewhat (58 - 65 %).

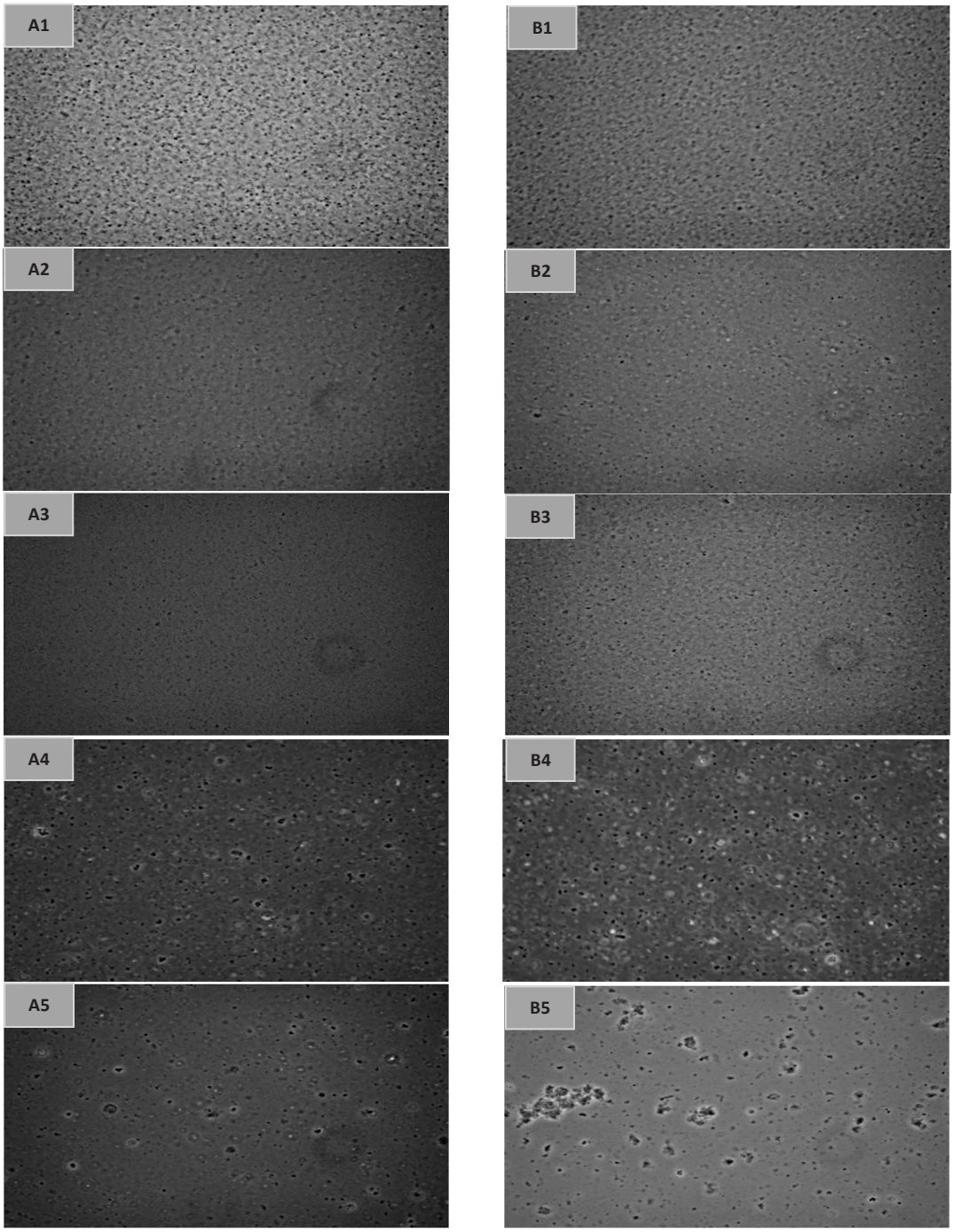

Figure 5.5: Microscopic images (x100 magnification) of structures formed after addition of HMW-MD and LMW-MD (20 w/v %) to HMW-C (0.175 w/v %) (A series) and LMW-C (0.175 w/v %) (B series) coated liposomes (0.5 w/v %) and the change in the structure upon redispersion of spray dried powders. 1: coated liposomes; 2: after addition of LMW-MD; 3: reconstituted spray dried samples prepared with LMW-MD; 4: after addition of HMW-MD; 5: reconstituted spray dried samples prepared with HMW-MD

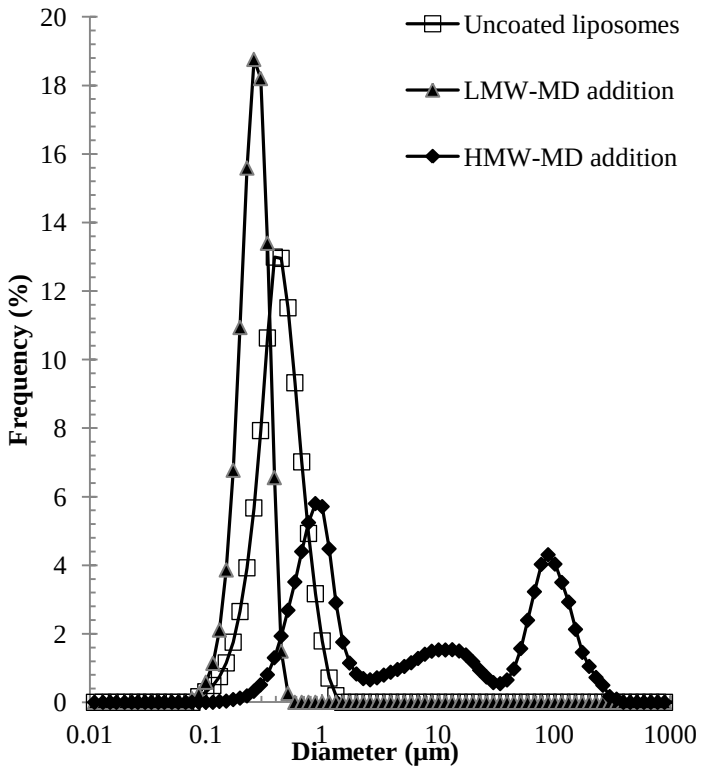

Figure 5 6: Volume based particle diameter distribution of uncoated liposomes (0.5 w/v %) before and after low and high molecular weight maltodextrin addition (20% w/v%)

5.4. Powder morphology

The drying of liquid precursor solutions containing dispersed polymers and discrete entities such as droplets or particles may yield a variety of different shapes and structures depending on both, the nature of the particulate matter and the dispersed polymer, and process parameters such as drying air and liquid precursor concentration. Many powder properties including particle size, flowability, and protection of core material from the environment have been reported to be directly related to their morphologies (Rosenberg and others 1985; Walton 2000). The scanning electron microscopy images of liposomal powders generated in this study demonstrate that the morphology of spray dried powders mainly depended on the maltodextrin type used (Figure 5.8 and 5.9).

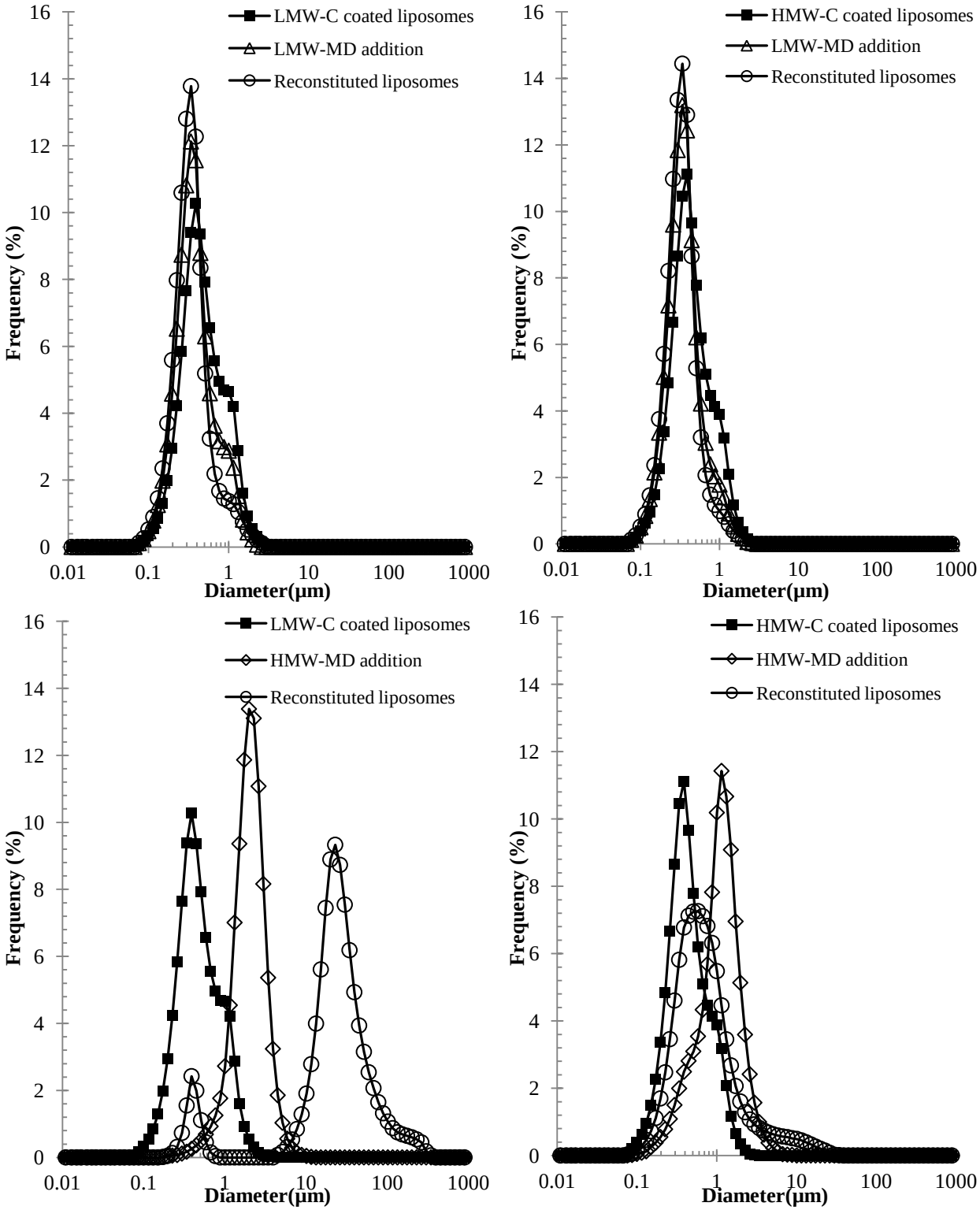

Figure 5.7: Volume based particle diameter distribution of low and high molecular weight chitosan (0.175 v/w %) coated liposomes before and after low and high molecular weight maltodextrin (20 w/v %) addition and after reconstitution of spray dried samples

Powders prepared from coated liposomes with low molecular weight maltodextrin were mostly spherical with some small indentations and wrinkles on their surfaces. Their diameter ranged between 1-5 μm, and most of the particles had average diameter of less than 5μm. The diameter range of coated liposomes spray dried with high molecular weight maltodextrin was larger (~2-10 μm) and most of the particles had sizes of ~10 μm. Smaller sized particles appeared broken and collapsed, and surfaces of all particles had characteristic concavities with deep dents (Figure 5.9). Such dents and wrinkles on the surface of spray dried powders have been reported in other studies also where carbohydrates excipients had been used (Sheu and Rosenberg 1998; Tonon and others 2011). It has been suggested that dent formation is related to skin formation around the particle. In the early stages of drying, the particle surface is initially a liquid with high solvent content. As soon as the atomized droplets come into contact with the dry air, evaporation occurs and a significant solvent concentration gradient between the surface and the interior of the droplets begins to develop. Depending on the evaporation speed and the rate with which the solvent may migrate from the interior to the surface, solids may precipitate from the solution at the surface of the particles, leading to the formation of a crust or skin. Depending on the mechanical properties of the developing skin, it may remain intact or may fracture (Walton 2000; Walzel and Furuta 2011).

Moreover, if the drying process takes place at a high temperature, the crust development may be followed by an internal bubble formation. The bubbles expand and begin to rupture the crust, in turn causing the particle to collapse, shrivel and re-inflate. Such a thermal expansion can also smooth out dents to a varying extent. The effectiveness of dent smoothing is dependent on the drying rate and the viscoelastic properties of the wall matrix. Nevertheless, smoothing of dents can occur only prior to solidification of the matrix, when the wall matrix is still elastic enough to undergo such structural changes (Sheu and Rosenberg 1998).

As a result, relatively smooth and shriveled particles with uneven surface structures are formed. According to the SEM pictures of the surface structure of powders prepared with low and high molecular weight maltodextrin, the powders had less dents, and a smoother surface when the molecular weight of the wall material was lower.

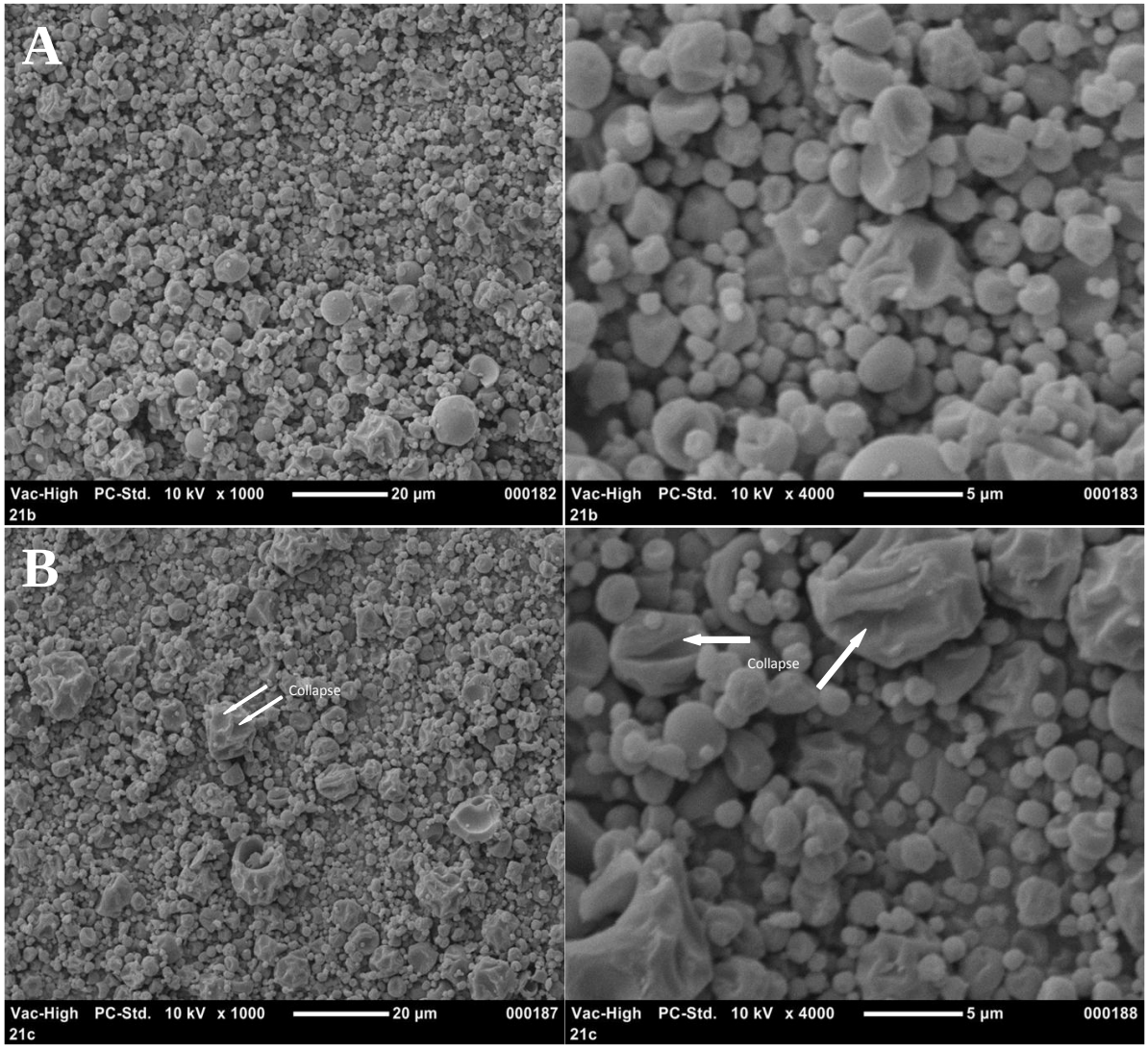

Figure 5.8: SEM images of coated liposomes (A: High molecular weight chitosan; B: Low molecular weight chitosan) spray dried in the presence of low molecular weight maltodextrin. Pictures were taken at X1000 and X4000 magnifications.

The less-dented structure of particles dried with low molecular weight maltodextrin may be attributed to the lower glass transition temperature and difference in sugar composition. High DE maltodextrins typically consist of a greater amount of low molecular weight sugars which may act as a plasticizer preventing irregular shrinkage during drying. The average molecular weight of the low molecular weight maltodextrin (DE 21) can be estimated to ca. 9000 kg/Kmol while for the high molecular weight maltodextrin (DE2) a value of 155 000 kg/ Kmol was given by (Avaltroni and others 2004). The glass transition temperature of the maltodextrins at outlet moisture content was determined based on a Gordon Taylor approximation to be 176°C and 86°C for the high and low molecular weight maltodextrin. In comparison to the inlet air temperature of 160°C and the outlet air temperature of

90°C these values indicate the difference in viscosity of the skin material at later stages of drying. The low molecular weight maltodextrin stays mobile through most of the drying, while the high molecular weight maltodextrin will not be able to shrink in the later phase and the skin rather wrinkles. The inverse relationship between surface dents and DE values of maltodextrins in our study is thus in agreement with the findings of various other authors (Sheu and Rosenberg 1998; Danviriyakul and others 2002; Walzel and Furuta 2011).

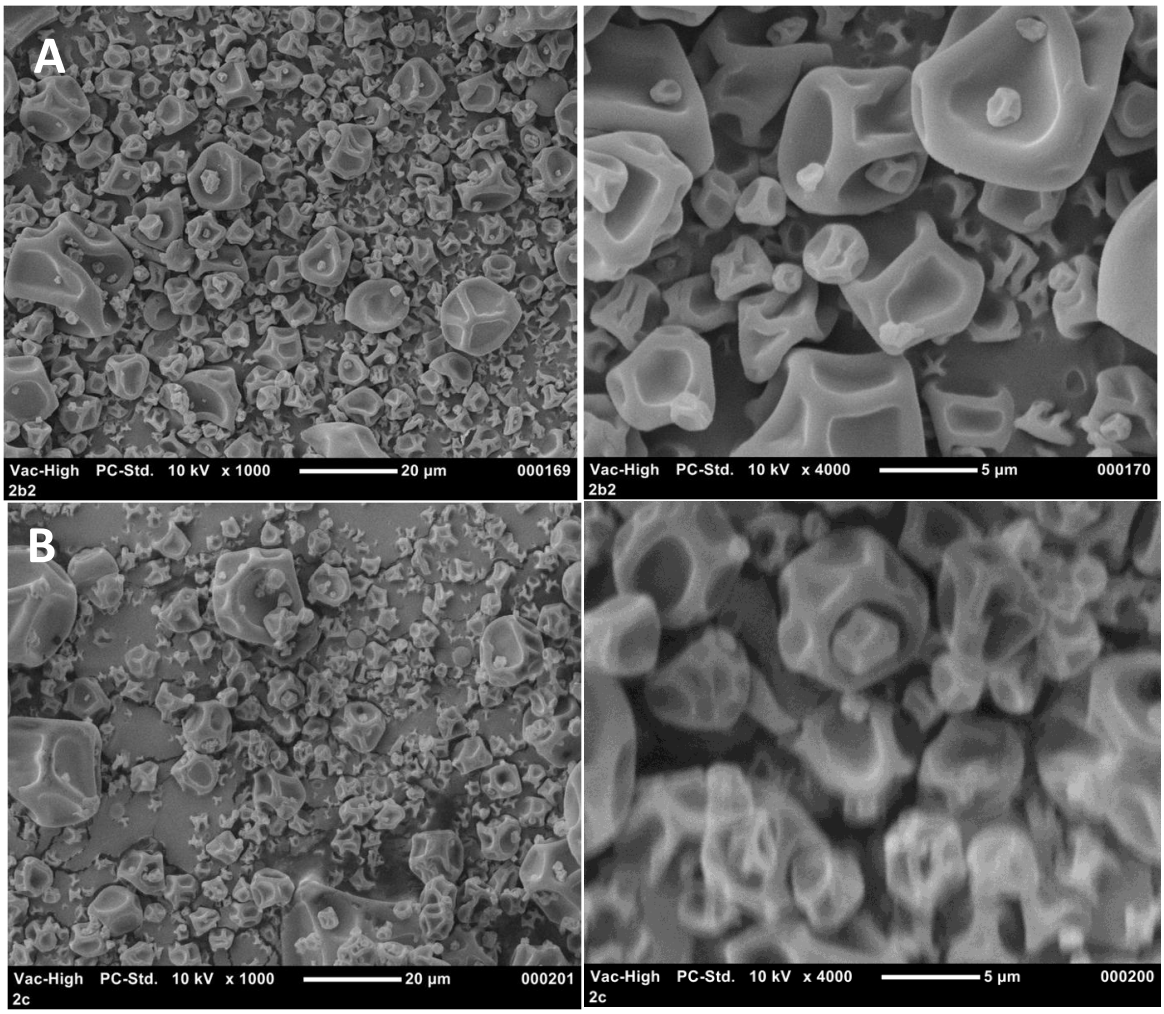

Figure 5.9: SEM images of coated liposomes (A: High molecular weight chitosan; B: Low molecular weight chitosan) spray dried in the presence of high molecular weight maltodextrin. Pictures were taken at x1000 and x4000 magnifications.

5.4.5. Reconstitution of coated liposomes

Due to the structural breakdown of uncoated liposomes upon addition of either low or high molecular weight maltodextrin (20 w/v %) before spray drying (see above), we spray dried only chitosan coated liposomes. The particle diameter of spray dried chitosan coated powders upon reconstitution was measured at different reconstitution

ratio (1:5, 1:10 and 1:20 weight of powder to weight of reconstituted dispersion) and at different times (1, 2, 4, 8 and 16 h). High molecular weight maltodextrin spray dried powders needed at least 16 h to be completely dissolved, in contrast to low molecular weight maltodextrin powders which could be rehydrated in less than 1 h. Mean particle diameter of reconstituted dispersions of low molecular weight maltodextrin powders were slightly smaller than those of pre-dried dispersions. The difference (~20 nm) was not significant for high molecular weight chitosan coated particles but was significant (~40 nm) for low molecular weight chitosan coated particles ($p<0.05$) (Table 5.3). All reconstituted dispersions prepared with LMW-MD had unimodal particle size distributions (Figure 5.7). A key property of dehydrated powders manufactured for consumer use is their ease of reconstitution (Hogekamp and Schubert 2003; Klinkesorn and others 2006).

We used a laser diffraction technique to determine the rate and efficiency of the powder dispersion. ~0.85 g powder was added to a continuously stirred buffer solution contained within the stirring chamber of a laser light diffraction particle size distribution analyzer (LA-950, Horiba, Japan), using a low buffer volume in the measurement chamber (~150 ml). The dispersibility of powders was then determined as the change in mean particle diameter as a function of time. The measurement was conducted only for coated liposomes prepared with LMW-MD, since HMW-MD powders needed at least 16 h to dissolve. The particle size reached a minimum value of ~350 nm for both high and low molecular weight chitosan coated liposomes after 6 min of stirring and remained constant thereafter. This rapid decrease in particle size indicated that the powder samples prepared with low molecular weight maltodextrin dissolved quickly and yielded homogenous dispersions.

Particle size of reconstituted high molecular weight maltodextrin powders increased compared to the size of pre-dried dispersions with the increase being significant for both high and low molecular weight coated liposomes ($p<0.05$). The increase was ~250 nm for high molecular weight chitosan coated liposomes whereas for low molecular weight chitosan coated ones, liposomes grew to more than 15 times their pre-dried size (Table 5.3). Powders prepared with high molecular weight maltodextrin had a bimodal distribution of reconstituted low molecular weight chitosan coated liposomes (Figure 5.7), and optical microscopy showed formation of large aggregates (Figure 5.5). The stabilizing effect of chitosan as a function of its

molecular weight during spray drying may be explained by "Hydration Forces Explanation" (HFE) theory. According to the HFE theory the presence of small solutes in membranes during dehydration prevents a close approach of the membrane bilayers, thereby reducing the probability of a structure breakdown that arises when the bilayers are in close proximity. The better protection provided by high molecular weight chitosan could be attributed to its molecular weight. Koster and coauthors stated that as long as the solutes remained in intermembrane regions, the protective effect of the solute was related to its molecular weight (Koster and others 2000). They reported for example that raffinose offered a substantially better protection than sucrose or trehalose. Each dry raffinose molecule has a molar volume that is equal to ~30 times that of a water molecule compared to ~18 times for sucrose and trehalose. In another study, the authors suggested that larger maltodextrins with molecular weights of 5000 and 12000 Da did not provide any stabilization since large polymers are partially or completely excluded from the interlamellar space and sequestered in the bulk phase during dehydration (Koster and others 2003). The results with coated liposomes and maltodextrins of the given size range (ca. 9000 Da) indicate the opposite.

5.5.Mechanistic insights

In our study, the surface of anionic phosphatidylcholine liposomes was coated with cationic chitosan using the layer-by-layer (LBL) depositioning method. Addition of chitosan to liposomes resulted in bridging flocculation when the amount of chitosan was not sufficient, and in depletion flocculation when there amount of free chitosan in the continuous phase was too high (Figure 5.10). An optimum chitosan concentration may be determined from optical microscopic images and particle diameter measurements.

Maltodextrin was then mixed with coated and uncoated liposomes to facilitate spray drying. There, liposome, chitosan and maltodextrin concentrations of 0.5, 0.175 and 20 (w/v %), respectively were used. Regardless of maltodextrin molecular weight, its addition to uncoated liposomes causes extensive flocculation making the system unsuitable for spray drying (Figure 5.10). In contrast, the structure of chitosan-coated liposomal dispersions did not change after maltodextrin addition.

We suggest that the adsorbed chitosan layer increases steric and electrostatic repulsion between liposomes, which in turn prevents that osmotic effects induced by addition of non-adsorbing polymer cause aggregation and breakdown of liposomes.

When chitosan coated liposomes were spray dried with maltodextrins and later reconstituted, all coated liposomes except those that had been coated with low molecular weight chitosan and spray dried with high molecular weight maltodextrin yielded back the original particle size distributions that liposomal dispersions had prior to spray drying. Mechanistically; one cam therefore conclude that the adsorption of a protective layer of biopolymer on the surface of liposomes in combination with the appropriate selection of a non-adsorbing polymer is required to generate a stable liquid precursor system that in turn resist the stresses of a spray drying process without compromising rehydration to an unacceptable level.

5.6.Conclusions

Liposomes are increasingly of great interest to food manufacturers for the delivery of various functional components such as flavors, antioxidants, antimicrobials, and bioactives. Recent studies have in particularly shown their ability to act as carriers for polyphenolics, a class of bioactives that is notoriously difficult to include in traditional oil-in-water emulsions. However, the difficulty of maintaining the structural integrity of liposomes in aqueous dispersion represents a challenge for their commercialization. Dehydration may increase their stability, resulting in an increased shelf-life and decreased distribution costs. Spray drying is one of the most economical processes to convert liquid precursors into dry powders. Prior to this study, spray drying of liposomes often led to their structural integrity being lost. The results of our study show for the first time that spray drying may be used to generate commercially feasible powders if combinations of adsorbing and non-adsorbing polymers are used in the formulation of the liquid precursor system. Clearly more research is needed to elucidate whether such powders also afford a higher chemical stability of liposomes to e.g. hydrolysis and oxidation and whether such an approach would reduce the leakage of encapsulated material. Nevertheless, the results should be of substantial interest to the food and pharmaceutical industry interested in delivering active ingredients.

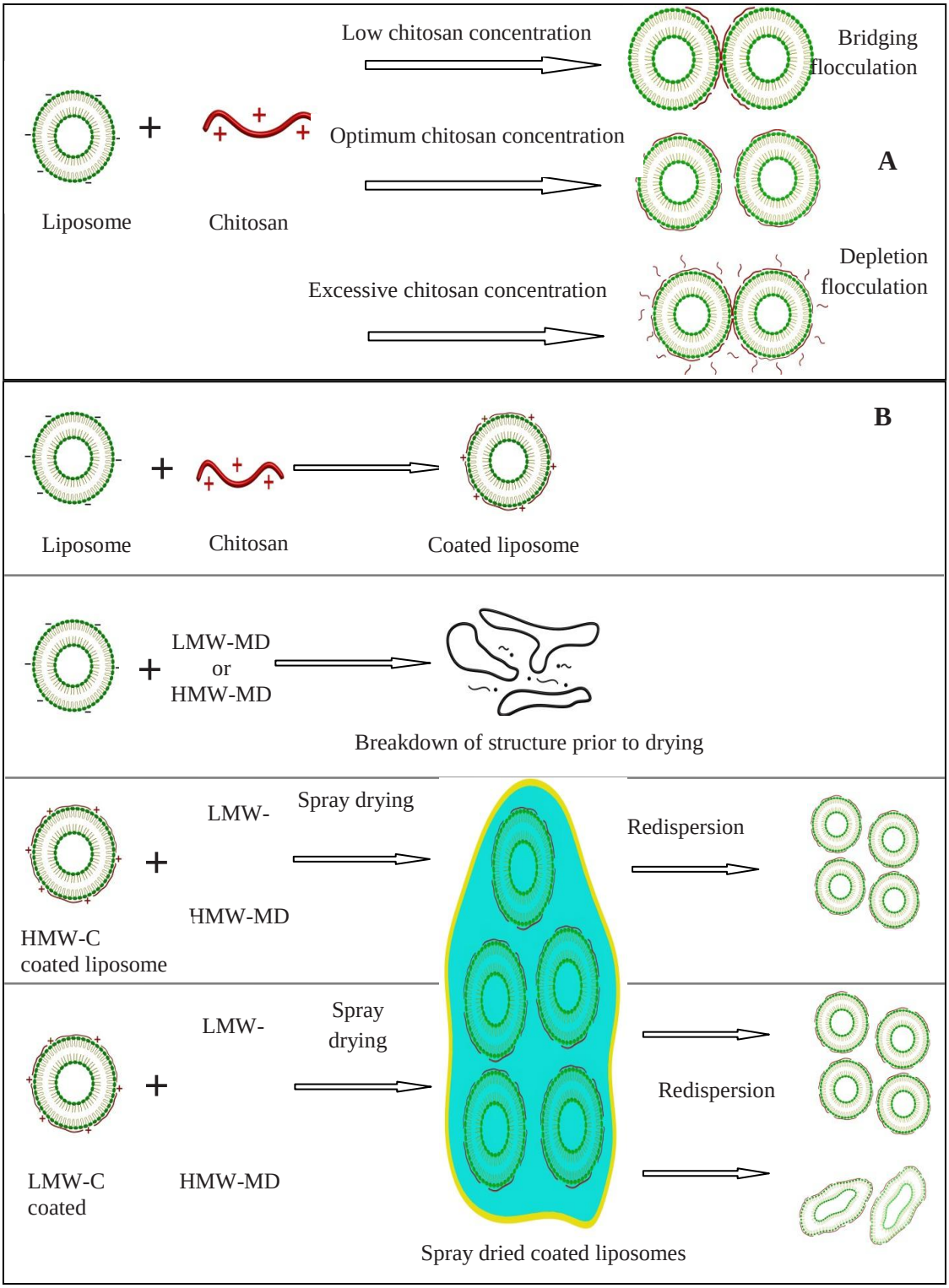

Figure 5. 10: Mechanistic image of different events occurred when chitosan added to liposomes (A) and when maltodextrin added to uncoated and chitosan coated liposomes and when spray dried liposome powders reconstituted (B).

REFERENCES

Adom, K.K., Liu, R.H. (2005). Rapid Peroxyl Radical Scavenging Capacity (PSC) Assay for Assessing both Hydrophilic and Lipophilic Antioxidants. *Journal of Agricultural and Food Chemistry*, 53(17), 6572-6580.

Anarjan, N., Mirhosseini, H., Baharin, B.S. and Tan, C.P. (2010). Effect of processing conditions on physicochemical properties of astaxanthin nanodispersions. *Food Chemistry*, 123(2), 477-483.

Anton, N., Benoit, J.P. and Saulnier, P. (2008). Design and production of nanoparticles formulated from nano-emulsion templates—A review. *Journal of Controlled Release*, 128(3), 185-199.

Anton, N. and Vandamme, T.F. (2009). The universality of low-energy nano-emulsification. *International Journal of Pharmaceutics*, 377(1–2), 142-147.

Aoki, T., Decker, E.A. and McClements, D.J. (2005). Influence of environmental stresses on stability of O/W emulsions containing droplets stabilized by multilayered membranes produced by a layer-by-layer electrostatic deposition technique. *Food Hydrocolloids*, 19(2):209-220.

Arnao, M.B. (2000). Some methodological problems in the determination of antioxidant activity using chromogen radicals: a practical case. *Trends in Food Science & Technology* ,11(11), 419-421.

Avaltroni, F., Bouquerand, P.E. and Normand, V. (2004). Maltodextrin molecular weight distribution influence on the glass transition temperature and viscosity in aqueous solutions. *Carbohydrate Polymers*, 58(3), 323-334.

Azuma, K., Ippoushi, K., Ito, H., Higashio, H. and J. T. (2002). Combination of lipids and emulsifiers enhances the absorption of orally administered quercetin in rats. *Journal of Agricultural and Food Chemistry*, 50(6), 1706-1712.

Baxter, S., Zivanovic, S. and Weiss, J. (2005). Molecular weight and degree of acetylation of high-intensity ultrasonicated chitosan. *Food Hydrocolloids*, 19(5), 821-830.

Benzie, I.F., Chung, W. and Strain, J.J. (1999). Antioxidant reducing efficiency of ascorbate in plasma is not affected by concentration. T*he Journal of Nutritional Biochemistry*, 10(3), 146-150.

Benzie, I.F. and Strain, J.J. (1996). The Ferric Reducing Ability of Plasma (FRAP) as a Measure of "Antioxidant Power": The FRAP Assay. *Analytical Biochemistry*, 239(1):70-76.

Blijdenstein, T.B.J., Winden, A.J., Vliet. T., Linden. E. and Van Aken, G.A. (2004). Serum separation and structure of depletion- and bridging-flocculated emulsions: a comparison. *Colloids and Surfaces A: Physicochemical and Engineering Aspects*, 245(1-3), 41-48.

Boots, A.W., Li, H., Schins, R.P.F., Duffin, R., Heemskerk, J.W.M., Bast, A. and Haenen, G.R.. (2007). The quercetin paradox. *Toxicology and Applied Pharmacology*, 222(1), 89-96.

Boots, A.W., Haenen, G.R. and Bast, A. (2008). Health effects of quercetin: From antioxidant to nutraceutical. *European Journal of Pharmacology*, 585(2-3), 325-337.

Bouchon, P. and Aguilera, J. (2008). Scanning Electron and Transmission Electron Microscopies in Food Analysis. *Handbook of Food Analysis Instruments.* CRC Press.

Brand-Williams, W., Cuvelier, M.E. and Berset, C. (1995). Use of a free radical method to evaluate antioxidant activity. *LWT - Food Science and Technology*, 28(1), 25-30.

Cao, G., Sofic, E. and Prior, R.L. (1997). Antioxidant and Prooxidant Behavior of Flavonoids: Structure-Activity Relationships. *Free Radical Biology and Medicine*, 22(5), 749-760.

Casagrande, R., Georgetti, S., Verri, W., Jabor, J., Santos, A. and Fonseca, M. (2006). Evaluation of functional stability of quercetin as a raw material and in different topical formulations by its antilipoperoxidative activity. *AAPS PharmSciTech* ,7(1), E64-E71.

Chan, H.K. and Kwok, P.C.L. (2011). Production methods for nanodrug particles using the bottom-up approach. *Advanced Drug Delivery Reviews*, 63(6), 406-416.

Chaubal, M. and Popescu, C. (2008). Conversion of Nanosuspensions into Dry Powders by Spray Drying: A Case Study. *Pharmaceutical Research*, 25(10), 2302-2308.

Chen, C., Han, D., Cai, C. and Tang, X. (2010). An overview of liposome lyophilization and its future potential. *Journal of Controlled Release*, 142(3)-299-311.

Chen, H., Khemtong, C,, Yang, X., Chang, X. and Gao, J. (2011). Nanonization strategies for poorly water-soluble drugs. *Drug Discovery Today*,16(7–8), 354-360.

Choe, E. and Min, D.B. (2006). Chemistry and Reactions of Reactive Oxygen Species in Foods. *Critical Reviews in Food Science and Nutrition*, 46(1), 1-22.

Chuah, A.M., Kuroiwa, T., Ichikawa, S., Kobayashi, I. and Nakajima, M. (2009). Formation of biocompatible nanoparticles via the self-Assembly of chitosan and modified lecithin. *Journal of Food Science*, 74(1), N1-N8.

Chun, J.Y., Choi, M.J., Min, S.G and Weiss J. (2013). Formation and stability of multiple-layered liposomes by layer-by-layer electrostatic deposition of biopolymers. *Food Hydrocolloids*, 30(1), 249-257.

Conxita, S., Isabel, S., Alejandro, F.A., Jordi, N., Nuria, A., Jose, G., Alicia, M., Carmen, G.l. and Carmen, P. (2009). Nanoemulsion formation by low-energy methods and functional properties. *Structure and Functional Properties of Colloidal Systems*. CRC Press, 457-482.

Coupland, J. (2005). Beyond Hard Spheres. *Handbook of Functional Lipids.* CRC Press, 163-176.

Da Silva Malheiros, P., Daroit, D.J. and Brandelli, A. (2010). Food applications of liposome-encapsulated antimicrobial peptides. T*rends in Food Science &Technology*, 21(6), 284-292.

Dalgleish, D. (2004). *Food Emulsions.* CRC Press.

Danviriyakul, S., McClements, D.J., Decker, E., Nawar, W.W. and Chinachoti, P. (2002). Physical Stability of Spray-Dried Milk Fat Emulsion as Affected by Emulsifiers and Processing Conditions. *Journal of Food Science*, 67(6), 2183-2189.

Di Mattia, C.D., Sacchettia, G., Mastrocolaa, D. and Pittia, P. (2009). Effect of phenolic antioxidants on the dispersion state and chemical stability of olive oil O/W emulsions. *Food Research International*, 42(8), 1163-1170.

Dickinson E. (2009). Hydrocolloids as emulsifiers and emulsion stabilizers. *Food Hydrocolloids*, 23(6)-1473-1482.

Donsì, F., Senatore, B., Huang, Q. and Ferrari, G. (2010a). Development of Novel Pea Protein-Based Nanoemulsions for Delivery of Nutraceuticals. *Journal of Agricultural and Food Chemistry*, 58(19), 10653-10660.

Donsì, F., Wang, Y., Li, J. and Huang, Q. (2010b). Preparation of Curcumin Sub-micrometer Dispersions by High-Pressure Homogenization. *Journal of Agricultural and Food Chemistry*, 58(5):2848-2853.

Douglas, D. (2003). *Food Emulsion*s.CRC Press.

Erlund, I. (2004). Review of the flavonoids quercetin, hesperetin, and naringenin. Dietary sources, bioactivities, bioavailability, and epidemiology. *Nutrition Research*, 24(10), 851-874.

Flanagan, J., Kortegaard, K., Neil, P.D, Rades, T and Singh, H. (2006). Solubilisation of soybean oil in microemulsions using various surfactants. *Food Hydrocolloids*, 20(2–3), 253-260.

Floury, J., Desrumaux, A. and Legrand, J. (2002). Effect of ultra-high-pressure homogenization on structure and on rheological properties of soy protein-stabilized emulsions. *Journal of Food Science*, 67(9), 3388-3395.

Gao, L., Liu, G., Wang, X., Liu, F., Xu, Y. and Ma, J. (2011). Preparation of a chemically stable quercetin formulation using nanosuspension technology. *International Journal of Pharmaceutics*, 404(1–2), 231-237.

Gao, L., Zhang, D. and Chen, M. (2008). Drug nanocrystals for the formulation of poorly soluble drugs and its application as a potential drug delivery system. *Journal of Nanoparticle Research*, 10(5), 845-862.

Gao, Y., Wang, Y., Ma, Y., Yu, A., Cai, F., Shao, W. and G. Z. (2009). Formulation optimization and in situ absorption in rat intestinal tract of quercetin-loaded microemulsion. *Colloids and Surfaces B: Biointerfaces*, 71(2), 306-314.

Garti, N. (2000). Food Emulsifiers and Stabilizers. *Food Shelf Life Stability*. CRC Press.

Garti, N. (2002). Food Emulsifiers. *Physical Properties of Lipids.* CRC Press.

Gharsallaoui, A., Saurel, R., Chambin, O. and Voilley, A. (2011). Pea (*Pisum sativum, L*.) protein isolate stabilized emulsions: A novel system for microencapsulation of lipophilic ingredients by spray drying. *Food and Bioprocess Technology*,1-11.

Gibis, M., Vogt, E. and Weiss, J. (2012). Encapsulation of polyphenolic grape seed extract in polymer-coated liposomes. Food & Function 3(3):246-254.

Goldbach, P., Brochart, H. and Stamn, A. (1993a). Spray-drying of liposomes for a pulmonary administration. I. Chemical stability of phospholipids. *Drug Development and Industrial Pharmacy*, 19(19), 2611-2622.

Goldbach, P., Brochart, H. and Stamn, A. (1993b). Spray-drying of liposomes for a pulmonary administration. II. Retention of encapsulated materials. D*rug Development and Industrial Pharmacy*, 19(19), 2623-2636.

Goula, A.M. and Adamopoulos, K.G. (2008). Effect of maltodextrin addition during spray drying of tomato pulp in dehumidified air: II. Powder properties. *Drying Technology*, 26(6), 726-737.

Gutiérrez, J.M., González, C., Maestro, A., Solè, I., Pey, C.M. and Nolla, J. (2008). Nano-emulsions: New applications and optimization of their preparation. *Current Opinion in Colloid Interface Science*, 13(4), 245-251.

Guzey, D., Kim, H.J. and McClements, D.J. (2004). Factors influencing the production of o/w emulsions stabilized by β-lactoglobulin–pectin membranes. *Food Hydrocolloids*, 18(6), 967-975.

Guzey, D. and McClements, D.J. (2006). Formation, stability and properties of multilayer emulsions for application in the food industry. *Advances in Colloid and Interface Science* 128–130, 227-248.

Guzey, D. and McClements, D.J. (2007). Impact of electrostatic interactions on formation and stability of emulsions containing oil droplets coated by β-lactoglobulin−pectin complexes. *Journal of Agricultural and Food Chemistry* 55(2), 475-485.

Han, R.M., Zhang, J.P. and Skibsted, L.H. (2012). Reaction dynamics of flavonoids and carotenoids as antioxidants. *Molecules*, 17(2), 2140-2160.

Harrigan, P.R., Madden, T.D. and Cullis, P.R. (1990). Protection of liposomes during dehydration or freezing. *Chemistry and Physics of Lipids*, 52(2):139-149.

Heim, K.E., Tagliaferro, A.R. and Bobilya, D.J. (2002). Flavonoid antioxidants: chemistry, metabolism and structure-activity relationships. *The Journal of Nutritional Biochemistry*, 13(10), 572-584.

Helgason, T., Gislason, J., McClement,s D.J., Kristbergsson, K. and Weiss, J. (2009). Influence of molecular character of chitosan on the adsorption of chitosan to oil droplet interfaces in an in vitro digestion model. *Food Hydrocolloids*, 23(8), 2243-2253.

Hogekamp S & Schubert H. 2003. Rehydration of food powders. Food Sci. Technol. Int 9:223-235.

Hollman, P.C.H., van Trijp, J.M.P., Mengelers, M.J.B., de Vries, J.H.M. and Katan, M.B. (1997). Bioavailability of the dietary antioxidant flavonol quercetin in man. *Cancer Letters*, 114(1–2), 139-140.

Hu, J., Johnston, K.P. and Williams, R.O. (2004). Nanoparticle engineering Processes for enhancing the dissolution rates of poorly water soluble drugs. *Drug Development and Industrial Pharmacy*, 30(3), 233-245.

Huang, D., Ou, B., Hampsch-Woodill, M., Flanagan, J.A. and Deemer, E.K. (2002a). Development and validation of oxygen radical absorbance capacity assay for lipophilic antioxidants using randomly methylated β-Cyclodextrin as the solubility enhancer. *Journal of Agricultural and Food Chemistry*, 50(7), 1815-1821.

Huang, D., Ou, B., Hampsch-Woodill, M., Flanagan, J.A. and Prior, R.L. (2002b). High-throughput assay of oxygen radical absorbance capacity (ORAC) using a multichannel liquid handling system coupled with a microplate fluorescence reader in 96-Well format. J*ournal of Agricultural and Food Chemistry*, 50(16), 4437-4444.

Huang, D., Ou, B. and Prior, R.L. (2005). The chemistry behind Antioxidant Capacity Assays. *Journal of Agricultural and Food Chemistry*, 53(6), 1841-1856.

Huang, Q., Yu, H. and Ru, Q. (2010). Bioavailability and Delivery of Nutraceuticals Using Nanotechnology. *Journal of Food Science*, 75(1), R50-R57.

Ingvarsson, P.T., Yang, M., Nielsen, H.M., Rantanen, J. and Foged, C. (2011). Stabilization of liposomes during drying. *Expert Opinion on Drug Delivery*, 8(3), 375-388.

Jacobs, C., Kayser, O. and Müller, R.H. (2000). Nanosuspensions as a new approach for the formulation for the poorly soluble drug tarazepide. *International Journal of Pharmaceutics*, 196(2), 161-164.

Jafari, S., He, Y. and Bhandari, B. (2007a). Optimization of nano-emulsions production by microfluidization. *European Food Research and Technology*, 225(5), 733-741.

Jafari, S., Assadpoor, E., He, Y. and Bhandari, B. (2008). Re-coalescence of emulsion droplets during high-energy emulsification. *Food Hydrocolloids*, 22(7), 1191-1202.

Jafari, S., He, Y. and Bhandari, B. (2007b). Production of sub-micron emulsions by ultrasound and microfluidization techniques. *Journal of Food Engineering*, 82(4), 478-488.

Jayant, L. (2011). Scaling up and processing nutraceutical dispersions. *Handbook of Nutraceuticals Volume II*. CRC Press, 239-259.

Karadag, A., Ozcelik, B. and Saner, S. (2009). Review of methods to determine antioxidant capacities. *Food Analytical Methods*, 2(1), 41-60.

Karlene, M. and Derick, R. (2006). Emulsions for the delivery of nutraceutical lipids. *Nutraceutical and Specialty Lipids and their Co-Products.* CRC Press. 281-300.

Kasaai, M.R., Arul, J. and Charlet, G. (2000). Intrinsic viscosity–molecular weight relationship for chitosan. *Journal of Polymer Science Part B: Polymer Physics*, 38(19), 2591-2598.

Kaufman, V.R. and Garti, N. (1984). Effect of cloudy agents on the stability and opacity of cloudy emulsions for soft drinks. *Journulof Food Technology*, 19 255-261.

Keck, C.M. and Müller, R.H. (2006). Drug nanocrystals of poorly soluble drugs produced by high pressure homogenisation. *European Journal of Pharmaceutics and Biopharmaceutics*, 62(1), 3-16.

Keller, B.C. (2001). Liposomes in nutrition. *Trends in Food Science & Technology*, 12(1), 25-31.

Klinkesorn, U. and McClements, D.J. (2009). Influence of chitosan on stability and lipase digestibility of lecithin-stabilized tuna oil-in-water emulsions. *Food Chemistry*, 114(4),1308-1315.

Klinkesorn, U., Sophanodora, P., Chinachoti, P., Decker, E.A. and McClements, D.J. (2006). Characterization of spray dried tuna oil emulsified in two-layered interfacial membranes prepared using electrostatic layer-by-layer deposition. *Food Research International*, 39, 449-457.

Klinkesorn, U., Sophanodora, P., Chinachoti, P., McClements, D.J. and Decker, E.A. (2005). Increasing the oxidative stability of liquid and dried tuna oil-in-water emulsions with electrostatic layer-by-layer deposition technology. *Journal of Agricultural and Food Chemistry*, 53(11), 4561-4566.

Klinkesorn, U., Sophanodora, P., Pavinee, C. and McClements, D.J. (2004). Stability and rheology of corn oil-in-water emulsions containing maltodextrin. *Food Research International*, 37, 851–859.

Knaul, J.Z., Kasaai, M.R., Bui, V.T. and Creber, K.A.M. (1998). Characterization of deacetylated chitosan and chitosan molecular weight review. *Canadian Journal of Chemistry*, 76(11), 1699-1706.

Koster, K.L., Lei, Y.P., Anderson, M., Martin, S. and Bryant, G. (2000). Effects of Vitrified and Nonvitrified Sugars on Phosphatidylcholine Fluid-to-Gel Phase Transitions. *Biophysical Journal*, 78(4), 1932-1946.

Koster, K.L., Maddocks, K.J. and Bryant, G. (2003). Exclusion of maltodextrins from phosphatidylcholine multilayers during dehydration: effects on

membrane phase behaviour. *European Biophysics Journal*, 32(2), 96-105.

Krause, K.P. and Müller, R.H. (2001). Production and characterisation of highly concentrated nanosuspensions by high pressure homogenisation. *International Journal of Pharmaceutics*, 214(1–2), 21-24.

Laguerre, M., Lecomte, J. and Villeneuve, P. (2007). Evaluation of the ability of antioxidants to counteract lipid oxidation: Existing methods, new trends and challenges. *Progress in Lipid Researc*h, 46(5),244-282.

Laguerre, M., Giraldo, L.J., Lecomte, J., Figueroa-Espinoza, M.C., Bruno, B., Weiss, J., Decker, E.A. and Villeneuv, P. (2010). Relationship between hydrophobicity and antioxidant ability of "Phenolipids" in emulsion: A parabolic effect of the chain length of rosmarinate esters. *J. Agric. Food Chem*, 58(5), 2869–2876.

Laye, C., McClements, D.J. and Weiss, J. (2008). Formation of biopolymer-coated liposomes by electrostatic deposition of chitosan. *Journal of Food Science*, 73(5), N7-N15.

Lesmes, U. and McClements, D.J. (2009). Structure–function relationships to guide rational design and fabrication of particulate food delivery systems. *Trends in Food Science & Technology*, 20(10), 448-457.

Li, H., Zhao, X., Ma, Y., Zhai, G., Li, L. and Lou, H. (2009). Enhancement of gastrointestinal absorption of quercetin by solid lipid nanoparticles. *Journal of Controlled Release*, 133(3), 238-244.

Li, J.L., Cheng, Y.Q., Wang, P., Zhao, W.T., Yin, L.J. and Saito, M. (2012). A novel improvement in whey protein isolate emulsion stability: Generation of an enzymatically cross-linked beet pectin layer using horseradish peroxidase. *Food Hydrocolloids*, 26(2), 448-455.

Li, Y., Hu, M., Xiao, H., Du, Y., Decker, E.A. and McClements, D.J. (2010). Controlling the functional performance of emulsion-based delivery systems using multi-component biopolymer coatings. *European Journal of Pharmaceutics and Biopharmaceutics*, 76(1), 38-47.

Lin, C.C., Lin, H.Y., Chen, H.C., Yu, M.W. and Lee, M.H. (2009). Stability and characterisation of phospholipid-based curcumin-encapsulated microemulsions. *Food Chemistry*, 116(4), 923-928.

Liu, P., Rong, X., Laru, J., van Veen, B., Kiesvaara, J., Hirvonen, J., Laaksonen, T. and Peltonen, L. (2011). Nanosuspensions of poorly soluble drugs: Preparation and development by wet milling. *International Journal of Pharmaceutics*, 411(1–2), 215-222.

Liu, W. and Guo, R. (2006). Interaction between flavonoid, quercetin and surfactant aggregates with different charges. *J Colloid Interface Sci*., 302(2), 625-632.

Lo, Y.I., Tsai, J.C. and Kuo, J.H. (2004). Liposomes and disaccharides as carriers in spray-dried powder formulations of superoxide dismutase. *Journal of Controlled Release*, 94(2–3), 259-272.

Lucas-Abellán, C., Fortea, I., Gabaldón, J.A. and Núñez-Delicado, E. (2007). Encapsulation of quercetin and myricetin in cyclodextrins at acidic pH. *Journal of Agricultural and Food Chemistry*, 56(1) 255-259.

MacDonald-Wicks, L.K., Wood, L.G. and Garg, M.L. (2006). Methodology for the determination of biological antioxidant capacity in vitro: a review. *Journal of the Science of Food and Agriculture*, 86(13), 2046-2056.

Mady, M.M. and Darwish, M.M. (2010). Effect of chitosan coating on the characteristics of DPPC liposomes. *Journal of Advanced Research*, 1(3), 187-191.

Malheiros, P.S., Daroit, D.J. and Brandelli, A. (2010). Food applications of liposome-encapsulated antimicrobial peptides. *Trends in Food Science & Technology*, 21(6), 284-292.

Malmsten, M. (2002). Emulsions. *Surfactants and Polymers in Drug Delivery*. CRC Press doi: 10.1201/9780824743758.ch6

Mason, T.G., Wilking, J.N., Meleson, K., Chang, C.B. and Graves, S,M. (2006). Nanoemulsions: formation, structure, and physical properties. *Journal of Physics: Condensed Matter*, 18(41), R635. doi:10.1088/0953-8984/18/41/R01

McClements, D.J. (2000). Comments on viscosity enhancement and depletion flocculation by polysaccharides. *Food Hydrocolloids*, 14(2), 173-177. doi: 10.1016/S0268-005X(99)00065-X

McClements, D.J. and Weiss, J. (2005). *Lipid Emulsions*,6th ed.:John Wiley & Sons, Inc.

McClements, D.J. (2005a). Characterization of emulsion properties. *Food Emulsions.* CRC Press. doi: 10.1201/9781420039436.ch11

McClements, D.J. (2005b). Colloidal interactions. *Food Emulsions.* CRC Press. doi: 10.1201/9781420039436.ch3

McClements, D.J. (2005c). Emulsion formation. *Food Emulsions.* CRC Press. doi: 10.1201/9781420039436.ch6

McClements, D.J. (2005d). Emulsion ingredients. Food Emulsions. CRC Press. doi: 10.1201/9781420039436.ch4

McClements, D.J. (2005e). Emulsion stability. *Food Emulsions*. CRC Press. doi: 10.1201/9781420039436.ch7

McClements, D.J. (2005f). Food Emulsions Principles, Practices, and Techniques. 2nd Ed. CRC Press. doi: 10.1201/9781420039436.ch1

McClements, D.J. (2007). Critical review of techniques and methodologies for characterization of emulsion stability. C*ritical Reviews in Food Science and Nutrition*, 47(7), 611-649. doi:10.1080/ 10408390 701289292

McClements, D.J., Decker, E.A. and Weiss, J. (2007). Emulsion-based delivery systems for lipophilic bioactive components. *Journal of Food Science*, 72(8), R109-R124.

McClements, D.J. (2008). Lipid-based emulsions and emulsifiers. *Food Lipids Chemistry, Nutrition, and Biotechnology*. CRC Press. doi: 10.1201/9781420046649.ch3

McClements, D.J., Decker, E.A., Park, Y. and Weiss, J. (2009). Structural Design Principles for Delivery of Bioactive Components in Nutraceuticals and Functional Foods. *Critical Reviews in Food Science and Nutrition*, 49(6), 577-606.

McClements, D.J. (2010). Design of nano-laminated coatings to control bioavailability of lipophilic food components. *Journal of Food Science*, 75(1), R30-R42. doi: 10.1111/j.1750-3841.2009.01452.x

McClements, D.J. and Li, Y. (2010). Structured emulsion-based delivery systems: Controlling the digestion and release of lipophilic food components. *Advances in Colloid and Interface Science*, 159(2), 213-228.

McClements, D.J. (2011). Edible nanoemulsions: fabrication, properties, and functional performance. Soft Matter 7(6):2297-2316.

McClements, D.J. and Rao, J. (2011). Food-grade nanoemulsions: Formulation, fabrication, properties, performance, biological fate, and potential toxicity. *Critical Reviews in Food Science and Nutrition*, 51(4), 285-330.

McClements, D.J. (2012a). Advances in fabrication of emulsions with enhanced functionality using structural design principles. *Current Opinion in Colloid & Interface Science*, 17(5), 235-245.

McClements, D.J. (2012b). Crystals and crystallization in oil-in-water emulsions: Implications for emulsion-based delivery systems. *Advances in Colloid and Interface Science*, 174, 1-30.

Meeren, PVd., Cocquyt, J. and Vanderdeelen, J. (2004a). Surface Charge Analysis. *Handbook of Food Analysis*, 2nd Edition -3 Volume Set. CRC Press. p. 1825-1836.

Meeren, PVd., Dewettinck, K. and Saveyn, H. (2004b). Particle Size Analysis. *Handbook of Food Analysis*, 2nd Edition -3 Volume Set. CRC Press. p. 1805-1823.

Merisko-Liversidge, E. and Liversidge, G.G. (2011). Nanosizing for oral and parenteral drug delivery: A perspective on formulating poorly-water soluble compounds using wet media milling technology. *Advanced Drug Delivery Reviews*, 63(6), 427-440.

Miller, C. (2010). Behavior of Emulsions and Microemulsions. *Nanoscience.* CRC Press. p. 493-511.

Mitri, K., Shegokar, R., Gohla, S., Anselmi, C. and Müller, R.H. (2011). Lutein nanocrystals as antioxidant formulation for oral and dermal delivery. *International Journal of Pharmaceutics* 420(1), 141-146.

Moore, J., Yin, J.J. and Yu, L. (2006). Novel fluorometric assay for hydroxyl radical scavenging capacity (HOSC) estimation. *Journal of Agricultural and Food Chemistry*, 54(3),617-626.

Mozafari, M.R., Chad, J., Sophia, H. and Costas, D. (2008a). Nanoliposomes and Their Applications in Food Nanotechnology. *Journal of Liposome Research*, 18(4), 309-327.

Mozafari, M.R., Flanagan, J., Matia-Merino, L., Awati, A., Omri, A., Suntres, Z.E. and Singh, H. (2006). Recent trends in the lipid-based nanoencapsulation of antioxidants and their role in foods. *Journal of the Science of Food and Agriculture*, 86(13), 2038-2045.

Mozafari, M.R., Khosravi-Darani, K., Borazan, G.G., Cui, J., Pardakhty, A. and Yurdugul, S. (2008b). Encapsulation of food ingredients using nanoliposome technology. *International Journal of Food Properties* 11(4), 833-844.

Müller, R.H. and Peters, K. (1998). Nanosuspensions for the formulation of poorly soluble drugs: I. Preparation by a size-reduction technique. *International Journal of Pharmaceutics* 160(2), 229-237.

Mun, S., Decker, E.A. and McClements, D.J. (2006). Effect of molecular weight and degree of deacetylation of chitosan on the formation of oil-in-water emulsions stabilized by surfactant–chitosan membranes. *Journal of Colloid and Interface Science*, 296(2), 581-590.

Narang, A.S., Delmarre, D. and Gao, D. (2007). Stable drug encapsulation in micelles and microemulsions. *International Journal of Pharmaceutics*, 345(1–2), 9-25.

O'hagan, P., Hasapidis, K., Coder, A., Helsing, H. and Pokrajac, G. (2005). Particle Size Analysis of Food Powders. *Encapsulated and Powdered Foods.* CRC Press. p. 215-245.

Ogawa, S., Decker, E.A. and McClements, D.J. (2003). Production and characterization of O/W emulsions containing cationic droplets stabilized by lecithin−chitosan membranes. *Journal of Agricultural and Food Chemistry*, 51(9), 2806-2812.

Ogawa, S., Decker, E.A. and McClements, D.J. (2004). Production and characterization of O/W Emulsions containing droplets stabilized by lecithin−chitosan−pectin mutilayered membranes. *Journal of Agricultural and Food Chemistry*, 52(11), 3595-3600.

Ostertag, F., Weiss, J. and McClements, D.J. (2012). Low-energy formation of edible nanoemulsions: factors influencing droplet size produced by emulsion phase inversion. *Journal of Colloid and Interface Science*,.388(2), 95-102. doi:10.1016/j.jcis.2012.07.089

Ou, B., Hampsch-Woodill, M. and Prior, R.L. (2001). Development and validation of an improved oxygen radical absorbance capacity assay using fluorescein as the fluorescent probe. *Journal of Agricultural and Food Chemistry*, 49(10), 4619-4626.

Ou, B., Huang, D., Hampsch-Woodill, M., Flanagan, J.A. and Deemer, E.K. (2002). Analysis of antioxidant activities of common vegetables employing oxygen radical absorbance capacity (ORAC) and ferric reducing antioxidant power (FRAP) assays: A comparative study. *Journal of Agricultural and Food Chemistry*, 50(11),3122-3128.

Pa, J.H. and Yu, T.L. (2001). Light scattering study of chitosan in acetic acid aqueous solutions. *Macromolecular Chemistry and Physics*, 202(7), 985-991.

Payet, L. and Terentjev, E.M. (2008). Emulsification and stabilization mechanisms of O/W emulsions in the presence of chitosan. *Langmuir*, 24(21), 12247-12252.

Ping-Chung, K. (2010). The application of nanotechnology to functional foods and nutraceuticals to enhance their bioactivities. *Biotechnology in Functional Foods and Nutraceuticals*. CRC Press. doi: 10.1201/9781420087123-c24

Piskula, M.K. and Terao, J. (1998). Quercetin's solubility affects its accumulation in rat plasma after oral administration. *Journal of Agricultural and Food Chemistry*, 46(10),4313-4317.

Prior, R.L., Wu, X. and Schaich, K. (2005). Standardized methods for the determination of antioxidant capacity and phenolics in foods and dietary supplements. *Journal of Agricultural and Food Chemistry*, 53(10), 4290-4302.

Quemeneur, F., Rammal, A., Rinaudo, M. and Pépin-Donat, B. (2007). Large and giant vesicles "decorated" with chitosan: Effects of pH, salt or glucose stress, and surface adhesion. *Biomacromolecules*, 8(8), 2512-2519.

Quemeneur, F., Rinaudo, M., Maret, G. and Pepin-Donat, B. (2010). Decoration of lipid vesicles by polyelectrolytes: mechanism and structure. *Soft Matter*, 6(18), 4471-4481.

Rabinow, B.E. (2004). Nanosuspensions in drug delivery. *Nat Rev Drug Discov*, 3(9), 785-796.

Rogerio, A.P., Dora, C.L., Andrade, E.L., Chaves, J.S., Silva, L.F.C., Lemos-Senna, E. and Calixto, J.B. (2010). Anti-inflammatory effect of quercetin-loaded microemulsion in the airways allergic inflammatory model in mice. *Pharmacological Research*, 61(4), 288-297.

Rosenberg, M., Kopelman, I.J. and Talmon, Y. (1985). A Scanning Electron Microscopy Study of Microencapsulation. *Journal of Food Science*, 50(1), 139-144.

Sadurní, N., Solans, C., Azemar, N. and García-Celma, M.J. (2005). Studies on the formation of O/W nano-emulsions, by low-energy emulsification methods, suitable for pharmaceutical applications. *European Journal of Pharmaceutical Sciences*, 26(5), 438-445.

Sahoo, N.G., Kakran, M., Shaal, L.A., Li, L., Müller, R.H., Pal, M. and Tan, L.P. (2011). Preparation and characterization of quercetin nanocrystals. *Journal of Pharmaceutical Sciences*, 100(6), 2379-2390.

Schramm, L. and Stasiuk, E. (2005). Emulsions. *Finely Dispersed Particles Micro-, Nano-, and Atto-Engineering*. Edited by Jyh-Ping Hsuand Aleksandar M . Spasic. CRC Press. doi: 10.1201/9781420027662.ch4

Seyoum, A., Asres, K. and El-Fiky, F.K. (2006). Structure–radical scavenging activity relationships of flavonoids. *Phytochemistry*, 67(18), 2058-2070.

Shaw, L.A., McClements, D.J. and Decker, E.A. (2007). Spray-dried multilayered emulsions as a delivery method for ω-3 fatty acids into food systems. *Journal of Agricultural and Food Chemistry*, 55(8), 3112-3119.

Shegokar, R. and Müller, R.H. (2010). Nanocrystals: Industrially feasible multifunctional formulation technology for poorly soluble actives. *International Journal of Pharmaceutics*, 399(1–2),129-139.

Sheu, T.Y. and Rosenberg, M. (1998). Microstructure of microcapsules consisting of whey proteins and carbohydrates. *Journal of Food Science*, 63(3):491-494.

Singare, D.S., Marella, S., Gowthamrajan, K., Kulkarni, G.T., Vooturi, R. and Rao, P.S. (2010). Optimization of formulation and process variable of nanosuspension: An industrial perspective. *International Journal of Pharmaceutics*, 402(1–2), 213-220.

Solans, C., Izquierdo, P., Nolla, J., Azemar, N. and Garcia-Celma, M.J. (2005). Nano-emulsions. *Current Opinion in Colloid & Interface Science*, 10(3–4), 102-110.

Solans, C. and Solé, I. (2012). Nano-emulsions: Formation by low-energy methods. *Current Opinion in Colloid & Interface Science*, 17(5), 246-254.

Solans, C., Sole, I., Fernandez-Arteaga, A., Nolla, J., Azemar, N., Gutierrez, J., Maestro, A., Gonzalez, C. and Pey, C. (2009). Nano-Emulsion formation by low-energy methods and functional properties. *Structure and Functional Properties of Colloidal Systems*..Edited by Roque Hidalgo-Alvarez CRC Press. doi: 10.1201/9781420084474-c21

Somasundaran, P., Raymond, F., Somil, M., Thomas, W. and Nissim, G. (2006). Emulsions and Their Behavior. *Surfactants in Personal Care Products and Decorative Cosmetics*, Edited by Linda D Rhein, Mitchell Schlossman, Anthony O'Lenick, and P . Somasundaran. 3rd Edition. CRC Press.doi: 10.1201/9781420016123.ch8

Stepanek, P. (1993). Data analysis in dynamic light scattering. Oxford University Press.

Tadros, T., Izquierdo, P., Esquena, J. and Solans, C. (2004). Formation and stability of nano-emulsions. *Advances in Colloid and Interface Science* 108–109, 303-318.

Tan, C.P. and Nakajima, M. (2005). β-Carotene nanodispersions: preparation, characterization and stability evaluation. *Food Chemistry*, 92(4), 661-671.

Taylor, T.M., Weiss, J., Davidson, P.M. and Bruce, B.D. (2005). Liposomal nanocapsules in food science and agriculture. *Critical Reviews in Food Science and Nutrition*, 45(7-8), 587-605.

Thanasukarn, P., Pongsawatmanit, R. and McClements, D.J. (2006). Utilization of layer-by-layer interfacial deposition technique to improve freeze–

thaw stability of oil-in-water emulsions. *Food Research International*, 39(6), 721-729.

Tonon, R.V., Freitas, S.S. and Hubinger, M.D. (2011). Spray drying of açai (euterpe oleraceae mart.) juice: Effect of inlet air temperature and type of carrier agent. *Journal of Food Processing and Preservation*, 35(5), 691-700.

Valkonen, M. and Kuusi, T. (1997). Spectrophotometric assay for total peroxyl radical-trapping antioxidant potential in human serum. *Journal of Lipid Research*, 38(4), 823-833.

Van Eerdenbrugh, B., Van den Mooter, G. and Augustijns, P. (2008). Top-down production of drug nanocrystals: Nanosuspension stabilization, miniaturization and transformation into solid products. *International Journal of Pharmaceutics*, 364(1):64-75.

Verma, S., Kumar, S., Gokhale, R. and Burgess, D.J. (2011). Physical stability of nanosuspensions: Investigation of the role of stabilizers on Ostwald ripening. *International Journal of Pharmaceutics*, 406(1–2), 145-152.

Vogt, M., Kunath, K. and Dressman, J.B. (2008). Dissolution enhancement of fenofibrate by micronization, cogrinding and spray-drying: Comparison with commercial preparations. *European Journal of Pharmaceutics and Biopharmaceutics*, 68(2), 283-288.

Wach, A., Pyrzynska, K. and Biesaga, M. (2007). Quercetin content in some food and herbal samples. *Food Chemistry*, 100(2), 699-704.

Walstra, P. (2002). Formation of Emulsions and Foams. *Physical Chemistry of Foods*. CRC Press.

Walton, D.E. (2000). The morphology of spray-dried particles a qualitative view. *Drying Technology*, 18(9), 1943-1986.

Walzel, P. and Furuta, T. (2011). Morphology and Properties of Spray-Dried Particles. *Modern Drying Technology*. Wiley-VCH Verlag GmbH & Co. KGaA. p. 231-294.

Wanasundara, P.K. and Shahidi, F. (2005). Antioxidants: Science, Technology, and Applications. *Bailey's Industrial Oil and Fat Products*. John Wiley & Sons, Inc.

Wang, W., Bo, S., Li, S. and Qin, W. (1991). Determination of the Mark-Houwink equation for chitosans with different degrees of deacetylation. *International Journal of Biological Macromolecules*, 13(5), 281-285.

Wang, X., Jiang, Y., Wang, Y.W., Huang, M.T., Ho, C.T. and Huang, Q. (2008). Enhancing anti-inflammation activity of curcumin through O/W nanoemulsions. *Food Chemistry*, 108(2), 419-424.

Weiss, J., Takhistov, P. and McClements, D.J. (2006). Functional Materials in Food Nanotechnology. *Journal of Food Science*, 71(9), R107-R116.

Wessman, P., Edwards, K. and Mahlin, D. (2010). Structural effects caused by spray- and freeze-drying of liposomes and bilayer disks. *Journal of Pharmaceutical Sciences*, 99(4), 2032-2048.

Wolfe, K.L. and Liu, R.H. (2007). Cellular antioxidant activity (CAA) assay for assessing antioxidants, foods, and dietary supplements. J*ournal of Agricultural and Food Chemistry*, 55(22), 8896-8907.

Wollenweber, C., Makievski, A.V., Miller, R. and Daniels, R. (2000). Adsorption of hydroxypropyl methylcellulose at the liquid/liquid interface and the effect on emulsion stability. *Colloids and Surfaces A: Physicochemical and Engineering Aspects*, 172(1–3), 91-101.

Wu, T.H., Yen, F.L., Lin, L.T., Tsai, T.R., Lin, C.C. and Cham, T.M. (2008). Preparation, physicochemical characterization, and antioxidant effects of quercetin nanoparticles. *International Journal of Pharmaceutics*, 346(1-2), 160-168.

Xu, X., Khan, M.A. and Burgess, D.J. (2012). Predicting hydrophilic drug encapsulation inside unilamellar liposomes. *International Journal of Pharmaceutics* , 423(2), 410-418. doi: 10.1016/j.ijpharm.2011.12.019

Yuan-Peng, Z., Boris, C. and Danilo, L. (2001). Liposomes in Drug Delivery. *Polymeric Biomaterials, Revised and Expanded*. Edited by Severian Dumitriu. CRC Press. doi: 10.1201/9780203904671.ch29

Yuan, Y., Gao, Y., Mao, L. and Zhao, J. (2008). Optimisation of conditions for the preparation of [beta]-carotene nanoemulsions using response surface methodology. *Food Chemistry*, 107(3), 1300-1306.

Zeeb, B., Gibis, M., Fischer, L. and Weiss, J. (2012). Crosslinking of interfacial layers in multilayered oil-in-water emulsions using laccase: Characterization and pH-stability. *Food Hydrocolloids*, 27(1), 126-136.

Zhang, Y., Zhang ,Y., Pan, Y., Wang, J., Zhang, L., Long, B. and Liu, X. (2006). Study on distribution of liposome nanoparticles loaded quercetin in mice. *Nanoscience*, 11(2), 89-94.

Zheng, Y., and Chow, A.H.L. (2009). Production and characterization of a spray-dried hydroxypropyl-β-cyclodextrin/quercetin complex. *Drug Development and Industrial Pharmacy*, 35(6), 727-734.

CURRICULUM VITAE

Name Surname:	**Ayşe KARADAĞ**
Place and Date of Birth:	**Istanbul, 14.06.1978**
Address:	**Bestekar Ziya Sok. 10/43 34730 Goztepe-Istanbul**
E-Mail:	**aykar78@yahoo.com**
B.Sc.:	**Yıldız Technical University, Chemical Eng., 2001**
M.Sc.	**Istanbul Technical University, Food Eng., 2005**

Professional Experience:

Visiting PhD student at Hohenheim University**,** Stuttgart-GERMANY, Food Structure and Functionality lab (April 2011-April 2012), **Supervisor:** Prof.Dr. Jochen Weiss

Visiting PhD student at Rutgers University, New Jersey-USA, Dept.of Food Science, Nanotechnology lab. (Jan 2010-Feb 2011)**, Supervisor:** Prof.Dr. Qingrong Huang

Researcher in a FP7 project entitled as COLORSPORE (contract No: 207948), Istanbul Technical University, TURKEY (Nov 2008-Dec 2009), **Supervisor:** Prof.Dr. Beraat Ozcelik

Business Development and Scientific Affairs-Specialist worked as a specialist in a project entitled as "*From Farm to Fork Food Safety Specialist Training Program*" (No: TR/06/B/F/PP-178050) funded by **EU** as **Leonardo B type project**. (Nov 2006- Aug 2008) at Kalite Sistem Laboratories Group- Istanbul

Ar-Ge- Project Manager in charge of managing the project (Project no: 280/T26) supported by **TUBITAK-TTGV**. (March 2004 -Feb 2006) at Muradoglu Tea Industry –Istanbul and Rize

Awards and Fellowhips

- **2nd place** in George F. Stewart: Graduate Student Research Paper Competition of Institute of Food Technologists (**IFT**), 23-25 June, 2012, Las Vegas, USA
- Fellowship provided by Erasmus Exchange Program for 6 months
- Fellowship provided by Rutgers University for 5 months

List of Publications

- **Karadag, A**., Ozcelik, B., Saner, S. **2009**. *Review of Methods to Determine Antioxidant Capacities*. Food Analytical Methods, Vol.2, No. 1, 41-60.
- Ozcelik, B., **Karadag, A**., Cinbas, T., Yolci, P. **2009**. *Influence of Extraction Time and Different Sage Varieties on Sensory Characteristics of a Novel Functional Beverage by RSM.* Food Science and Technology International, Vol. 15, No. 2, 111-118
- **Karadag, A.,** Gunes G. **2008**. *The effects of gamma irradiation on the quality of ready-to-cook meatballs*. Turk. J. Vet. Anim. Sci., Vol. 32, 2008, 269-274
- **Karadağ, A**., Ömeroğlu, P.Y. ve Saner, S.**2008** "*Gıda muhafazasında yeni yöntemlerin* kullanılması", Gıda Güvenliği Degisi, No: 1, s. 50-56
- **Karadağ A,** Güneş G, **2005** "*Gama ışınlarının gıdaların besin değeri üzerindeki etkileri*", Dünya Gıda, No. 9, s. 55-60
- **Karadag, A**., Avci, N., Ozcelik, B. **2011**. Effects of microwave process on Turkish black tea quality. International Food Congress-Novel Approaches in Food Industry (NAFI), 390-395, 26-29 Mayıs, İzmir.
- **Karadag, A**., Ozcelik, B. **2010**. *Yağlarda Biyoteknolojik Uygulamalar ve Yapılandırılmış Yağlar* in GIDA BIYOTEKNOLOJISI, 1st ed., Nobel Publishing house, 343-374
- **Karadag, A**., Ilyasoglu, H., Gultekin. M., and Ozcelik, B. **2009**. *Determination of antioxidant capacity of Bacillus indicus HU36 spores as a part of COLORSPORE Project in FP7*, IFT (Institute of Food Technologists), June 06-09, Anaheim, OC.
- **Karadag, A**., Özçelik, B., **2009**. *Stability of carotenoid nanodispersions against heating, salt, pH, relative humidity and light*. Nanomats International Conference on Nanomaterials and Nanosystems, 10-13 August, Istanbul.
- Ozcelik, B., **Karadağ, A**., İlyasoğlu, H., **2009**. *Karotenoid Üreten Probiyotik Bakterilerin Nanoenkapsülasyonu*. İTÜ Nano-Bilim ve Nano-Teknoloji Çalıştayı Özetler Kitabı, 12-13 Şubat 2009, sy 65, İstanbul.
- **Karadag, A.,** Gunes G., December 08-10 **2007**, *Quality characteristics of ready-to-cook meatball as affected by gamma irradiation.* 5th Food Engineering Conference, Istanbul.
- Yolcu, P., Saner, S., **Karadag, A. 2007** *Application of Technical Requirements of ISO/IEC 17025 into a routine aflatoxin analysis laboratory*, IUPAC XII th International Symposium on Mycotoxins and Phycotoxins, May 21-25, Istanbul
- **Karadag, A.,** Yolcu P., Saner, S. **2007** *Review of mycotoxins alerts in RASFF belongs to 2002-2006*, May 25, 2007, 3rd National Mycotoxins Symposium, Istanbul
- Saner, S., Ömeroğlu, P.Y. ve **Karadağ, A**. **2007**. Tarım İlaçları ve Gıda Güvenliği AB ile Son Yasal Düzenlemeler. Tatım İlaçları Kongre ve Segisi Bildiriler Kitabı, 25-26 Ekim 2007, sy 24-35
- **Karadag, A.,** Avci, N., and Ozcelik, B. **2006** *Improvement of Turkish Black Tea Quality by Application of Novel Microwave Technology*, IFT (Institute of Food Technologists), June 24-28, Orlando, FL.,

- **Karadag, A.,** Avci, N., and Ozcelik, B. **2006** *Effect of microwave process on antioxidant activity and phenolics of Turkish green tea***,** IFT (Institute of Food Technologists), June 24-28, 2006, Orlando, FL.
- Ozcelik B., **Karadag, A.,** Tulay, C. and Yolcu, P. **2004** *Investigating Influence of Extraction Time and Different Sage Types on Sensory Characteristics of a Novel Functional Beverage by RSM*, IFT (Institute of Food Technologists), July 12-16, Las Vegas, NV.

PUBLICATIONS/PRESENTATIONS ON THE THESIS

- **Karadag, A.**, Ozcelik, B., Shramek, M Kohlus, R. and Weiss, J. **2013**. *Presence of* electrostatically-adsorbed polysaccharides improves spray drying of liposomes. *Journal of Food Science*, 78(2), E206-E221. doi: 10.1111/1750-3841.12023
- **Karadag, A**., Yang, X., Ozcelik, B. and Huang, Q. **2013**. Optimization of conditions for the preparation of quercetin nanoemulsions using response surface methodology. Journal of Agricultural and Food Chemistry, 61(9), 2130-2139, doi: 10.1021/jf3040463
- **Karadag, A.**, Ozcelik, B., Shramek, M Kohlus, R. and Weiss, J. **2012**. *Presence of electrostatically-adsorbed polysaccharides improves spray drying of liposomes.* IFT (Institute of Food Technologists), June 23-25, Las Vegas-NV, **Awarded**
- **Karadag, A**.,Ozcelik, B. and Huang, Q. **2013.** *Preparation of Quercetin Sub-micrometer Dispersions by High-Pressure Homogenization.* Journal of Agricultural and Food Chemistry-Submitted, under review process